The University Of Sheffield.

Understanding the tribological interactions between plantar skin and sock textiles through the development of biofidelic test-beds

Diyana Nurfathiah Tasron

A thesis submitted in partial fulfilment of the requirements for the degree of
Doctor of Philosophy

The University of Sheffield
Faculty of Engineering
Department of Mechanical Engineering

October 2016

Department of Mechanical Engineering

Understanding the tribological interactions between plantar skin and sock textiles through the development of biofidelic test-beds

Diyana Nurfathiah Tasron

Submitted for the degree of Doctor of Philosophy
October 2016

Foot friction blisters are one of the most common dermatological injuries experienced by those actively involved in outdoor physical pursuits. The frictional interaction between the human skin and textile fabric is acknowledged as being an important aspect in blister development. Despite growing research in this area, relatively little is known about the friction interaction between plantar skin and textiles.

The ultimate aim of this thesis is to achieve enhanced understanding of the complex tribological interactions between human plantar skin and sock textiles. The first part of this thesis primarily focusses on experimental studies conducted on the sock-insole and skin-sock interfaces. Due to the lack of existing standard testing protocols, novel testing protocols were developed and used as a standard testing procedure throughout the experimental studies. The friction study on the entire plantar region was conducted in dry textile conditions whereas the friction study on the plantar aspect of the first metatarsal head (1MTH) was carried out in three significantly different moisture conditions (dry, low moisture and wet). Findings gained from a friction study on the 1MTH region of the foot were then used for validations in the second half of this thesis which concerns the development of a range of prototype biofidelic test-beds to mimic the frictional behaviour of 1MTH region.

A set of prototype biofidelic test-beds were developed after considering the appropriate geometry, materials and manufacturing processes. Each test-bed is a two-layer polymer-based physical skin model, with the outer layer representing the epidermal dermal tissue and

the inner layer representing the dermal subcutaneous tissues. A steel hemisphere was also embedded within the test-bed to simulate the 1MTH bone. Nine test-beds of differing inner Young's modulus were made with four of them having texture on their surface layer, obtained from a mould of an actual human foot. All test-beds were subjected to deformation and friction tests in order to validate their performances in the respective aspects, when compared with data obtained from human testing.

It is hoped that the understanding gained from the study will close the gaps in the existing knowledge of plantar skin – sock textile friction which can be applied into future foot friction blister studies.

Keywords: Skin tribology, plantar skin, first metatarsal head, friction blisters, running socks, moisture, biofidelic test-beds

Acknowledgements

First and foremost, I would like to express my special appreciation and thanks to my supervisors, Dr Matt Carré and Prof Roger Lewis for their tremendous support, patience, encouragement and inspiration throughout the past four years. I would have been completely lost without them.

I would like to thank Dr Farina Hashmi (University of Salford) for kindly letting me visit and use the research facilities at the School of Podiatry for the collaborative work. I also thank her for providing the training to conduct the foot assessments and to use the skin characterisation devices. Her assistance during the participant recruitment is also greatly appreciated. I would also like to extend my gratitude to Ciaran Wright for his support in using the foot loading device.

I am grateful to Prof Olga Troynikov and Sit Hana Nasir (RMIT University) for the opportunity to collaborate on the sock textile study and for their clarifications on some of the textile testing equipment and terminologies.

My sincere thanks also go to Jamie Booth, Les Morton and Ben Kitchener for their technical support in equipment design and software programming.

I have deeply appreciated the camaraderie provided by all my colleagues in MB21 office: Dr Raman Maiti, Almaky Almagirby, Zing Lee, Daniel Ura, Asim Zaheer, Xueqing Zhang, Victor Gonzalez and Fathi El-Shukri. They have been a great source of friendships, collaboration and stimulating discussions.

I owe my deepest gratitude to both my sisters, Dalila Tasron and Dinie Tasron, for their assistance during the human testing. They also tirelessly motivate me through the ups and downs of my PhD journey.

Finally, my most profound appreciation and gratitude goes to my parents, Dr Tasron Surat and Mrs Rohani Jaffar for providing me with unfailing support and immense encouragement throughout my years of study. Most importantly, I thank them for simply believing in me. To them I dedicate this thesis.

Table of contents

List of figures

List of tables

Abbreviations

1MTH	first metatarsal head
ABS	anti-blister sock
ANOVA	analysis of variance
AOTI	accumulative one-way transport index
AU	Arbitrary unit
BF	biofidelic
COF	coefficient of friction
CRS	cotton-rich sock
DCOF	dynamic coefficient of friction
E-D	epidermal-dermal
FT	friction test
LMo	low moisture
MMT	moisture management tester
NT	non-textured
OCT	optical coherence tomography
OMMC	overall moisture management capacity
SC	stratum corneum
SD	standard deviation
SEE	standard error of estimate
ST	soft tissue
T	textured

Nomenclature

A	contact area (m^2)
Ap	projected contact area
a	contact radius
d	diameter (mm)
E	Young's modulus (N/m^2)
Eeq	equivalent Young's modulus (N/m^2)
E^*	reduced Young's modulus (N/m^2)
F	applied normal force (N)
F_{ad}	adhesion force (N)
F_{def}	deformation force (N)
F_F	friction force (N)
F_T	total friction force
h	indentation depth (mm)
h_c	contact depth (mm)
L	original length (mm)
L_o	unstrained length (mm)
L_1	strained length (mm)
n	sample size
p	probability of a statistical test
P	contact pressure (N/m^2)
r	Pearson's / Spearman's statistical correlation
R	radius (mm)
R^2	squared Pearson's correlation coefficient
R_a	roughness (μm)
R_0	immediate skin extensibility
R_2	gross elasticity of skin (U_a/U_f) (N/m^2)
R_5	net elasticity of skin (U_r/U_e) (N/m^2)
R_6	viscoelasticity on extensibility portion of skin (U_v/U_e) (N/m^2)
R_7	biology elasticity of skin (U_r/U_f)
S	stiffness (N/m)
T	temperature
U_a	skin recovery following removal of Cutometer® vacuum
U_f	skin distensibility
U_r	skin immediate retraction
U_v	skin viscoelasticity
V	sliding velocity (m/s)
δ	displacement (mm)
μ	dynamic coefficient of friction
ν	Poisson's ratio
τ	shear stress (N/m^2)

Chapter 1

Introduction and literature review

1.1 General introduction

The plantar aspect of the foot is one of the areas of the human body where the thickest skin is found, along with the palms and the back [2]. During walking and running, feet are continuously subjected to pressure, impact, friction and shear forces [3], which when combined with individual's skin physiological characteristics and certain environmental effects can lead to various dermatological injuries. The incidence of dermatological injuries associated with athletic pursuits has significantly increased in the recent decades due to an increasing number of people participating in various competitive and recreational sports to enhance their physical health and well-being.

According to Mailler & Adams [4], foot friction blisters are the most common dermatological injuries among marathon runners, with an incidence level as high as 39% in a survey conducted on 265 entrants after the New York City Marathon in 1994. The percentage of blister incidence was also reported to be as high as 24% of 301 experienced wilderness hikers [5, 6]. Although friction blisters rarely pose a severe threat to overall health they can be painful and often result in significant increase in plantar shear stress [7] which may subsequently lead to other types of injuries. For competitive athletes, blisters could impede their athletic performance and have an adverse effect on success, as experienced by Roger Federer (2005 Australian Open) and Maria Sharapova (2006 Australian Open) [7]. Diabetic patients are often advised to get their blisters treated immediately as failure to do

this may cause damage to the deeper tissue layers leading to necrosis [8]. Although extensive studies have been carried out relating to blister formation, the complex interplay of various contact and environmental parameters that contribute to blistering is not fully understood. The reason for this is found in limited understanding of the plantar skin friction and how it is influenced by loading, contact surface and moisture conditions.

This thesis describes comprehensive experimental studies carried out over the course of three-year PhD study to examine the friction interaction between human plantar skin and running sock textile fabrics.

In this chapter, the fundamental concepts of skin anatomy are described and skin mechanical properties are presented. An overview of the theoretical background of skin friction is also included, followed by an outline of the complex interplay of various parameters influencing the skin friction. Additionally, various experimental techniques used for measuring skin properties in previous studies are reviewed to provide better understanding of the development of foot friction blisters.

1.2 Structure and function of human skin

The human integumentary system includes two major components: the skin and its derivatives (hair, sebaceous and sweat glands, and nails) accounting for approximately 7% of our total body weight [9] as illustrated in Figure 1.1. Skin being the largest organ in a human body with a surface area of 1.5 to 2m^2 in a typical adult [10], acts like a shield that protects our internal systems against the hostile external world. It is also the principal site for interaction with the surrounding surfaces throughout the course of our everyday lives. The thickness of the skin varies based on the gender and age of the individual which is due to the genetic and hormonal differences [11] as well as its anatomical location [12, 13] on the body. Males tend to have much thicker skin than females in most, if not all, anatomic locations [11]. The skin on the eyelids and in the post-auricular region is considered to be the thinnest with a thickness of approximately 0.5mm in comparison to the skin on palms and plantar aspect of the feet which is much thicker [9, 14]. A study by Sun *et al*. [15] reported plantar thickness

ranging from 5.16mm under the big toe to 18.87mm under the heel. In addition, the heel pad thickness of elderly (older than 60 years) adults was found to be significantly different than that of young adults (less than 40 years). This is due to the thickening of plantar soft tissue with age [16]. Certain medical conditions such as diabetes mellitus have also known to cause reduction of the plantar thickness which could result in the loss of compliance [17, 18].

Most of the human body surface is covered with non-glabrous (hairy) skin whereas some other parts such as the palms, fingertips, ears and lips as well as the plantar aspect of the feet are covered with glabrous (non-hairy) skin. The surface of glabrous skin is grooved with ridges and furrows to provide friction necessary for gripping [19] and locomotion. Although hair follicles are absent in glabrous skin, the eccrine sweat glands, whose ducts penetrate the centre of the ridges, are far more concentrated than in non-glabrous skin [9].

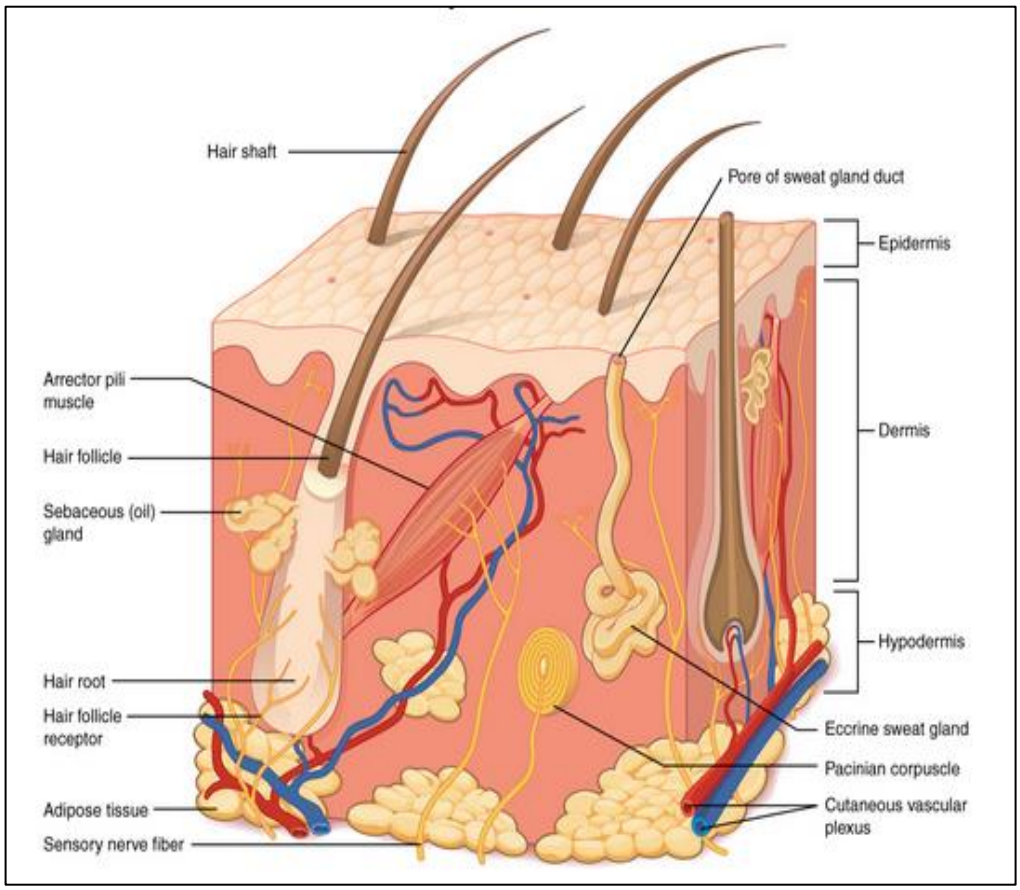

Figure 1.1: A schematic diagram of human skin and its derivatives (image reproduced from [20]).

Human skin is a complex multi-layered structure comprising of three functional layers: namely the epidermis and dermis, which are anchored to each other by a dermal-epidermal junction, and the hypodermis (also known as the subcutaneous layer). The epidermis is the outermost layer that serves as a protection shield against the external environment. It also functions to prevent extreme water loss from the body. The dermis is the deeper layer, much thicker (5 to 7 times) than the epidermis. It consists of papillary (the interface between the epidermis and the dermis) and reticular layers and acts like a scaffold, providing the structural support and elasticity to the skin [21]. Within the dermis layer, blood vessels, sensory receptors, sweat glands, hair and skin appendages can be found intricately woven with a network of closely-packed elastin and collagen fibres, embedded in interstitial fluids and water. The reticular layer contains a higher density of elastin and collagen fibres compared with the papillary layer. The dermis also helps to regulate the body temperature by secreting sweat through sweat pores. The hypodermis is made up of loose connective and subcutaneous tissues and attaches the whole skin structure to underlying structures of muscles and bones [9]. The hypodermis also serves as a shock absorber (using structural fat and stored fat) and as a thermal insulator [21]. It has been shown that with ageing, the skin gradually becomes looser and appears wrinkled due to the incremental loss of elastins over time [22].

1.1.1 Epidermis

Some researchers considered that the role of the epidermal layer in determining the mechanical properties of the skin is so small that it can often be neglected [23, 24], with an exception for the palms and plantar aspect of the feet. These researchers assumed that the collagen-rich dermis dominates the way the skin mechanically behaves. Since the pivotal focus of this PhD study is on foot friction blisters, a deeper understanding on the epidermal layer structure is therefore important.

The epidermal layer is a stratified tissue which can be further divided into five sub-layers as shown in the Figure 1.2. From the deep to the superficial layers of epidermis: stratum basale (also known as stratum germinativum), stratum spinosum, stratum

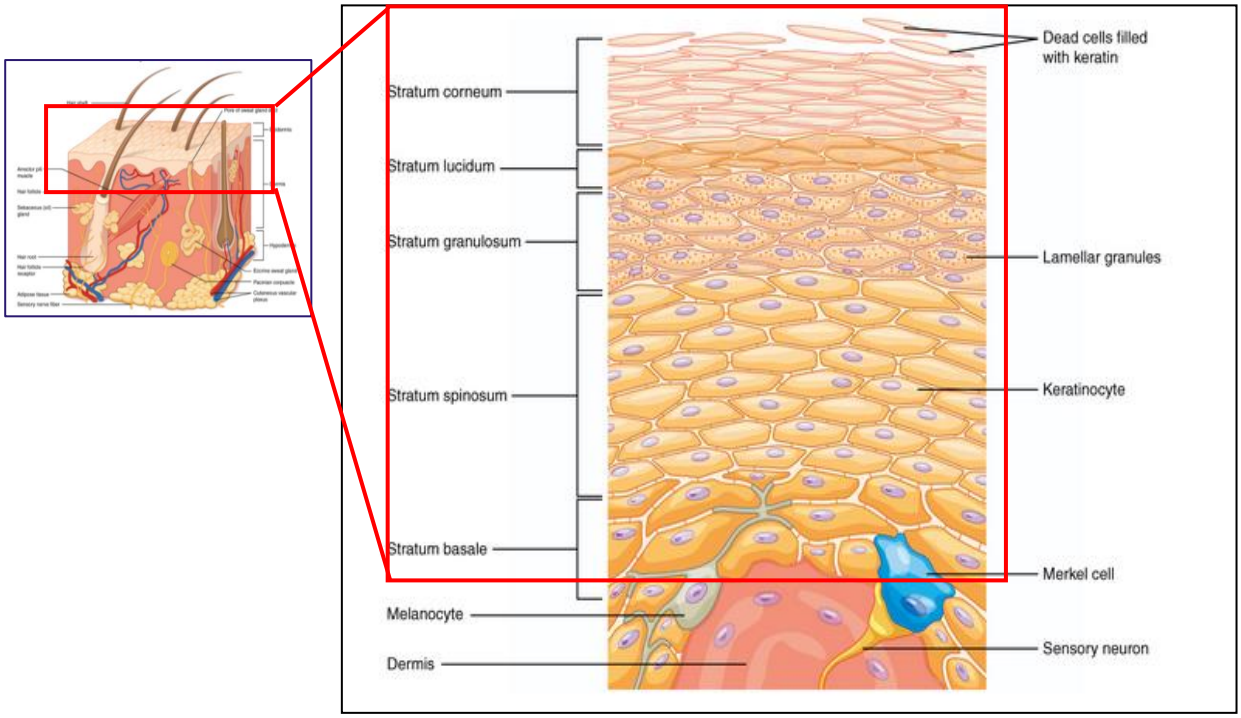

Figure 1.2: A schematic diagram of the epidermis sub-layers and its specialised cells (image reproduced from [20]).

granulosum, stratum lucidum and stratum corneum (a cornified layer consisting of flattened dead cells). Each sub-layer is defined by the shape, position, morphology and state of differentiation of the keratinocyte which is the primary cell of the epidermis, accounting for 90% to 95% of the epidermal cells [25]. The epidermal layer undergoes constant desquamation (shedding) and cell renewal occurs every 25 to 45 days to balance out the cell loss [9, 26]. A hydrolipid film composing of water and sebum, which is secreted from sweat and sebaceous glands, covers the stratum corneum to keep the skin well-hydrated and to prevent water loss [27, 28]. According to Cua *et al.* [29], there is no significant difference in terms of the stratum corneum moisture level in relation to gender.

The epidermal layer plays a central role in defining the surface properties of human skin which can be primarily attributed to the surface roughness, presence of superficial sebum and skin moisture. These attributing factors in return influence the friction between the skin and contact surface [21, 30, 31] which will be discussed throughout the latter part of this chapter.

1.3 Skin mechanical properties

The skin possesses both elastic and viscous properties. The elastic properties of human skin are mainly from the dermis, with some contributions from the epidermis whereas the viscous properties are due to the displacement of interstitial fluid through the intricate fibrous network during skin deformation [12]. In terms of its mechanical behaviour, the skin behaves as an anisotropic, non-linear viscoelastic material owing to its multi-layered and non-homogeneous nature [2, 11, 31-33]. It is generally characterised by a non-linear stress-strain relationship as shown in Figure 1.3 below.

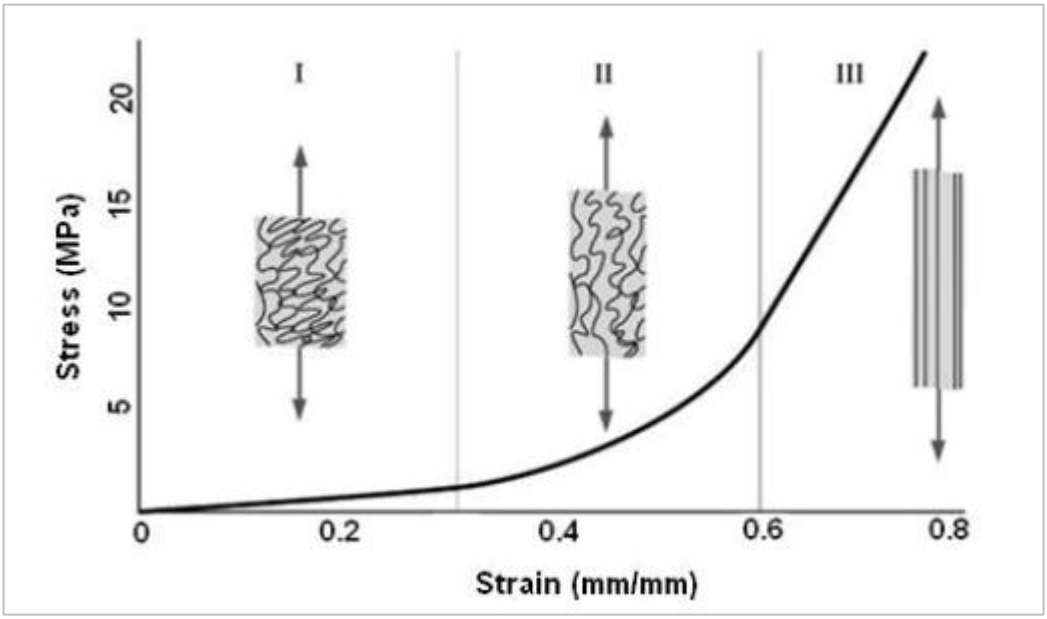

Figure 1.3: The non-linear stress-strain relationship exhibited by a normal human skin (image reproduced from [28]).

As discussed earlier, each skin layer is made up of different thicknesses and composed of various types of tissues which translates to different mechanical properties. Three separate stages can be observed from Figure 1.3. In stage I, a linear stress-strain relationship is exhibited by the dermis with a Young's modulus of 5kPa which is caused by the resistance to skin deformation provided by the network of elastin fibres within the layer. In stage II, a non-linear stress-strain relationship can be seen starting at 0.3 strain value due to the gradual extension of the collagen fibres. In the final stage III, all collagen fibres are

fully extended, resulting in another linear stress-strain relationship. The slope of this relationship corresponds to the degree of skin stiffness (i.e. the steeper the slope, the stiffer the skin becomes). Beyond stage III, yielding and rupture of the collagen fibres occur [23].

Additionally, the mechanical properties of the skin are affected by various intrinsic and loading parameters as illustrated in Figure 1.4. Environmental conditions such as the temperature and relative humidity could also influence the properties of the skin as reported by Tomlinson *et al*. [34]. Geerlings *et al.* [34, 35] also found that the dynamic shear modulus (stiffness) of the skin decreases with increasing relative humidity which concurs with the findings reported by Hendriks & Franklin [36]. Another study by Edwards & Marks [37] utilised both in-vivo and in-vitro tests to compare the strength and elasticity of skins from two different age groups and concluded that the strength and elasticity continued to increase during maturation up to a point where these mechanical properties either plateau or reduce. This finding was in agreement with results published by Escoffier *et al.* [11] and Cua *et al.* [12] which had also noted the great reduction of elasticity and recovery capacities in older skin (aged 70 years and above) despite the small difference in thickness and extensibility. Understanding these findings is important to gain the fundamental knowledge in recruiting participants for the human testing.

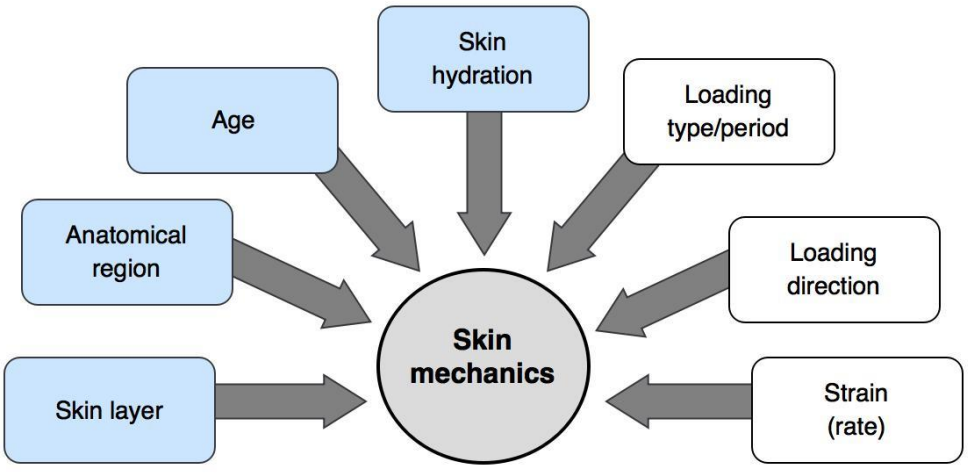

Figure 1.4: The mechanical properties of human skin are influenced by the loading factors (white boxes) and intrinsic skin parameters (grey-filled boxes) (image reproduced from [21]).

1.4 Frictional behaviour of human skin

1.4.1 Fundamentals of skin tribology

Skin friction is defined by the coefficient of friction (COF), μ between the skin and the interacting surface. COF is the ratio between the friction force, F_F acting in the horizontal direction of the skin surface and the normal load applied perpendicular to the skin surface, F_N.

$$\mu = \frac{F_F}{F_N}$$

The COF of human skin is a system property rather than a material property since it is highly determined by the contact surface material and its properties, the physiological characteristics of the skin itself (e.g. natural hydration state and sebum level), presence of any intermediate layers (e.g. added moisture, topical and cosmetic products), the mechanical contact parameters (e.g. normal load, sliding velocity and contact pressure), as well as the ambient conditions (e.g. ambient temperature and relative humidity) [21]. One of the earliest skin friction studies by Naylor [38] found that the human skin obeys Amontons' Laws as the COF of the skin was found to be independent of the applied loads. However, the findings obtained from an investigation conducted by Comaish & Bottoms [2] later disputed this and proved that human skin deviates from Amontons' Laws due to its complex viscoelastic nature which allows non-linear deformation when subjected to varying load.

Cua *et al.* [29] reported that although the skin dynamic COF varied considerably among the anatomical regions of the body, there was no significant variance in relation with age and gender. The authors further suggested that dynamic COF is more dependent on the water content and presumably sebum secretion. The relationship between skin hydration level and friction was also found in another skin friction studies by Derler *et al*. [39]. Skin with high hydration level has a tendency to produce higher friction due to increase in the real contact area following water absorption into the stratum corneum.

Numerous experimental techniques have been used to study the COF of human skin against various probe materials in either linear or rotary fashion. The diversity of

experimental techniques and loading conditions has made it extremely challenging to compare measurement results across studies. Linear techniques are found to be more convenient than the rotary techniques. Once the load is applied to an interface and the sliding motion begins, the normal and friction forces can easily be measured. The experimental results obtained using this technique are also easier to interpret since the nominal condition of the interface is the same. One challenge with the rotary techniques is the non-uniform loading distribution experienced by the contact regions which makes result interpretation to be slightly tricky [40]. A more detailed review on this particular topic has been published by Derler & Gerhardt [21], Sivamani *et al.* [41], Gitis & Sivamani [42] and Sivamani & Maibach [43].

Bowden and Tabor [44] proposed a theory on basic friction mechanisms in 1950 which has now been widely acknowledged and implemented by later studies. According to the theory, there are two important mechanisms involved in the frictional behaviour of skin in dry condition which are the deformation, F_{def} and adhesion, F_{ad} forces.

$$F = F_{def} + F_{ad}$$

The deformation mechanism is associated with the incomplete recovery of the energy dissipated by skin deformation (also known as hysteresis). However, for dry and smooth surfaces, the deformation mechanism of the skin friction is usually ignored. Therefore, the skin friction is assumed to be only related to the adhesion mechanism which is determined by the molecular attractive forces (e.g. Van der Waals forces, hydrogen bonds, electrostatic) as well as the area of contact where the adhesive bonds are formed [44].

$$F = F_{ad} = \tau A$$

where τ is the interfacial shear stress and A is the real contact area at the skin-interacting surfaces interface.

1.4.2 Previous experimental methods for measuring skin friction

A wide range of methodologies have been previously employed to measure and assess skin friction against various interacting surfaces as outlined in Table 1.1. Depending on the

objective of the studies, researchers often conduct the friction experiments using either unidirectional or reciprocating sliding interactions. In general, the measurement protocols can be divided into two main categories: a) experiments in which human subjects rub their skin against a surface [34] and b) loaded probes that are dragged against human skin [21, 45]. Both approaches can offer good insights on the friction mechanisms at the skin-surface interface, and the choice of which one to use can depend on equipment availability, repeatability, accuracy, ease of use and the extent to which the real-world scenario is simulated.

Table 1.1: A summary of some of the previous research on skin friction.

Tested skin	Interacting surfaces	Test methods	Applied load (N)	COF	Reference(s)
Dorsum of hand		Linear movement		(static) 0.25 – 0.55 0.2 – 0.48	[2]
Finger	Glass and steel	Finger sliding against surfaces	15 - 20	0.97 – 1.1	[19]
Back of heel	Rubber	Sliding probe			[45]
Lower leg	PE	Sliding probe	5	0.5 – 0.6	[46]
Forehead Volar forearm Palm Abdomen Upper back	Teflon	Rotating probe		0.34 0.26 0.21 0.12 0.25	[47]
Inner forearm	Glass	Sliding probe		0.27 – 0.36	[48]
Finger	Steel	UMT rolling probe	0.2	0.33 – 0.55	[49]
Forearm	Steel	Moving plate		0.24 – 0.64	[50]
Index finger	Wool fabric	Finger sliding against surface		0.42	[51]

1.5 Plantar skin

1.5.1 Vertical ground reaction force and peak plantar pressure during running

Running is one of the most common daily routines incorporated in an athlete's training programme. Depending on the running speed, each foot is off the ground between 70 and 80% of the time during gait [52]. While on the ground (i.e. during midfoot strike or push-off phase) the peak vertical ground reaction force experienced on each foot can approach more than twice body weight (i.e > 1600 N for an individual weighing ~ 85kg) [52, 53]. This value is further increased when performed on a hard surface combined with sport-specific movements such as stopping and braking [54]. Figure 1.5 shows the comparison between the vertical and horizontal ground reaction forces obtained from the same subject running at 3m/s. It can be seen that the horizontal ground reaction force experienced by the subject is considerably lower than the vertical ground reaction forces with a magnitude of approximately 13 times.

The large magnitude of vertical force may not be damaging when subjected to the entire plantar region of the foot. However, during midfoot strike and push-off phase, the plantar pressure resulted from the vertical ground reaction force was only distributed laterally across the forefoot region. The presence of bony prominences over this region substantially increase the peak pressure experienced by the plantar skin. Hennig & Milani [55] reported an in-shoe peak pressure of as high as 1018kPa under the first metatarsal head with a relative load of 26.5%. This is in agreement with a study carried out by Hayafune *et al.* [56] looking at the distribution of plantar pressure during walking where they found that the first and second metatarsal heads and the hallux shared 64% of the total load during the push-off phase. They reported a peak pressure value of 373 ± 172kPa under the first metatarsal head, accounting for 29.1% of the body weight.

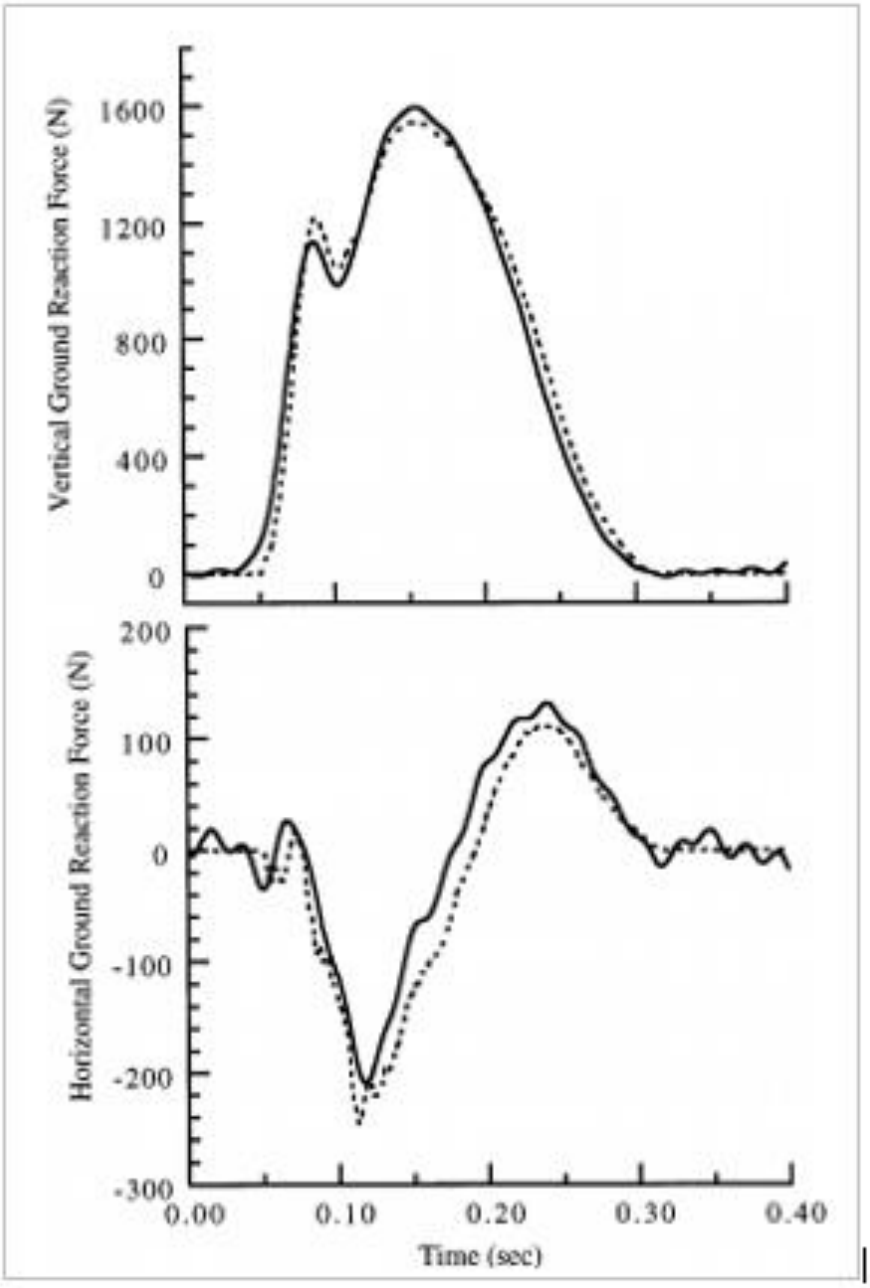

Figure 1.5: The vertical and horizontal forces experienced by each foot during running (image reproduced and adapted from [57]).

1.6 Friction blister formation

The skin has a unique protective mechanism that enables it to respond and adapt to the repetitive mechanical stress such as pressure, impact forces, shear, and friction [58, 59]. For example, as we grow older, our plantar skin becomes much thicker compared to our abdominal and facial skin since it is subjected to continuous trauma throughout our lives. Besides the physiological [60] and environmental factors, the degree of skin response and adaptation relies on the following factors [46, 61]:

1) the type and direction of the mechanical stress applied;
2) the magnitude of the mechanical stress applied per unit area of the skin;
3) the duration and rate at which the mechanical stress is applied.

However, during running the mechanical trauma may exceed the skin protective capability threshold and result in dermatological injuries such as friction blisters. As described in section 1.5, when the foot makes initial contact with the ground during running, the impact forces can reach of two to three times body weight [52, 62]. During this contact phase, the pressure distribution across the plantar skin in contact is affected by the design and fit of the shoe. The contact forces are partly translated into a shear component, causing a cyclic shear stress to be exerted to the plantar skin surface. The friction between the foot-sock interface and the normal pressure distribution limit the level of shear that can be applied. Initially, the outermost layer of the skin, the stratum corneum, will just be abraded due to skin desquamation (also known as shedding).

However, during prolonged loading, as the repeated shearing cycles persist, the forces are transmitted to the deeper epidermal layer. Once the surrounding tissues are unable to withstand the amount of forces which have been intensified beyond the threshold point, micro-tears start to occur within the stratum spinosum [60, 61, 63]. The number of micro-tears increases whilst the existing tears enlarge and begin to combine. Eventually, the stratum spinosum is separated from the stratum basale forming a vesicle, resulting in friction blisters [46]. The vesicle then fills with fluid [61] which has similar electrolyte compositions to the serum but only about one-third of the serum protein concentration [64]. The other three

epidermal layers on top of the stratum spinosum (stratum corneum, stratum lucidum and stratum granulosum) remain intact to form the blister roof [3, 61].

The recovery process is initiated in about 6 hours after blister formation as the cells in the blister base begin to absorb the amino acids and nucleosides required for the 'repair'. High mitotic activity can be detected at the base cells within 24 to 30 hours, followed by the formation of new granular layer at 48 hours. Finally, a new stratum corneum is visible by day 5 [61, 63, 65].

1.6.1 Risk factors contributing to blistering

The severity of blistering varies depending on the magnitude of the combined forces, the skin location, contact parameters and the environment as reported by Herring & Richie [66]. They found that 60.2% of the blister incidences occur in the forefoot region compared to the midfoot and rearfoot regions with 33.3% and 6.5% respectively. This can be linked to the high peak plantar pressure experienced by the forefoot region, as described earlier in section 1.5.

There are several factors that have been identified as influencing the probability of blister formation. These can be categorised as intrinsic and extrinsic factors. Intrinsic factors are defined as variables related to the subject himself/herself such as skin condition, moisture level, poor biomechanics, foot type and deformities. On the other hand, extrinsic factors are variables not related to the essential nature of the subject himself/herself which include the magnitude of normal and frictional forces, number of shear cycles, poorly-fitted footwear. These factors are further elaborated in Tables 1.2 and 1.3 respectively. Sulzberger *et al*. [61] further suggested that blisters may be readily developed if the skin area fulfils both of the following pre-requisites:

- The stratum basale is firmly anchored to the underlying dermis which will allow shearing to occur, thus creating an intra-epidermal cleavage (zone of damage);
- The stratum corneum is thick and more resistant to superficial abrasion compared to 'thin' skin such as the abdominal, thighs and forearms. Therefore, the shearing will be translated into the deeper epidermal layer and lead to blistering

It can be hypothesised that reducing one or more risk factors could dramatically reduce the probability of blister incidence and severity.

Table 1.2: A summary of qualitative correlations between the intrinsic risk factors and probability of blistering.

Intrinsic risk factor	Qualitative correlation	Reference(s)
Skin condition	Diabetic patients with peripheral neuropathy are more susceptible to blisters due to poor blood circulation resulting from nerve damage. Hyperhydrosis (excessive sweating) is also thought to increase susceptibility to blisters	[67]
Moisture level	Dry skin has been shown to reduce friction, whereas moist skin has been shown to increase friction due to increase in contact area resulted from suppler skin	[38]
Poor biomechanics	People with poor biomechanics tend to have non-uniform plantar pressure distribution, which when combined with excessive shearing will lead to blistering	-
Foot type	People with flat feet (pes planus) and high-arch feet (pes cavus) have higher incidence of blisters due to non-uniform pressure distribution across the feet	[65]
Foot deformities	The vertical plantar pressures against the metatarsal heads and calcaneus are dramatically increased in patient populations with foot deformities such as hallux valgus, diabetes mellitus with neuropathy and rheumatoid arthritis	[68]
Body temperature	An increased in body temperature, such as from vigorous activities, may evoke sweating. Profuse sweating increases moisture build-up within an in-shoe environment which could then increase the likelihood of developing blisters	[45]

Table 1.3: A summary of qualitative correlations between the extrinsic risk factors and probability of blistering.

Extrinsic risk factor	Qualitative correlation	Reference(s)
Intensity of activity	High-intensity activities put an individual at increased risk for developing blisters due to the increased impact forces.	[65]
Duration of the activity	Long-distance runners tend to have much higher chances of developing blisters than 100-metre runners	[4]
Additional load	Heavy loads increase the pressure acting on foot skin which over prolonged duration could increase the likelihood of blistering	[69, 70]
Improper footwear	Poorly-fitted footwear causes the anterior of the foot to slip and displace within the shoe. This could result in an increased shearing which has been shown to increase skin susceptibility to blistering	[71]
Type of socks	Acrylic socks with additional padding and double-sock systems have been proven to reduce blister incidence and severity among runners	[66, 72]
Lubricants application	Applying lubricating agents increases the friction coefficient and blister incidence significantly after 3 hours of its application	[65, 73]

Among the identified risk factors, increase moisture levels within the shoe primarily due to high level of perspiration and humid environment has been shown to be the most critical factor that poses additional risks to developing blisters. It has been reported that an athlete may evoke sweat losses of nearly three litres per hour during a long run in a warm and humid environment, resulting in approximately 10% reduction in body weight [74]. Presence of water in the skin-sock interface and moisture build-up in the stratum corneum [75] could strongly influence the skin friction. A significant increase in friction was observed when rubbing wet skin against dry fabrics, with larger increases being found for hairy skin (such as the forearms and thighs) compared to glabrous skin (palms and plantar surfaces) [76]. A study by Tomlinson *et al.* [34] (not using fabrics), found an increase in skin-surface

friction coefficients in a humid environment and attributed them to physical mechanisms including water absorption and capillary adhesion due to meniscus formation. In addition, the authors concluded that the effect due to viscous shearing of liquid bridges formed between the skin and the interacting surface was negligible.

Elevated temperature at the skin surface during rigorous sport activities where the feet are subjected to repeated rubbing could also increase the skin moisture levels through sweating. This is more prominent for shoes with poor air-permeability that create a barrier for heat transfer [74]. Sweat from the body will vaporise into the atmosphere much quicker compared to the sweat accumulated within an enclosed shoe environment. This will increase the presence of moisture at the plantar skin-sock textile interface and in return influence the friction [31, 34, 77]. It is therefore important for sock fabrics to have the capability to "wick" and transport the moisture away from the plantar skin into the external environment [78]. Furthermore, accumulated moisture at the plantar skin-sock textile interface has potential to bridge air gaps between fibres which subsequently increases the contact area between these two surfaces. This could lead to an increase in the friction and/or cause lubrication [3], in addition to influencing the thermal resistance and thermal conductivity of the sock fabrics [79].

The socks should not generate additional shear force at skin-sock textile interface since this could have a negative impact on the range of movement and could even potentially lead to friction blisters [3, 80], which introduce potential discomfort to the wearer [80].

1.6.2 Previous experimental investigations on friction blisters

There were few restrictions in using human subjects to conduct in-vivo blister studies between late 1950s and 1980s which allowed researchers to recruit as many people as they needed to be subjected to temporary pain and injury for the purpose of research. Naylor [46] was the first to publish a quantitative study on experimental friction blisters in 1955 after discovering the effect of varying moisture degree on the skin COF just a few months earlier [38]. The results obtained from this study confirmed his earlier study that both extremely dry and wet skin conditions resulted in a high value of COF in comparison to moist (intermediate

degree of moisture) skin. However, a study by Cua *et al*. [29] in 1990 did not fully concur with Naylor's conclusion as the authors found slight variations for the lower back and dorsal forearm.

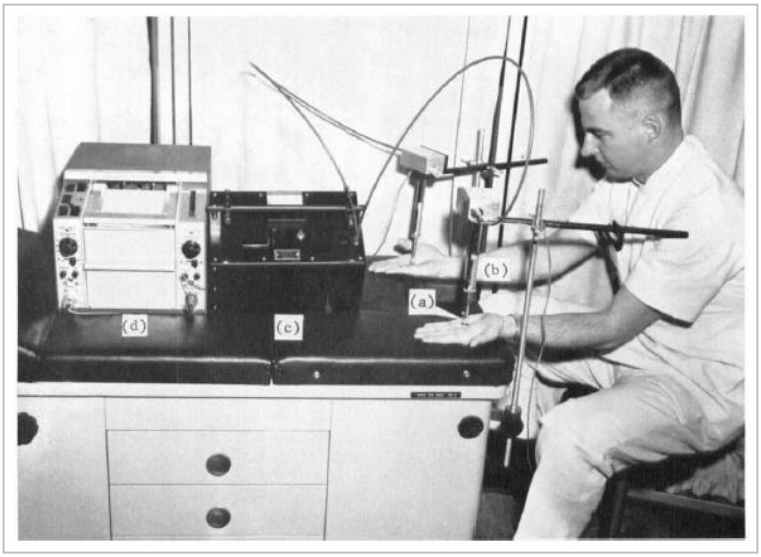

Figure 1.6: The experimental set-up modified from [38] , and used to create blisters in-vivo. The apparatus is capable of administering linear and twist rubbing onto the palmar surface of the volunteers (image reproduced from [61]).

The next definitive friction blister study was conducted by Sulzberger *et al*. [61] in 1966 and the authors found that blistering only occurred on the palms and soles. The most recent controlled in-vivo blister study was conducted by Hashmi *et al.* [45] by incorporating digital infrared thermographic imaging into the experimental apparatus as shown in Figure 1.7. The authors reasoned that the thermographic images could be useful in assessing temperature changes during blister formation without having to contact the foot skin (non-invasive assessment method). It was found that the temperature change on the test site from baseline to the onset of blister development is 5.1ºC. An immediate reduction in temperature was seen over a period of 60 minutes post-blister testing, which later gradually decreased to 0.8ºC slightly above the baseline reading. An ultrasound device was used to confirm the blister formation on the test site.

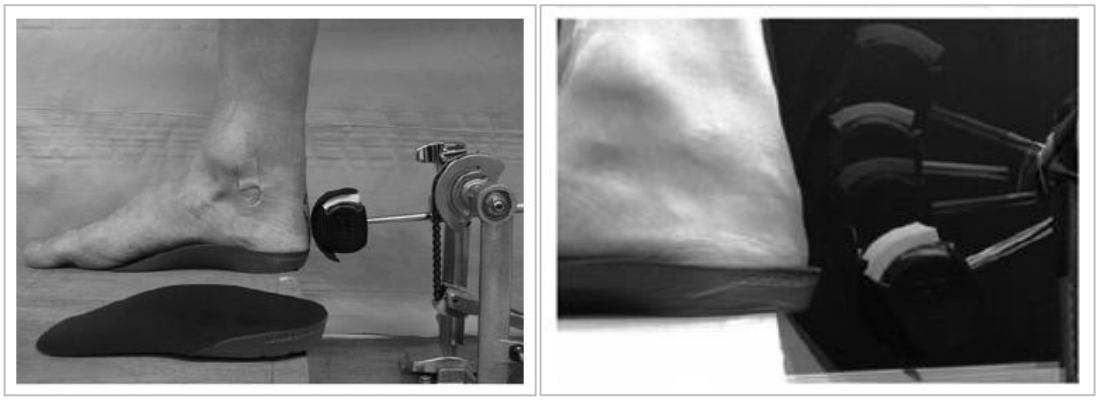

Figure 1.7: shows the load application mechanism used to manually apply a compression load of 70kPa on the posterior aspect of the heel (images reproduced from [45]).

1.6.3 In-silico investigations on friction blisters

In-silico modelling is a very useful and versatile tool that allows engineers to simulate and study realistic events which are usually rather difficult or impossible to be carried out physically. This is especially beneficial in skin tribological research which normally encompasses a wide range of skin physiological and frictional variations. A number of assumptions and model simplifications are always necessary in order to not over-complicate the model but the predicted results obtained from finite element simulation can be highly-comparable with the real case. Pan *et al.* [81] conducted a series of in-silico studies looking at blister deformation and stress under walking and running loading conditions. The authors' work employed a dynamic non-linear finite element model and assumed the skin to be hyperelastic, the muscles to be isotropic and elastic, and the bone to be a rigid body.

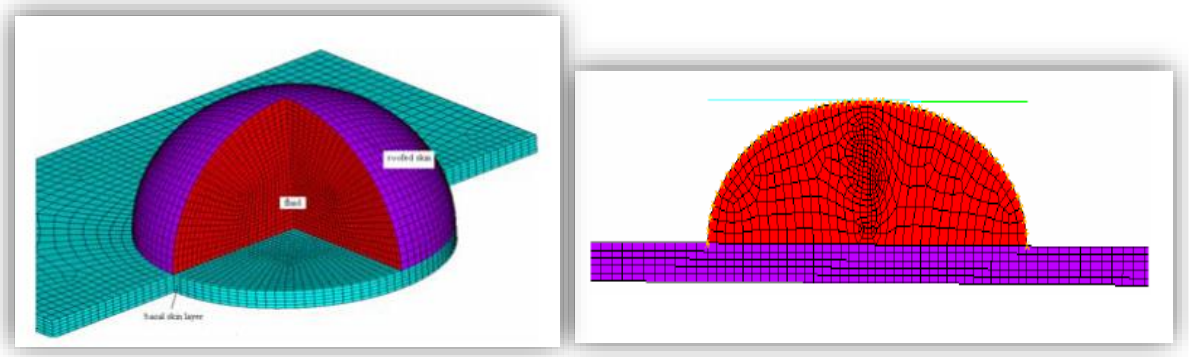

Figure 1.8: The three-dimensional (left) and two-dimensional (right) FE models of blister with radius ratio of 0.9 and 0.5 respectively were generated to study fabric-skin interactions (images reproduced from [81]).

1.6.4 Synthetic test-beds

Obtaining ethical approval before performing any tests on human subjects can be a difficult and time-consuming process. Furthermore, every individual does not produce similar response to mechanical stimulus which could be attributed to various reasons, including but not limited to, the difference in genetic makeup, medical conditions, gait, choice of footwear, and activity levels.

Guerra & Schwartz [1, 82] were the first researchers to develop a synthetic blister model, named the Synthetic Skin Simulant Platform (3SP), that serves as a research platform for friction blistering tests. The 3SP is made of a three-layer composite of elastomeric material to simulate the layered skin structure as shown in Figure 1.9 below and Table 1.3 summarizes what each layer of the 3SP represents and the type of materials used. The authors found that the blistered samples exhibit a similar appearance to skin blister, with the layers separation occurred between the epidermal simulant layer (ESL)-dermal simulant layer (DSL) interface. The degree of the blister area and severity of the surface damage were also found to correspond with the friction force. Higher friction force resulted in a larger blister area and severe surface damage. However, justifications on the choice of silicone materials used were not provided. Furthermore, the authors did not specify which part of the human skin was simulated by the 3SP model, hence making results validation and comparison impossible.

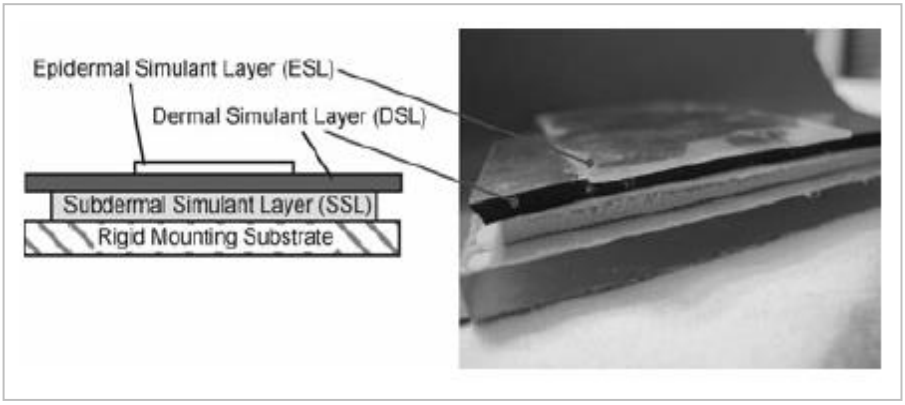

Figure 1.9: The 3SP layers developed by Guerra & Schwartz (image reproduced from [1]).

Table 1.4: A summary on the element of 3SP (information extracted from [1]).

Element of 3SP	Simulating role	Type of material / adhesive	Material thickness (mm)	Shore Hardness
ESL	stratum corneum	silicone rubber	0.8	40 A
ESL-DSL interface	dermal-epidermal junction	methyl-ethyl-ketone adhesive	-	-
DSL	dermis layer	polyurethane elastomer / neoprene rubber	3.18	40 OO / 30 A
DSL-SSL interface	-	silicone-based adhesive	-	-
SSL	tendons, muscles and fat	latex rubber	3.18	35 A
SSL-rigid mounting substrate interface	-	silicone-based adhesive	-	-
Rigid mounting substrate	-	paper-backed acrylic plate	-	-

An artificial fingertip made of a type of silicone rubber was constructed by Shao *et al.* [83] to be used in tactile measurements. The artificial fingertip has similar geometry and softness as human fingertip. The development of the artificial fingertip was then evaluated in terms of its deformation and friction properties against fifteen surfaces with varying degree of surface roughness. They found that the artificial fingertip exhibited different friction characteristics than a human fingertip due to the high adhesive shear stress it experienced during the sliding test. In comparison with the 3SP model study, this study provides a more

systematic approach in developing and testing synthetic skin models. The development of the biofidelic prototypes, described in Chapter 5 of this thesis, follows similar systematic approach conducted by Shao *et al.* [83], which allows comparisons to be made between the prototypes and human first metatarsal head.

1.6.5 Fabric friction measurement methods

Different types of fabric possess different degree of frictional properties depending on their nature of fabric, materials composition and knit pattern. This in return could influence the fabric performance in terms of its quality and comfort. There are two classical methods of measuring fabric friction: unidirectional and multidirectional methods.

The unidirectional method is the most commonly used measuring method consisting of a probe rubbed against the tested fabric which is fixed on the horizontal platform. The probe is connected to a sensor that allows the desired force to be applied. The Kawabata Evaluation System is one of the devices that operates based on this measuring method [84]. It has been widely used since the 1980s to assess the friction and roughness properties of fabrics in various loading conditions: compression, pure bending, tensile and shear [85, 86].

Bueno *et al.* [87] found that the Kawabata Evaluation System was not sufficiently appropriate to characterise the effects of finishing treatments on fabric friction and later developed a multidirectional tribometer. Unlike the unidirectional method, this device allows the friction of the fabric to be evaluated in all directions relative to its surface.

1.7 Aims and objectives of the thesis

The aims of this study are two-fold:

1) To evaluate the tribological interactions between the skin-sock interface and the interplay of contact and moisture parameters contributing to blistering

2) To design and develop biofidelic test-beds that closely match the mechanical and frictional properties of plantar region of the first metatarsal head. These test-beds are physical skin models that can be used in future friction blister studies

The main objectives of the study were to:

1) establish a friction methodology to assess the frictional behaviour between the skin-sock interface. This will include a moisture control and management protocol
2) devise a standardised protocol for the foot friction testing
3) assess the friction between the plantar aspect of the first metatarsal head (1MTH) and selected sock fabrics in different moisture conditions, using human participants
4) design and develop a range of biofidelic test-beds that closely-resemble the mechanical and frictional properties of the 1MTH plantar region
5) assess the friction between the biofidelic test-beds and selected sock fabrics in different moisture conditions
6) validate the biofidelic test-beds using the human friction data and recommend potential uses of these findings

The findings obtained from this study will contribute to existing knowledge gaps that are required in understanding plantar skin friction and friction blisters.

1.8 Structure of thesis

This thesis has been organised into six chapters that outline the key concepts of this study, as illustrated in Figure 1.10.

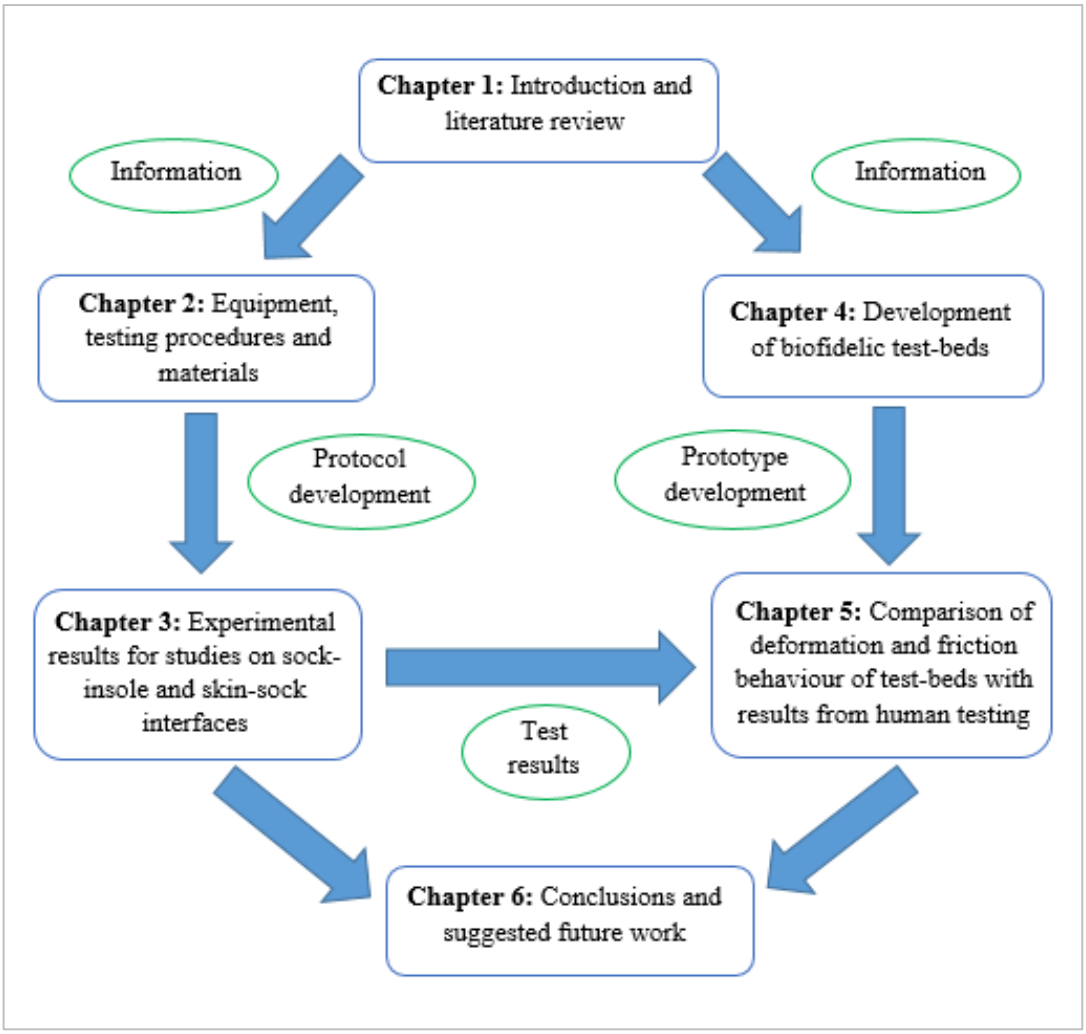

Figure 1.10: The key concepts outlined by each chapter of this thesis.

Chapter 1 presents a detailed review of the relevant literature and encompasses the fundamental concept of skin anatomy, skin friction, and skin mechanical properties. The later part of this chapter will also include a thorough review of foot friction blisters and various experimental techniques used for measuring skin friction and mechanical properties in previous studies.

Chapter 2 outlines the established testing protocols used in the human participant friction experiments as well as the equipment utilised to accomplish the purpose of this study.

Chapter 3 presents the experimental results obtained from the friction studies on sock-insole skin-sock interfaces. A novel moisture management protocol was established and was presented at the 12th biennial Footwear Biomechanics Symposium (FBS) of the International Society of Footwear Biomechanics Group and published in '*Tasron D, Maiti R, Hemming M, Lewis R, and Carré M. Investigating a methodology to measure moisture in skin–textile friction experiments. Footwear Science. 2015; 7(sup1): S15-S6 [88]'*.

Two different foot-sock friction methodologies were also investigated in order to select the most appropriate methodology for the friction investigations in this study. The outcome from this work was presented at the 11th conference of the International Sports Engineering Association (ISEA) and published in '*Carré M, Tasron D, Lewis R, and Hashmi F. Investigating foot-sock friction: A comparison of two different methodologies. Procedia Engineering. 2016;147:759-64 [89]'.*

This chapter also includes detailed experimental studies on the plantar skin against five different types of running socks. The outcome from this study was presented at the 7th Asia-Pacific Congress on Sports Technology (APCST) and published in '*Tasron D, Thurston T, and Carré M. Frictional behaviour of running sock textiles against plantar skin. Procedia Engineering. 2015; 112: 110-5 [90]*'.

The friction study was also carried out on the first metatarsal head in three different moisture conditions. The results from this study was presented at the 11th conference of the International Sports Engineering Association (ISEA) and published in '*Tasron D, Maiti R, Hemming M, Lewis R, and Carré M. Frictional interaction between running sock fabrics and plantar aspect of first metatarsal head in different moisture conditions. Procedia Engineering. 2016; 147: 753-8[91]*.

Chapter 4 describes the entire process involved in designing and developing a set of prototype biofidelic test-beds that closely mimic the mechanical and frictional properties of the human plantar aspect of the 1MTH.

Chapter 5 presents detailed comparisons of deformation and friction behaviour of the biofidelic test-beds with findings obtained from 1MTH skin-sock fabrics friction study.

Chapter 6 provides the main conclusions from this study in reference to the established objectives. The contributions of the thesis are also highlighted in this chapter along with a number of recommendations for future work.

Chapter 2

Equipment, testing procedure and materials

All equipment, testing procedure and materials that have been utilised and established are outlined in this chapter. Firstly, the sock materials used for testing throughout the PhD study are introduced. This is then followed by the descriptions of the development of two different devices used to measure the frictional behaviour of the plantar skin which include a foot friction rig and an instrumented foot loading device. The standard testing procedure used with respect to each equipment was also outlined. Additionally, this chapter describes the non-invasive commercial instruments used to monitor and assess various parameters related to skin such as the hydration level (using the Corneometer® CM825), temperature (using the Skin Thermometer ST500), deformability of the skin (using the Cutometer® MPA580) and skin topography (using an optical coherence tomography).

2.1 Friction equipment: foot friction rig (at The University of Sheffield)

Two approaches were used to measure foot-sock friction. The first approach used a foot friction plate rig adapted from a previous study [34], to measure the friction by sliding plantar skin against sock fabrics. It was developed at the University of Sheffield and includes two 50 kg-rated S-shaped load cells, capable of measuring the applied normal and friction forces as shown in Figure 2.1. A test plate was mounted on the rig to allow a sufficiently large sock test area while allowing the transmission of the normal and shear forces. The rig setup also includes a laptop installed with a LabView programme, a National Instruments hi-speed USB Carrier (NI 9162) and a National Instruments data acquisition card (N1 9237) as shown in

Figure 2.2. The NI 9237 combines the analogue and digital filtering to eliminate the noise and optimise the output signals.

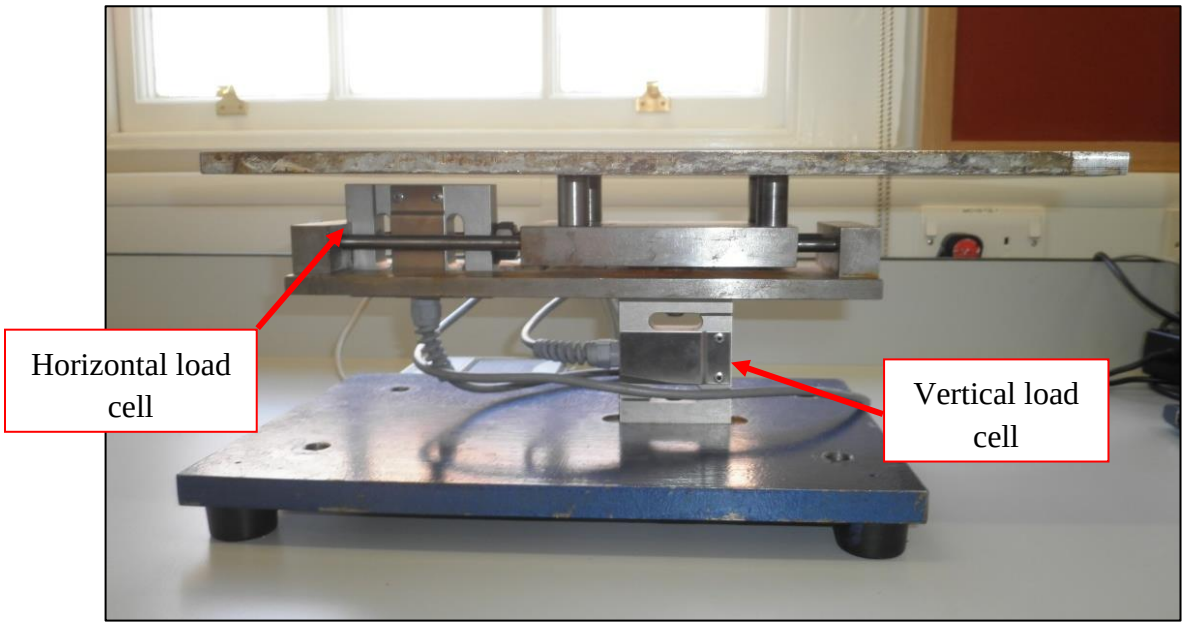

Figure 2.1: Foot friction plate rig. The vertical load cell measures the applied normal force whereas the horizontal load cell measures the friction force.

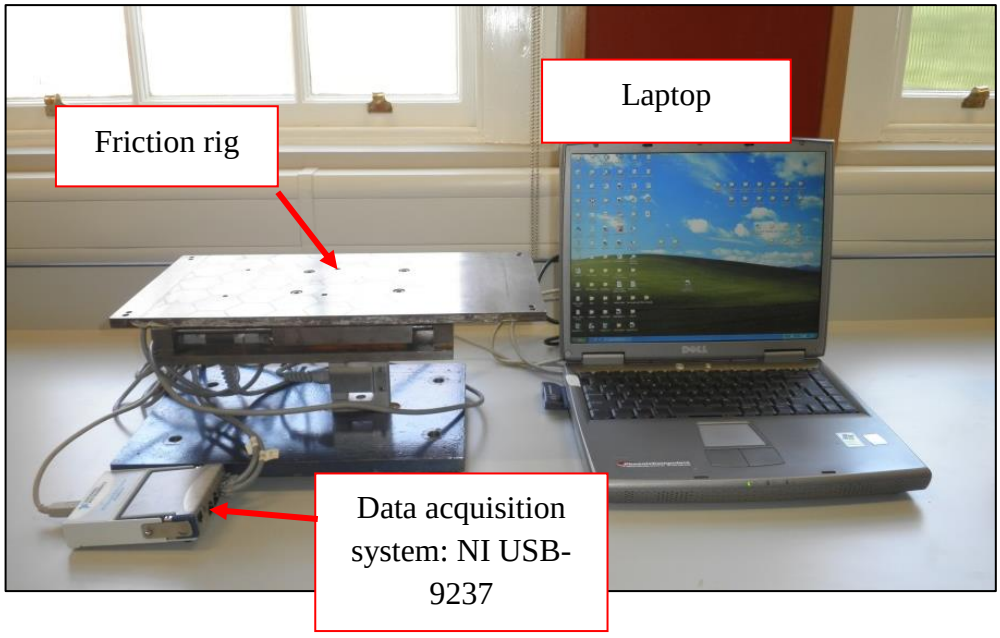

Figure 2.2: The foot friction rig setup.

2.1.1 Experimental procedure for foot friction rig

The sock materials were cut along the dorsal (top) line, opened out so that the inside surface of the plantar region was facing upwards, and stretched to approximately 50% level of strain in both vertical and horizontal directions before being secured to the rig plate with double-sided adhesive tape. This level of pre-straining had been selected based on the findings from the pilot study carried out to assess the effects of strain in sock fabrics on friction, which will be described in the following chapter. Anecdotally, the strain level was also found to reflect real-world conditions when the sock is being worn. In order to further prohibit any movement between the sock and the plate, clamps were also applied around the material sample perimeter, as shown in Figure 2.3. A test area of 102 mm×54mm was then marked on the plantar region of the sock to ensure that the sliding was performed on the desired region.

Participants were instructed to slide their feet across the plate. They needed to lift their toes throughout sliding to effectively isolate the 1MTH (see Figure 2.4). A friction test protocol was adapted from previous studies [34, 90, 92-95] whereby participants press their IMTH region against the test plate and then push their foot forwards across the sock surface, maintaining the initial level of normal load and a relatively consistent, self-monitored, sliding velocity. This process was repeated for a range of applied normal loads and this was observed and checked throughout testing.

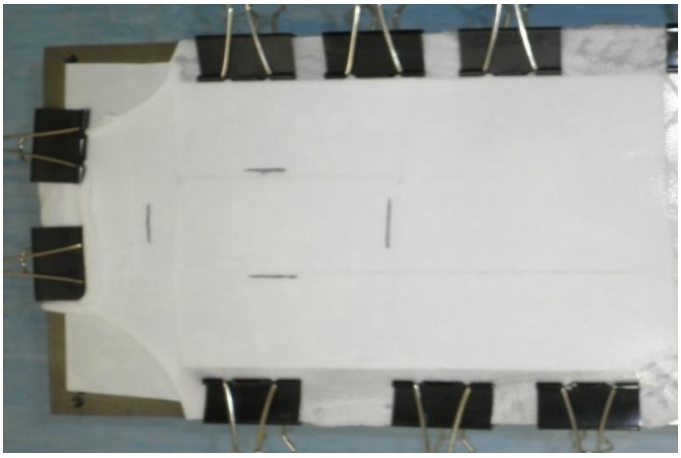

Figure 2.3: The set-up of the sock sample for friction testing.

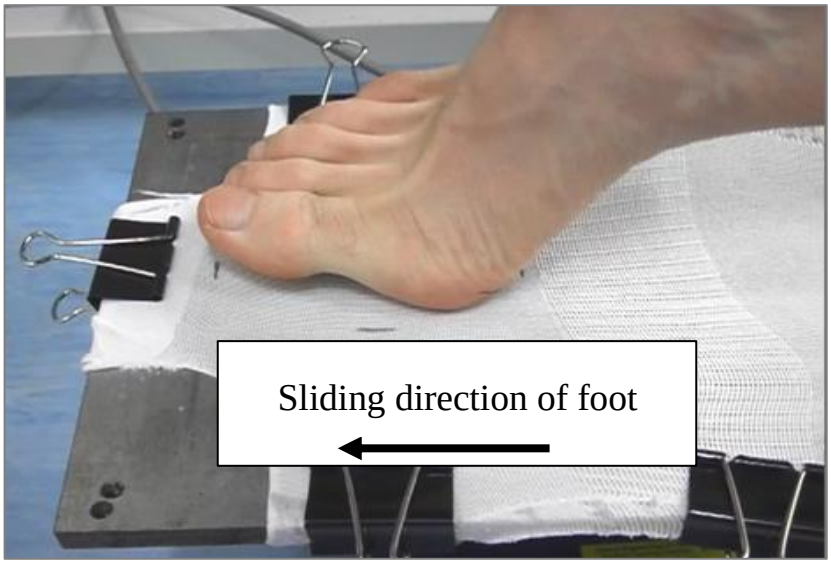

Figure 2.4: Friction testing conducted using the foot friction plate rig.

Figure 2.5 shows a typical example of raw force data collected from a participant using the foot friction plate rig. Both the applied normal load and friction force were plotted as a function of time to show the different phases of interaction as the 1MTH slid across the tested sock fabric. In phase (I) the applied normal (vertical) load and the friction force (horizontal) can be seen gradually increasing as the 1MTH is pressed on the plate and is then maintained by the participant. In this phase, there is no relative movement between the foot and the sock fabric. This is then followed by phase (II) whereby the friction force has reached a level able to overcome the limiting friction and the 1MTH begins to slide forward. The average of the stable, central region of both normal and friction forces data in phase (II) is selected to generate force values that relate to the dynamic coefficient of friction. The dynamic coefficient of friction (DCOF) is calculated by dividing the average friction force by the average normal force.

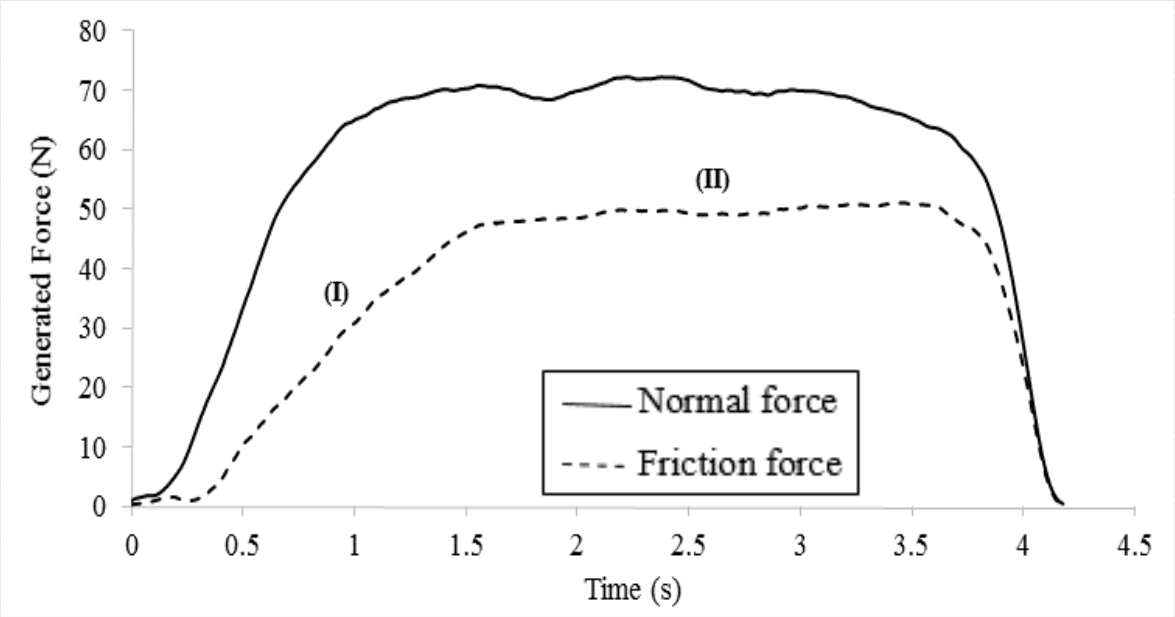

Figure 2.5: Typical force data output obtained from testing conducted using the foot friction plate rig.

2.2 Friction equipment: foot loading device (at The University of Salford, UK)

A second approach, an instrumented foot loading device, was also used to assess the friction interaction between the 1MTH and the sock fabrics. The device was designed and developed by Dr Farina Hashmi and Ciaran Wright (University of Salford) to apply repetitive compression and shear forces on plantar skin without relative sliding occurring. The device includes a compression actuator (SMC Pneumatics UK Ltd.), a compression load cell (Applied Measurements), a shear actuator (SMC Pneumatics UK Ltd.), a shear load cell (Applied Measurements) and an instrumented metal cylindrical probe, as shown in Figure 2.6.

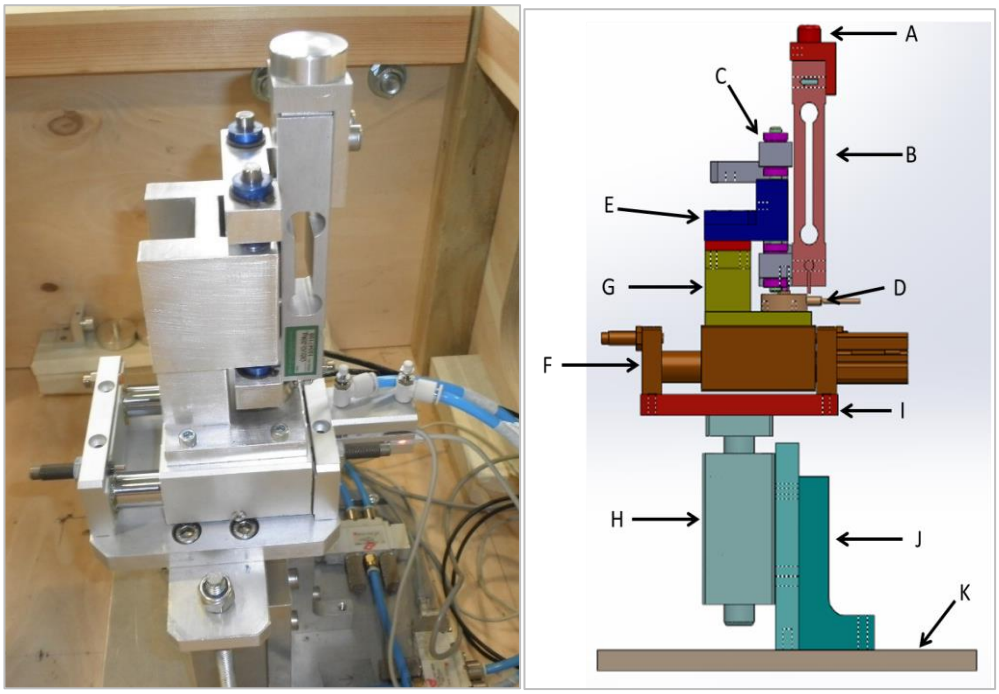

Figure 2.6: The foot loading device: A: instrumented probe; B: Shear load cell; C: slider; D: compression load cell; E: bracket; F: shear actuator; G: mounting plate; H: compression actuator; I: connecting plate; J: fixing brackets and K: base plate (The composite drawing on the right is reproduced from [96] with permission.)

The pneumatic actuators drive the cyclic motion of the probe and it is displacement-controlled through the use of two solenoid valves and a dedicated computer program, written by the research team at the University of Salford. In addition, the two load cells allow the compression (normal) and shear (friction) forces to be measured. The probe provides contact between the 1MTH skin and tested sock fabric, without interference from adjacent metatarsals. The ram pressure setting can be selected up to 0.75mbar to generate the desired range of applied compression loads on 1MTH.

2.2.1 Development of instrumented probe and platform

An instrumented probe was developed in order to apply the compression and shear forces against the 1MTH skin, simulating the same forward sliding foot movement as the friction testing conducted with the foot friction plate rig. In addition, it is important that the

instrumented probe has sufficiently large contact area to prevent it from digging into the skin during sliding as well as to provide sufficient area to mount the sock fabric on.

By using the 1 MTH peak pressure data and force values provided by Hayafune *et al*.[56], the contact area was determined to be 0.00052m^2, which was comparable to the contact area given by a 27 mm diameter probe which is 0.00057m^2 . The same probe was used throughout testing. A platform was also designed and developed to allow the participants to place their 1MTH over the instrumented probe. The platform was made of a sturdy wooden structure with two support rails for the Velcro straps that were used to position the foot in place. The entire set-up of the instrumented probe and platform is shown in Figure 2.7.

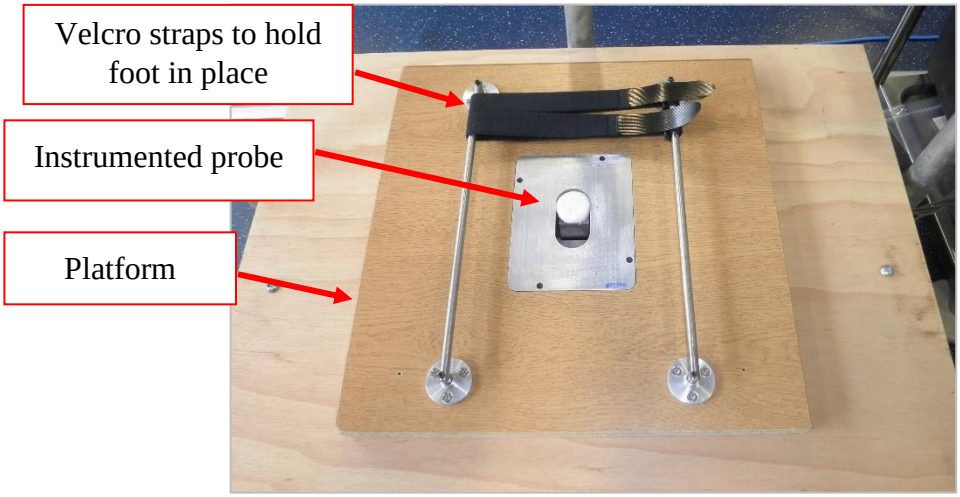

Figure 2.7: The platform and an instrumented probe used for the friction testing.

2.2.2 Experimental procedure for foot loading device

Participants were instructed to remain standing on the platform, as shown in Figures 2.8 and 2.9, with the probe pressed against the 1MTH region of the foot. Each sock material was stretched to approximately 50% strain (similar to the protocol used during friction testing using the foot friction plate friction plate rig) before being securely attached to the probe using double-sided adhesive tape. Straps were used to aid in the positioning of the participant's foot which also ensured that the conditions were consistent for repeated runs.

Initially, some trial runs were conducted and once the participant was familiar and comfortable with the procedure, and the foot positioning was deemed correct, the foot straps were applied.

When testing was initiated, the probe moved downwards away from the foot and was driven horizontally in the anterior-posterior direction for 250 mm. It was then driven upwards, making contact with the plantar aspect of the foot, before being driven in the posterior-anterior direction, whilst sliding across the 1MTH region. This motion made up one full loading cycle which was then repeated another time. Three different ram pressure settings of 0.2 mbar, 0.4 mbar and 0.6 mbar were used to generate a range of applied compression loads for different test-runs. For each pressure setting, the first two loading cycles were used to obtain data. Careful observation was made throughout testing to ensure that the probe contact remained in the 1MTH skin area for each sliding part of the loading cycle.

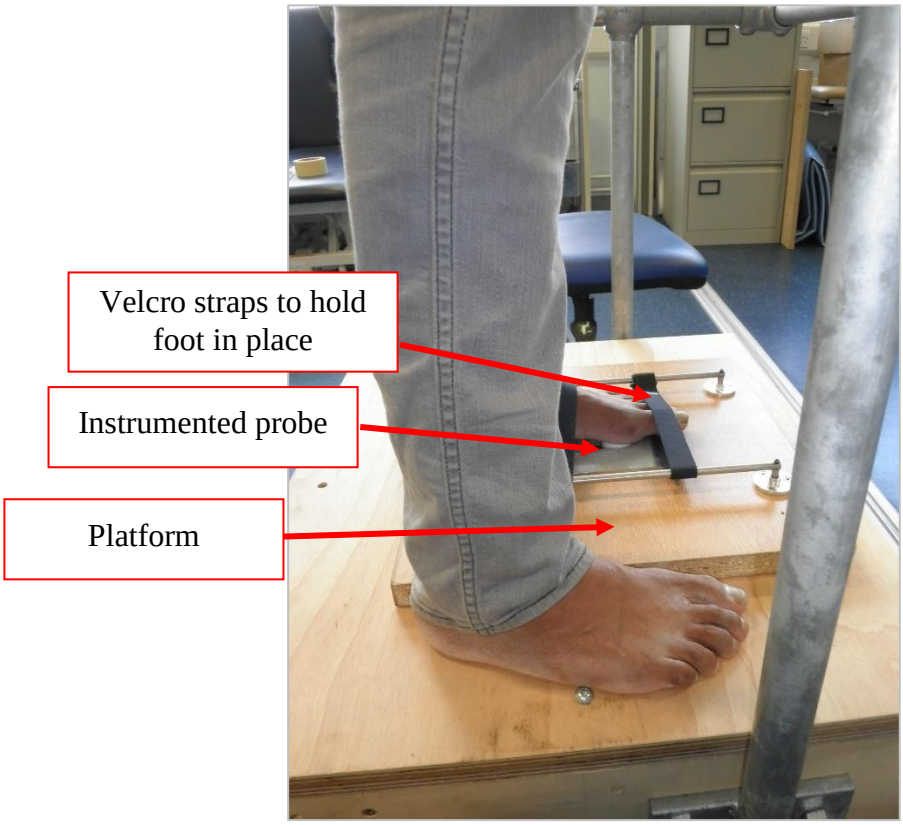

Figure 2.8: Participant standing on the platform whist placing the test foot on the instrumented probe.

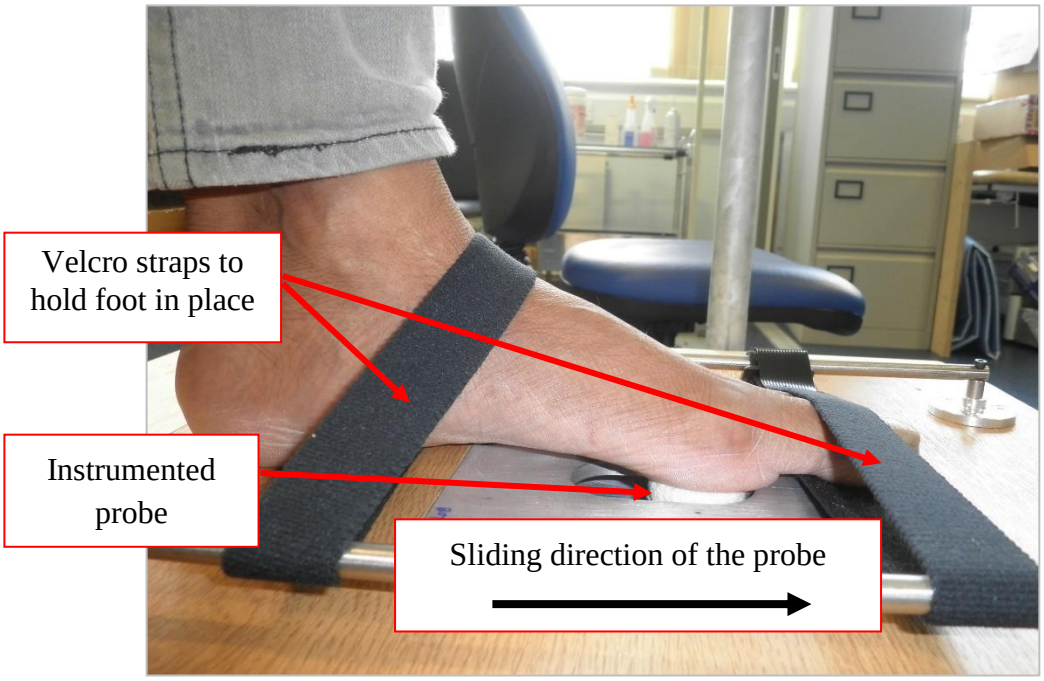

Figure 2.9: Friction testing conducted using the foot loading device.

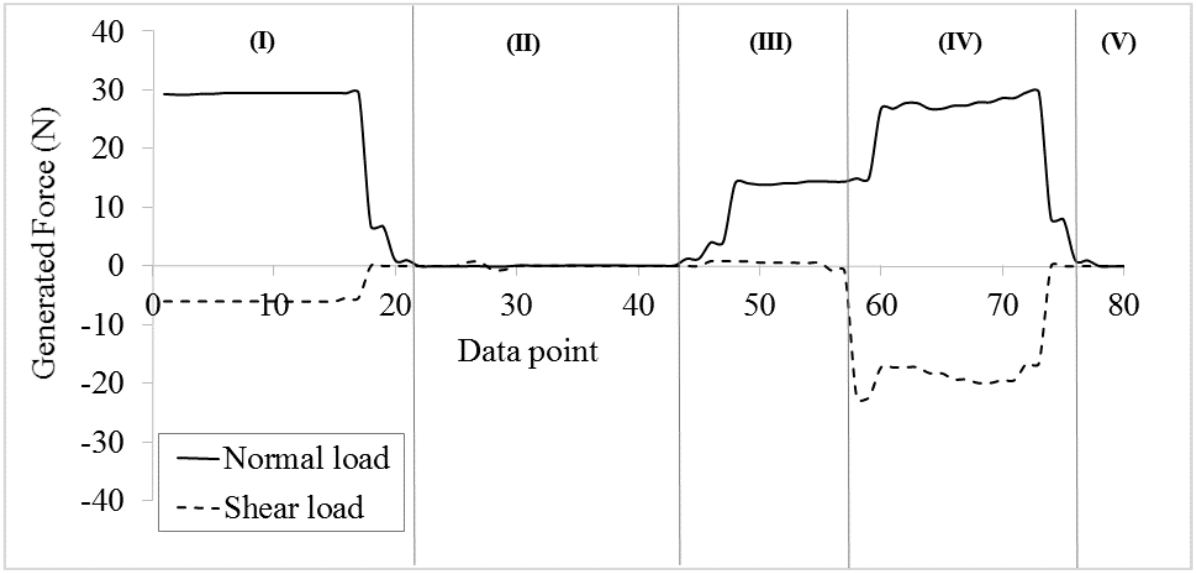

Figure 2.10: Typical force data output obtained from the friction testing conducted using the foot loading device.

Figure 2.10 shows a typical raw force data output obtained during testing using the foot loading device. The generated forces are shown plotted against the order of data point collected and can be divided into five different phases. The cyclic motion begins in phase (I) where the probe is pressed against the 1MTH region, before being moved away from the foot due to the unloading of the applied normal force. As the probe was driven towards the back of the foot, it was not in contact with the foot and therefore no forces were measured as indicated by Phase (II). Phase (III) shows the initial compression loading of the probe being pressed against the plantar aspect of the foot (more specifically at the rear of the 1MTH) before being driven horizontally by the actuator. In phase (IV), the probe actually began to move horizontally due to a relative constant shear load and the applied compression loading then increased further, thought to be a consequence of the probe sliding over the bony prominence in the 1MTH region. This general effect was seen in all the participants but to varying degrees depending on their respective anatomical variations. The probe was then unloaded in phase (V) and was made to repeat the entire cyclic motion (not shown in Figure 2.10).

Note that the transition between phase (I) and (II), where the probe is in unloading phase, is mirrored by the repeating action in the transition between phase (IV) and (V). In order to generate a dynamic coefficient of friction, the stable, central region of loading phase (IV) was used to obtain the average compression (normal) and shear (friction) force values. These values were then averaged with the measurements obtained from the second cyclic loading of the friction testing.

2.3 Skin characteristics equipment: Corneometer® CM825

Some commercially-available devices were used to monitor participant skin characteristics. The first was the Corneometer® CM825 (Courage and Khazaka Electronic, Cologne, Germany) used to measure and monitor the hydration level of the plantar aspect of the 1MTH as well as the tested sock fabrics at specific intervals throughout testing. The Corneometer® is widely used due to its ease of use and capability to monitor skin moisture using capacitance measurements [97]. Skin surface hydration changes the dielectric constant which alters the

capacitance of a measuring capacitor embedded in the probe head. The Corneometer® has also been shown to be capable of differentiating between dry and well-hydrated skin [98]. The measurement depth of the device is between 10 to 20 µm, ensuring that the measured reading only reflects the amount of moisture present within the stratum corneum layer without any influence from the moisture within the deeper skin layers (dermis and subcutaneous tissue). The moisture measurements are all reported in "arbitrary units" (AU) ranging from 0 to 120, where 0 indicates no moisture present whereas 120 indicates a maximum measurement according to the capability of the device.

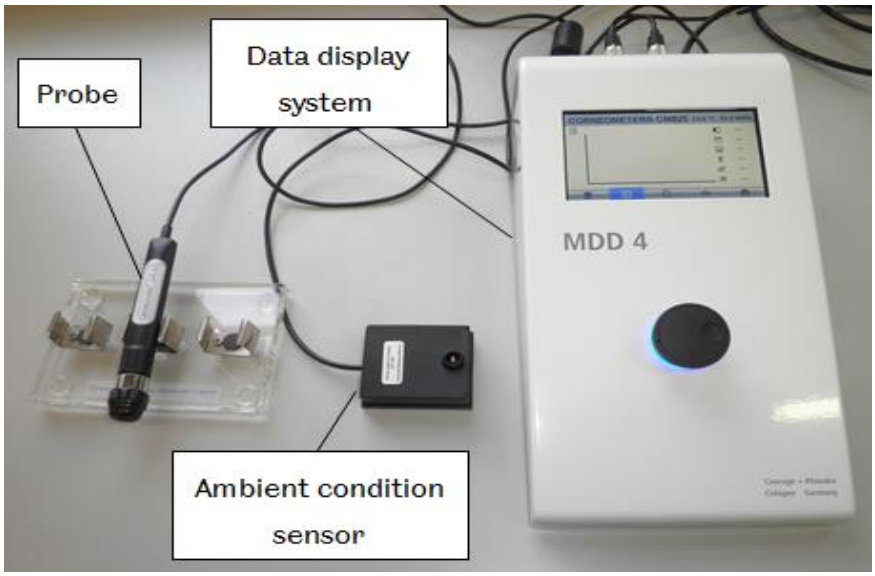

Figure 2.11: The Corneometer® CM 825 device.

2.3.1 Skin moisture control protocol using the Corneometer® CM825

Prior to any testing, participants were required to clean their foot that was to be tested for 1 minute using a room temperature water bath, to remove any contaminants and sock fibres. The foot was then dried with paper towels and allowed to acclimatise to room conditions for between 8 to 10 minutes. Hydration measurements were performed on the 1MTH region at specific intervals: 1) prior to cleaning; 2) after cleaning and acclimatisation; 3) prior to friction tests and 4) immediately after each friction test. The hydration readings taken after cleaning and acclimatisation were considered as the baseline foot hydration level and used

for subsequent analyses. Cleaning and acclimatisation was repeated before changing the sock materials, halfway through testing, to remove any sweat or contaminant build-up and ensure consistency.

2.4 Skin characteristics equipment: Cutometer® MPA580

A second skin test, the Cutometer® MPA580, was a non-invasive device used to measure the deformability of the upper skin layer using vacuum pressure which deforms the skin mechanically based on suction principle. The device consists of a handheld probe equipped with a suction head (available in 2, 4, 6, and 8 mm diameter aperture) and an operating unit which includes a vacuum pump that can generate intended pressure up to 500mbar. The skin was drawn into the aperture of the probe head with defined vacuum pressure. An integrated optical lens allows the absorption depth of the skin into the probe to be measured by converting the change in light intensity into millimetre (mm).

There are four different measuring modes offered by the Cutometer which are:

- Mode 1 – measurement with constant negative pressure
- Mode 2 – measurement with linear rising and falling negative pressure
- Mode 3 – measurement with constant followed by linear falling negative pressure
- Mode 4 – measurement with linear rising negative pressure followed by abrupt release of the negative pressure

Each mode gives different set of parameters than the others. Mode 1 has been widely documented in literature and the measurements obtained using this particular mode provide important insight of the skin mechanical properties. A study by Hashmi & Malone-Lee [99] also utilised Mode 1, in varying pressure settings of 100, 200, 300, 400, and 500 mbar, to evaluate and compare the elasticity between the weight-bearing and non-weight-bearing foot skin. The maximum displacement readings were then plotted against pressure. The non-weight-bearing dorsal skin was shown to have highest elasticity compared with the other two weight-bearing skin areas on the plantar skin. They also found that the displacement readings on average were overestimated with fairly low percentages of error for all tested skin sites.

Figure 2.12 shows a typical strain-time curve obtained from a human skin using the Cutometer® device. Each deformation parameter and its representation is briefly explained in Table 3.3.

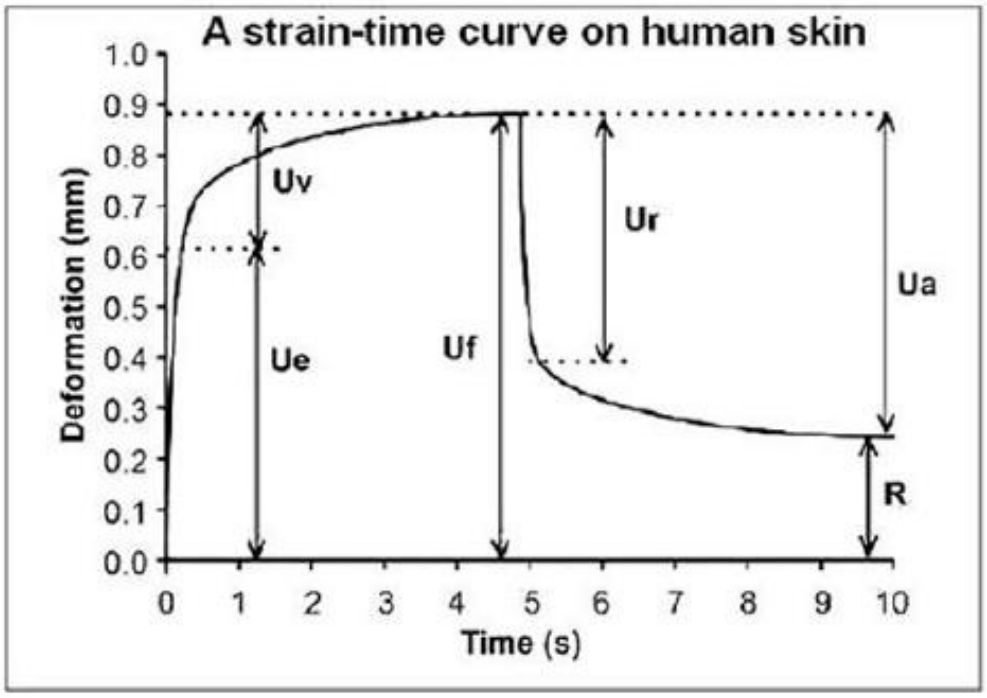

Figure 2.12: A typical strain-time curve obtained from the human skin using the Cutometer® MPA580 in Mode 1 (image reproduced from [12]).

Table 2.1: Deformation parameter and its representation obtained from [11].

Parameter	Parameter representation
Ue	Immediate deformation denoting the elastic component of the skin
Uv	Delayed deformation reflecting the viscoelasticity component of the skin
Uf	Maximal deformation
Ur	Immediate retraction
Ua	Final retraction after vacuum removal
Ua/Uf	Gross elasticity of the skin
Ur/Ue	Net elasticity of the skin
Uv/Ue	The viscoelasticity portion on the elastic region of the curve
Ur/Uf	Biological elasticity

2.4.1 Experimental procedure for Cutometer® MPA580

Similar to the skin moisture management protocol using the Corneometer® CM825, participants were first required to clean and acclimatised their foot to the room conditions. The Cutometer® probe was cleaned using a medical-grade alcohol swab prior to use to ensure that no contaminants will be transferred onto the test region. The test region was then marked to ensure that the exact same area can be tested. A probe with 8 mm diameter aperture was selected for the elasticity measurements to allow full deformation of skin to be measured. One full 60-second strain-time cycle, with 30 seconds under negative pressure of 500mbar and 30 seconds off-time, was used. The highest negative pressure setting of 500mbar was chosen for the measurements of the relatively thicker and stiffer plantar skin.

Figure 2.13: A Cutometer® probe in use to obtain elasticity measurements of the plantar skin.

2.5 Skin characteristics equipment: Optical Coherence Tomography (OCT)

Optical coherence tomography (OCT) is a non-invasive optical imaging technique widely used in the dermatology and medicine for diagnosing skin disease. OCT allows cross-sectional assessment of living tissues in real-time. The principle of OCT imaging is very similar to that of ultrasound imaging, which measures the delays in the echo time reflected by the acoustic waves. OCT, on the other hand, measures the time delays of the back-scattered infrared light and generates a two-dimensional image [100] with a lateral dimension of 6 mm and a penetration depth of approximately 2 mm [31]. Five sub-surface OCT images were obtained from a participant's 1MTH using a VivoSight system (Michelson Diagnostics). The measurements were performed before and after 1MTH friction measurements. An algorithm, with anisotropic filtering to remove speckle noise and prior knowledge of the multiple channel foci in the multi-beam, was used to measure the morphological parameters from the images which included the thickness of the stratum corneum (SC) and roughness of the outermost skin layer and the SC junction. This study was conducted in collaboration with Dr Raman Maiti.

2.6 Tested running sock materials

In order to assess the frictional interaction between the plantar skin against sock fabrics, a variety of running socks were required. Initially, for the preliminary study, five different

types of commercially available running socks were selected due to their differing material composition and knit patterns. The characteristics of these socks are given in Table 2.2.

Table 2.2: Characteristics of five different socks used in the preliminary studies.

Sock	Material compositions	Knit pattern
A	75% cotton, 17% polyester, 6% nylon, 2% elastane	Terry jersey
B	100% cotton	Simple jersey
C	40% wool, 31% cotton, 19% nylon, 8% elastane	Terry jersey
D	99% nylon, 1% elastane	Simple jersey
E	100% synthetic nylon	Simple jersey

The simple jersey and terry jersey are the most widely used knit patterns in running socks. The single jersey is usually formed with a single yarn of material, producing a relatively thin fabric. On the other hand, terry jersey uses a second yarn to create loops with the back yarns, producing a thicker fabric compared to the single jersey [3]. The difference between these two knit patterns are show in Figure 2.14.

(a) 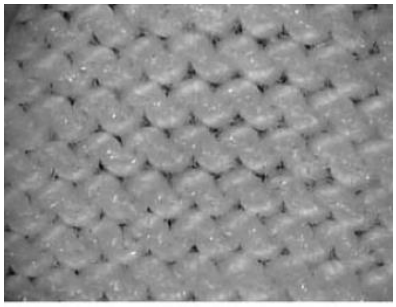 (b) 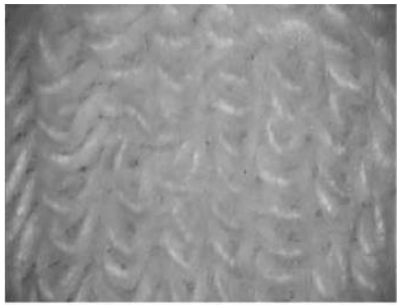

Figure 2.14: The two most commonly used knit patterns in running socks: (a) simple jersey and (b) terry jersey (images reproduced from [3]).

Upon completing the preliminary study, two out of five of these running socks were chosen to be used for further friction experiments which are a cotton-rich sock, Sock A and a predominantly nylon sock, Sock D. However, due to the limited availability of Sock A, an alternative sock was obtained and used. It was manufactured by the same manufacturer as

Sock A and was made of similar material composition and knit pattern. Table 2.3 provides the characteristics of the socks used for further friction testing.

Table 2.3: Characteristics of the selected socks used for further friction testing.

Sock	Material compositions	Knit pattern
Anti-blister "ABS"	99% nylon and 1% elastane	Simple jersey
Cotton-rich "CRS"	70% cotton, 29% nylon, and 1% elastane	Terry jersey

In order to reflect the real-world use, all newly-purchased running socks were hand-washed using water and a mild liquid detergent and left to air-dry at room temperature for at least 72 hours prior to the test. Pre-washing the socks ensured the removal of any contaminants trapped within the sock fibres as well as to maintain their dimensional stability.

2.7 Establishing a standard fabric moisture management protocol using the Corneometer® CM825

2.7.1 Introduction

It is widely known that natural moisture content in human skin and the presence of moisture at the skin-fabric interface can strongly influence the friction [31, 34, 77], as described in Chapter 1. However, it was noticed at the beginning of the study, that there was a lack of a standard moisture control protocol for textile experiments. This means that research in this area can be challenging to carry out and presents difficulties in comparing different studies. Presently, quantifying the change in the amount of moisture that has taken place within the fabric by weighing them pre- and post-test was the most commonly used technique by researchers [101]. In another study by Van Amber *et al.* [102] the socks were placed in a washing machine and submitted to a time-varying wetting cycle prior to testing to achieve damp socks (i.e. a technique adapted from a study by Laing *et al.* [103]). Although these two methods may have their own practical advantage in studies conducted in a small scale or in accordance to the standard textile testing procedure, they are not considered to be the most

time-efficient techniques for a large scale human testing. A large scale human testing may be defined as an experiment which involves a large number of participants (i.e. usually more than 10 people) and/or long-duration and complex testing procedures.

Therefore, a standard moisture control protocol is required to allow the same protocol to be easily implemented throughout the study thus ensuring consistency in the measuring technique and allowing comparison between studies to be made. A two-part pilot study was therefore undertaken to: (1) establish a moisture control protocol for fabrics, using the Corneometer® and (2) to assess the protocol in a participant study. It is worth to note that this study was not designed to evaluate the frictional performance of the tested sock materials.

2.7.2 Tested sock fabrics

The wool-rich (40% wool, 31% cotton, 19% nylon and 8% elastane) and cotton-rich (70% cotton, 29% nylon, and 1% elastane) socks were used for purpose of this pilot study. These socks were chosen due to the high percentage of hydrophilic fibres composed in the socks (i.e. cotton and wool) which will help to absorb and retain the added moisture. The characteristics details of the socks could also be found in Table 2.2 and 2.3.

2.7.3 Experimental procedure

In the first part of this study three specimens of each wool-rich and cotton-rich sock were prepared. The sock samples were mounted onto a rigid metal plate and water was applied to the inside of the plantar region using a spray bottle. The water was sprayed directly onto a targeted area of 40mm radius and each spray delivered approximately 1.4 ± 0.1 ml of water. Five Corneometer® readings were then taken in dry condition and also after applications of 1, 2, 3, 5, and 10 consistent sprays. The measurements were then averaged and plotted with standard deviations as displayed in Figure 2.15 below.

2.7.4 Results and discussion

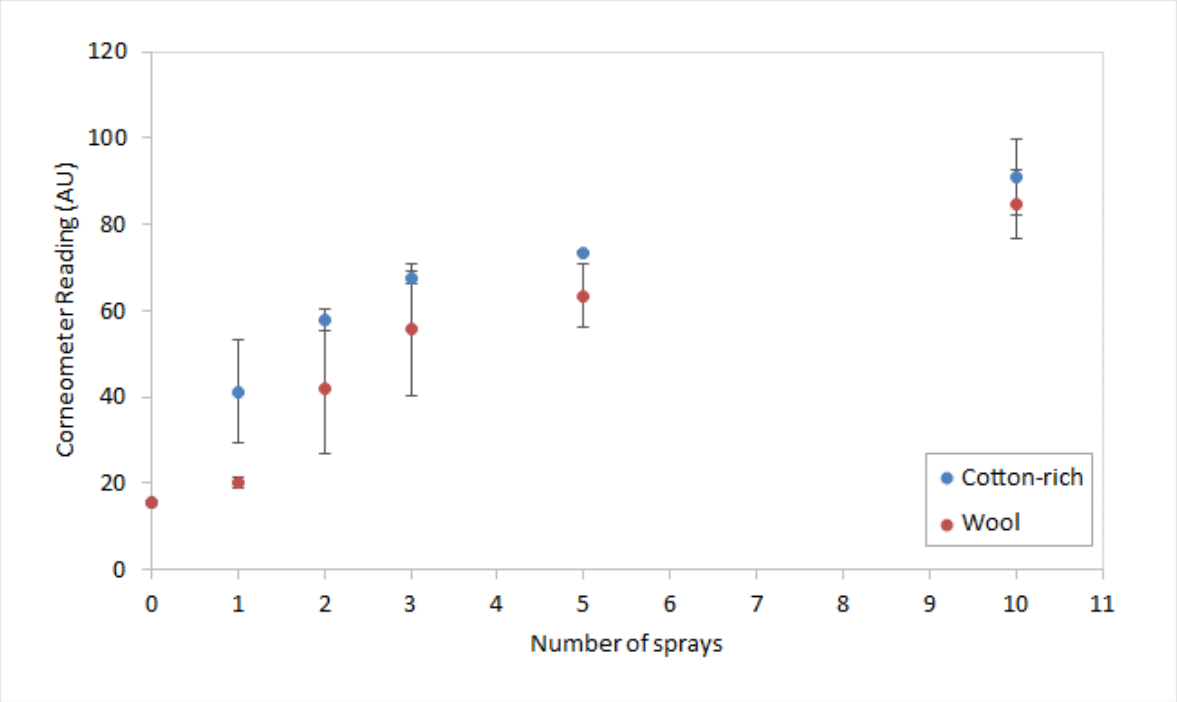

Figure 2.15: The Corneometer® readings obtained in relation to the number of calibrated sprays.

It can be seen that in dry condition, both sock materials gave similar Corneometer readings, indicating that the results were not influenced by differing capacitance values of the materials compositions themselves. The Corneometer readings steadily increased with the number of sprays and showed relatively similar trend for both types of socks. These findings suggested that the Corneometer® CM825 device can be used as a reliable indicator to quantify the amount of moisture in sock fabrics.

This protocol was then further assessed in the second part of the study where two healthy subjects (one female aged 26 and male aged 31) were recruited to complete a running session that included three running sessions of 15-, 30-, and 45-minute duration. It should be noted that since the objective of this study is to measure moisture accumulation in the socks, the speed of running was not measured. Both subjects were only required to run continuously at their comfortable pace for the targeted duration. Prior to running, subjects were required to clean their feet with room temperature water and let them acclimatised to the room

conditions for 15 minutes. Subjects were then instructed to wear a wool-rich sock on one foot and a cotton-rich sock on the other. Both feet were then wrapped with cling film and plastic bags to induce maximum sweating throughout the running duration. A total of 10 Corneometer readings were then obtained on the dorsal and plantar regions of the socks, pre- and post- each running session.

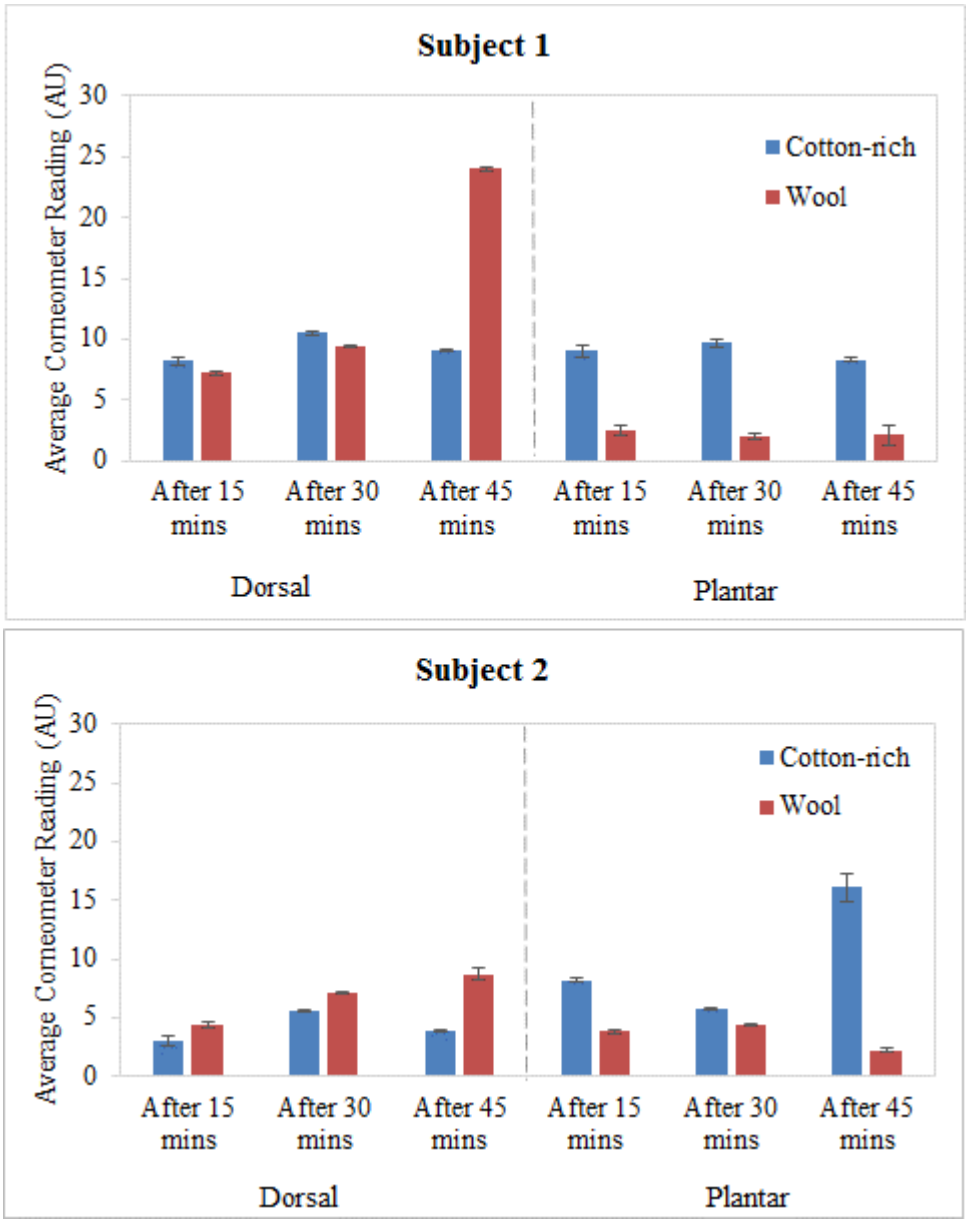

Figure 2.16: The Corneometer® readings obtained from each sock material after respective running bout: (Top) Subject 1 and (Bottom) Subject 2.

Figure 2.16 shows the average Corneometer readings obtained from both sock materials after each running session, for both subjects. The error bars represent the standard deviations of the data sets. It can be seen that the moisture levels of the sock materials were at the lower end of the Corneometer scale even after a 45-minute run. It can also be deduced that Subject 1 produced higher moisture level on the dorsal part of the sock compared with Subject 2, suggesting that different individuals vary in the way they regulate moisture within a shoe environment.

From this two-part pilot study, it can be concluded that the Corneometer shows promise as a methodology to monitor moisture change within a sock fabric. When compared with the benchmark technique of weighing the sock before and after testing, this newly-established protocol, which has been implemented and demonstrated in the following studies [90, 92-94], was found to be the a quicker approach in measuring moisture levels in both human skin and sock fabrics. In addition, the software used with the Corneometer allows the measurement data to be recorded automatically onto the computer, hence eliminating the need to manually record them. Since the moisture in skin and sock fabrics evaporates into the atmosphere over time, the quick Corneometer approach may be able to provide more accurate representation of the moisture amount as it allows a high number of measurements to be taken within a short window of time.

Chapter 3

Experimental results for studies on sock-insole and skin-sock interfaces

Current knowledge on the sock-on-insole and plantar skin-on-sock interactions is still very limited despite extensive advancement in both skin tribology and textile research areas. Progress in plantar skin research may have been hindered by the challenges in obtaining quantitative physical properties such as coefficient of friction and elastic modulus, in addition to the lack of appropriate experimental setup and standard experimental protocol. The beginning of this chapter describes a comparison of two different foot – sock friction measuring methodologies alongside a few series of pilot studies that were undertaken to address this issue. The results from these obtained serve as a starting point and necessary foundation to further developing the direction of this PhD research. The latter part of this chapter discusses the more in-depth studies carried out on friction between plantar skin in the first metatarsal head region and sock fabrics.

3.1 Pilot study 1: A comparison of two different methodologies in measuring foot-sock friction

3.1.1 Introduction

Two different methodologies for assessing the friction between foot skin and sock fabrics were presented and discussed earlier in Chapter 2. The first approach uses a foot friction plate rig developed at the University of Sheffield, which requires participants to slide their foot over a test plate whilst maintaining a targeted normal load at a relatively consistent sliding speed. The second approach uses a pneumatically-driven foot probe loading device designed at the University of Salford, which requires the participants to stand still on a platform whilst the probe is applied to, and then driven across, the plantar aspect of foot. Both approaches allow friction coefficients to be calculated from load data collected during the sliding phase of movement. The main purpose of this investigation is to compare the results from both methodologies and to consider which approach offers the best promise for continued work in the foot-skin friction area. To the author's knowledge, this type of comparison has not been considered prior to this investigation.

3.1.2 Study participants and test conditions

The investigation consists of two separate studies that took place at two different institutions and six healthy participants (4 males and 2 females; average age in years, 28.5 ± 5.3 SD) were recruited to take part in both studies. The first study was conducted at the University of Sheffield (hereafter will be referred to as Study A) whereas the second study was conducted three months later at the University of Salford (hereafter will be referred to as Study B). Ethics approval for Study A was granted by the Ethics Committee of the Department of Mechanical Engineering and Dermatology Research Unit, University of Sheffield (application number 002074) whereas for Study B, ethics approval was obtained from the University of Salford's College Research Ethics Panel (application number HSCR15-21).

In order to be eligible for both studies, participants must be aged between 20 to 45 years old and have healthy plantar skin especially the area under the 1MTH. This age group has been selected to be appropriate for the purpose of this investigation for a number of reasons. According to a previous research conducted by Escoffier *et al*. [11], the structure and mechanical properties of the skin remain somewhat constant until around 70 years of age. However, to achieve the purpose of this investigation, people in the age range of 20 to 45 are more likely to be healthy with less risk of having skin pathologies and actively involved in running. In addition, this age group is selected due to their availability within the university.

Participants with the following conditions were also excluded from taking part in both studies:

- having acute or chronic wounds such as unhealed ulcers and blisters;
- having any foot skin disorders such as eczema, athletes' foot, dermatitis, psoriasis, or fungal infections;
- having a known disease such as rheumatoid arthritis, diabetes and cardiovascular disease;
- having any allergies that could be triggered by latex, silicone-based materials, surgical spirit or any alcohol based topical preparations;
- having impaired peripheral that compromises skin integrity and/or neurological status.

In addition, all participants underwent the following assessments prior to the start of both studies in accordance to the 'Guidelines for the Prevention and Management of Foot Problems for People with Diabetes'.

- **Vascular Assessment**

  The dorsalis pedis and posterior tibial artery were palpated. If both pedal pulses in one foot were not palpable, the participant was identified as "increased risk" and therefore was not eligible to participate.

- **Neurological Assessment**

  A 10g Monofilament was used to identify neuropathy at three sites which are under the hallux and the first and fifth metatarsals. The application of the monofilament was repeated twice at the same site but alternated with at least one 'sham' application in which no filament was applied. If the participant correctly answered 2 out of 3 applications, protective sensation was considered present at each site. However, if the protective sensation was absent with 2 out of 3 incorrect answers and the participant was considered to be at risk of ulceration and therefore was not eligible to participate.

Prior to the recruitment, the author had received sufficient training from an HCPC registered podiatrist, Dr Farina Hashmi from the University of Salford. All participants provided their informed written consent prior to testing.

It is worth noting that in both Studies A and B, the testing for each participant took between 4 to 4.5 hours to complete. Due to the extended period of testing, recruiting a large number of participants who are able to attend both studies at the specified dates was not feasible. A sample size of 6 was therefore decided to be appropriate to achieve the objective of both studies.

In both studies, the tested foot was initially cleaned with water (at room temperature) to remove any contaminants and sock fibres and then dried with a paper towel and allowed to acclimatise to the room conditions for a period of 10 minutes. The Corneometer® CM825 (Courage and Khazaka, Germany) was used to measure and monitor the skin hydration of the 1MTH area at specific intervals using following a standard test protocol highlighted earlier in Chapter 3, to ensure that comparable test conditions were achieved. All testing was performed in laboratory conditions with a temperature of between 20ºC to 22ºC and a relative humidity of 40 to 60%.

3.1.3 Tested sock materials

The same two types of commercially available running socks were used in both studies. One is marketed as "anti-blister" sock and the other as "cotton-rich" sock. Each sock had different

material composition and knit patterns, as provided in Table 3.1. The order of testing for each sock material was counter-balanced for each participant.

Table 3.1. Characteristics of the running socks used in this study.

Sock type	Material compositions	Knit pattern	Material thickness (mm)
Anti-blister "ABS"	99% nylon and 1% elastane	Simple jersey	1.18 ± 0.04 SD
Cotton-rich "CRS"	70% cotton, 29% nylon, and 1% elastane	Terry jersey	2.62 ± 0.08 SD

3.1.4 Data and statistical analysis

Statistical analysis was undertaken using SPSS 22.0 (Chicago, USA). The Shapiro-Wilk test was used to confirm that any data sets were normally distributed (at significance level $p > 0.05$) before Pearson's correlation analysis was employed to determine the relationship strength between two parameters.

3.1.5 Experimental procedure

For Study A, friction tests were carried out using the established protocol explained in Chapter 2 earlier (please refer to section 2.1 for detailed explanation). Study B was conducted using the protocol outlined in Chapter 2 (please refer to section 2.2 for detailed explanations). All friction tests were conducted in dry condition where no additional moisture was added to the sock materials. Data from both approaches was collected and assessed before being compared to each other.

3.1.6 Results and discussion

The generated raw force data from both methodologies have been described in detail in Sections 2.1.1 and 2.2.2 respectively.

For comparison, the averaged normal and dynamic (sliding) friction forces from both studies are shown in Figure 3.1(a) (for the anti-blister sock) and Figure 3.1(b) (for the cotton-rich sock). Both studies were able to distinguish between the participants to some degree and gave the same general trend whereby the dynamic friction force increases with the normal force. Study A achieved normal loads ranging between approximately 10 to 200 N, with the upper level more representative of pedestrian loading. Study B was capable of achieving normal (compression) loads in the approximate region of 10 to 40 N and in trial runs attempts to increase this load level, either through the ram pressure setting or the initial foot positioning, led to the risk of discomfort to participants. Although this normal load range is lower than that seen in walking and running, it is higher than the level used typically in other skin friction studies [51, 104, 105]. Table 3.2 summarises the statistical data obtained from both Study A and Study B.

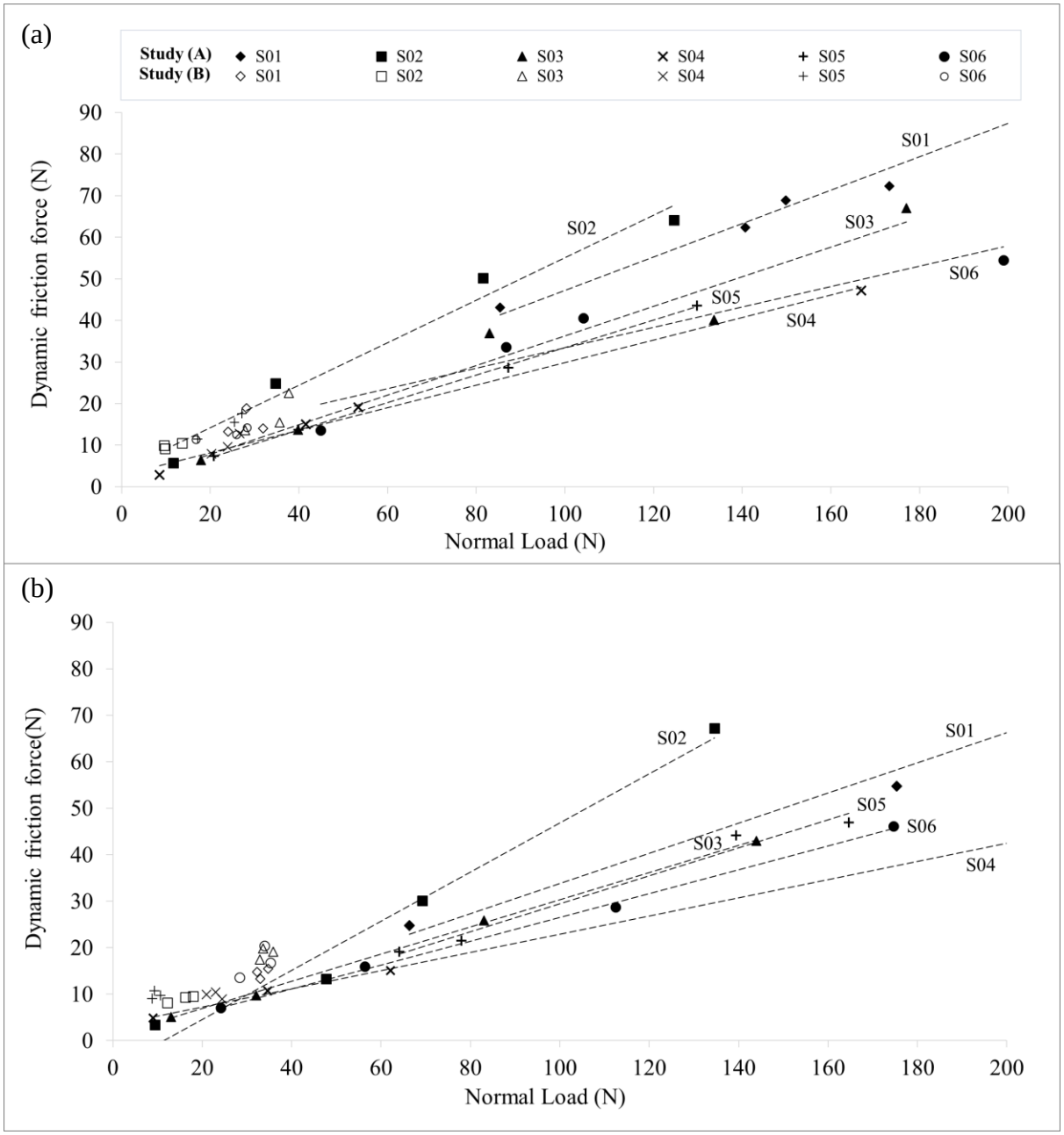

Figure 3.1: Normal and friction force data for both studies with linear fits applied to Study A data for (a) the anti-blister sock; (b) the cotton-rich sock.

Both Figure 3.1(a) and Figure 3.1(b) contain linear fits of the participant data from Study A. The Pearson's R^2 and p values reported in Table 3.2 indicate the strength and significance of the linear fits. Since the participant results obtained from Study B did not produce any significant linear fits for both sock types (see Figure 3.2 and Table 3.2), the fits were therefore omitted for clarity. Linear regression was also carried out on the participant datasets combined from both studies and the Pearson's R^2 and p values for these are also tabulated in Table 3.2, where the dynamic coefficients of friction (DCOF) are also presented for Study A. It is worth to note that these DCOF values were not reproduced in Study B (see Figure 3.2).

It can be seen in Figure 3.1(a) that for the anti-blister sock data, participant results were found to compare well between studies and the data for most the participants in Study B was also well-described by these linear fits. For the anti-blister sock linear fits based on Study A alone, many of the datasets produced strong relationships with R^2 equal to 0.95 or above. All the datasets gave linear fits that were significant at $p < 0.05$, except participant S06 which also produced the weakest fit at $R^2 = 0.885$.

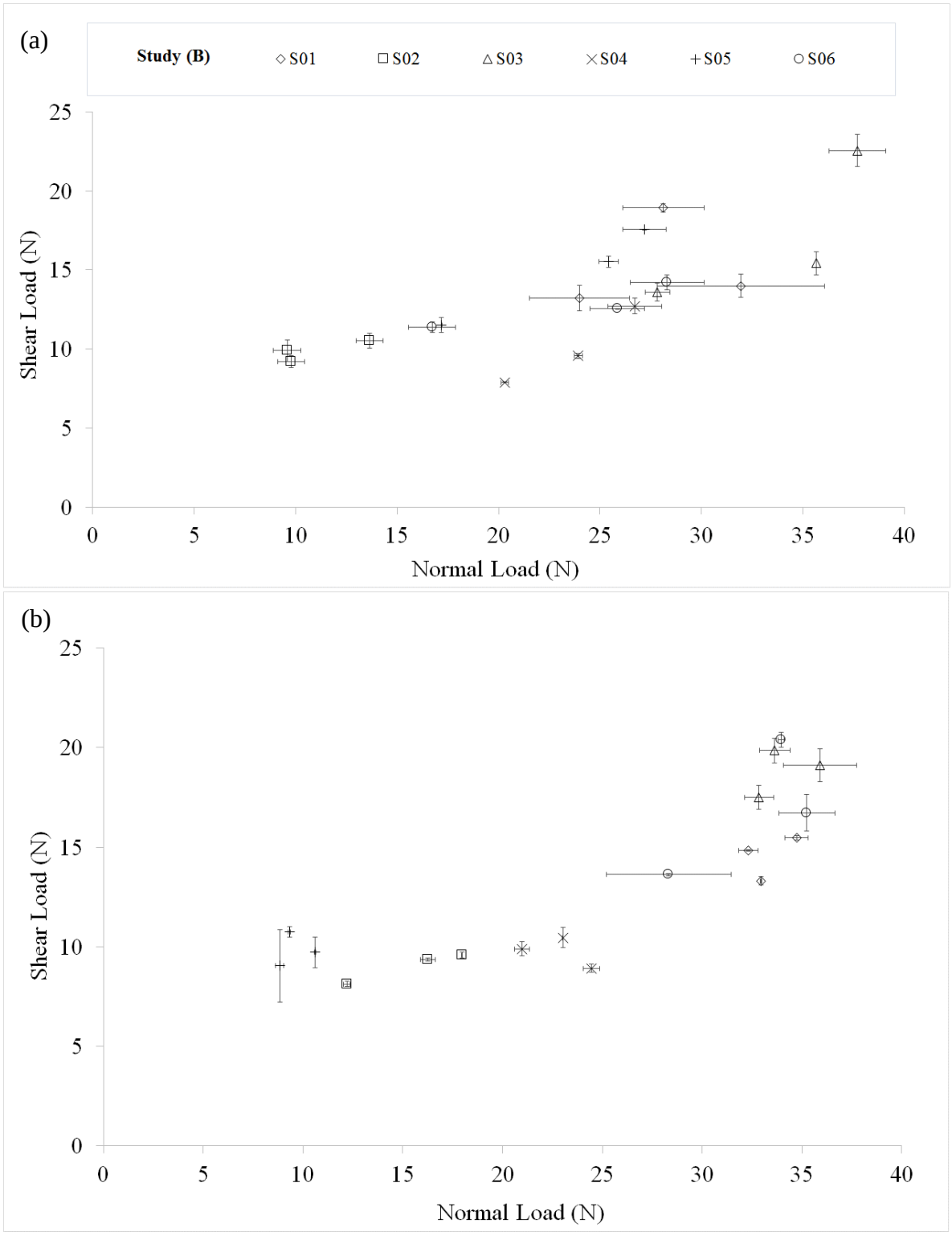

Figure 3.2: Normal and friction force data for Study B: (a) the anti-blister sock; (b) the cotton-rich sock.

Table 3.2: Summarised statistical data obtained from Study A and Study B. The level of significance is indicated by * ($p < 0.05$).

Sock type	Subject	Study A			Study B	
		R^2 value	p-value	DCOF	R^2 value	p-value
"ABS"	S01	0.987	0.001*	0.45	0.021	0.907
	S02	0.970	0.015*	0.59	0.690	0.376
	S03	0.947	0.005*	0.37	0.628	0.418
	S04	0.990	0.005*	0.33	0.938	0.161
	S05	1.000	0.000*	0.34	0.970	0.111
	S06	0.885	0.059	0.34	0.829	0.271
"CRS"	S01	0.990	0.005*	0.34	0.279	0.646
	S02	0.975	0.013*	0.40	0.980	0.090
	S03	0.999	0.000*	0.33	0.196	0.708
	S04	0.999	0.000*	0.33	0.299	0.631
	S05	0.978	0.137*	0.30	0.023	0.903
	S06	0.998	0.001*	0.27	0.538	0.476

On the other hand, analysis of the data from the cotton-rich sock tests in Figure 3.1(b) shows less close friction behaviour between the two studies, although the DCOF values from the Study A dataset and combined dataset gave good comparison for all of the participants except S02 and S04. In terms of sock frictional performance, the cotton-rich sock was consistently found to produce lower friction than the anti-blister sock for each set of participant data (in the dry conditions tested). This finding was confirmed in an additional study that included more participants which is described in the latter part of this chapter.

In general, both approaches gave similar results in terms of the trends observed and the participant and textile-specific friction values produced. This was despite the fact that the level of loading differed between the methodologies as well the interaction between foot skin and sock; Study A used one area of the foot sliding across the sock surface, whereas Study B used one area of sock sliding across the foot surface. This has given confidence that both approaches have validity in further studies of skin-fabric frictional interactions. The approach

used in Study B is recommended for situations where it is difficult for participants to control the loading in a consistent manner and/or in a particular location. However, the approach used in Study A (with the current set-up as previously explained in Chapter 2) allows greater range of normal loading to be applied, that is more representative of pedestrian interactions, and therefore more likelihood that statistical differences can be found between datasets using different input parameters.

3.1.7 Conclusion

Two different methodologies to measure foot skin-fabric frictional interaction was described and compared in this investigation. The first testing approach has been selected for use in further foot skin-sock friction experiments due to its capability of achieving higher normal loading conditions. To the author's knowledge, this topic has not been investigated in previous studies. Therefore, the findings from this comparison can be used to provide some insights in deciding the most appropriate methodology for foot skin-fabric frictional testing.

3.2 Pilot study 2: Investigating the friction between a sock and chosen shoe insole

3.2.1 Introduction

As a starting point of the project, a pilot study was carried out to investigate the frictional behaviour of a shoe insole, which is one of the important interfaces within the in-shoe environment, against five different types of sock materials.

3.2.2 Tested sock materials and insole

A variety of commercially-available running sock materials were selected due to their differing fibre compositions and knit patterns as presented in Table 3.3. All socks were obtained from single layer socks except for the double layer sock which consists of an inner layer (for skin-sock interface) and an outer layer (for sock-insole interface). For the double sock, only the outer layer was used for the pilot study as it directly interacts with the shoe

insole during gait. These socks have been reported to be the most commonly-used socks by pedestrians and runners alike. In contrast, selecting a 'standard' insole to be used for the testing was proven to be more challenging due to the limited information available from shoe manufacturers on the materials and compositions of their shoe insoles. Upon careful observations of multiple insoles from various types of trainers, an insole deemed to be of a 'standard' style was obtained from a running shoe. It consists of a homogenous textile layer adhered to a 3mm thick backing foam and has not been submitted to any use prior to the friction tests (see Figure 3.3).

Table 3.3: Characteristics of socks used for the sock-insole pilot study.

Sock type	Fibre compositions	Knit pattern
Cotton-rich "Sock A"	75% cotton, 17% polyester, 6% nylon, 2% elastane	Terry jersey
100% cotton "Sock B"	100% cotton	Simple jersey
Wool-rich "Sock C"	40% wool, 31% cotton, 19% nylon, 8% elastane	Terry jersey
Anti-blister "Sock D"	99% nylon, 1% elastane	Simple jersey
Double-layer (outer) "Sock E-o"	54% cotton, 44% nylon and 2% elastane	Simple jersey

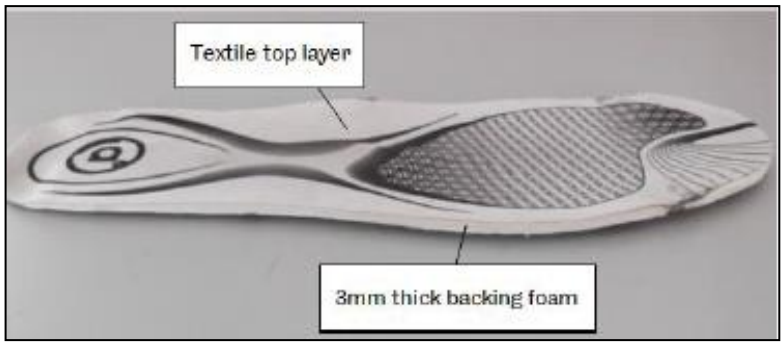

Figure 3.3: Shoe insole selected for testing.

3.2.3 Experimental procedure

Since the insole was made up of two distinct layers, two separate friction experiments were carried out using the foot friction plate rig. The first experiment was conducted against the insole in its entirety (i.e. including the backing foam) whereas the second friction experiment was carried out against the textile layer only (i.e. without the backing foam). Similar to the friction experimental protocol described in section 2.1 of Chapter 2, the shoe insole was mounted and adhered on the plate, as shown in Figure 3.4 and the sock materials were then pushed across the insole surface.

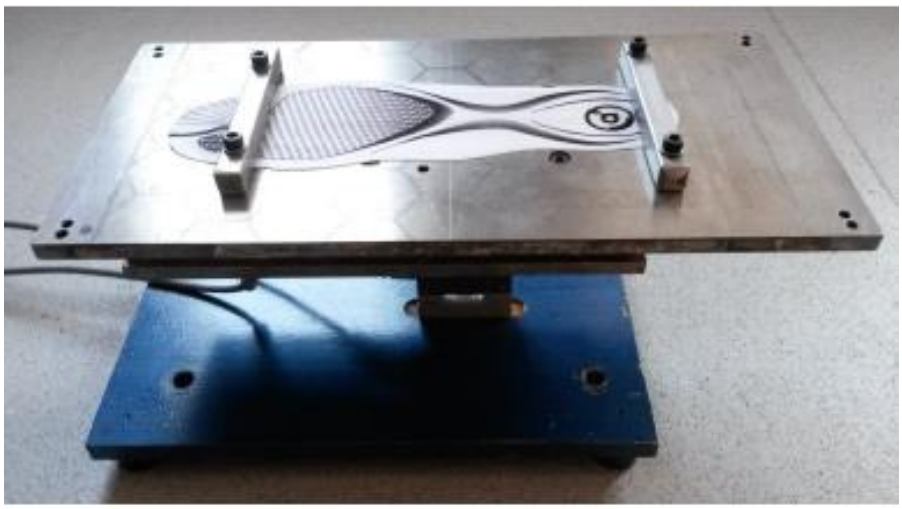

Figure 3.4: Shoe insole adhered on the foot friction plate rig.

The tested sock material was mounted on a carrier made of a medium-density fibres (MDF) template with a contact area of 5cm^2, as shown in Figure 3.5. The MDF was chosen to be a suitable material for the mounting as it was relatively stiff compared to the textiles and easy to machine and shape. The shape of the template was created by simplifying the shape of the forefoot truncated to form a semi-ellipse, with the curved section used at the front of the movement direction to prevent digging in from occurring. The contact area was obtained by computing: ½ x π x semi-major axis x semi-minor axis of the semi-ellipse. The sock materials were strained at 20% level and carefully adhered to the template using double-

sided adhesive. In each run of tests, ten different ranges of normal load were applied in a gradually increasing manner up to 300N and the sliding friction forces were averaged across the dynamic region of the raw friction data, as previously explained in Section 2.1.1. All friction tests were conducted in a dry condition.

Figure 3.5: (left) The MDF mounting used as the sock carrier; and (right) a sock material adhered to the template with a 20% strain level.

3.2.4 Results and discussion

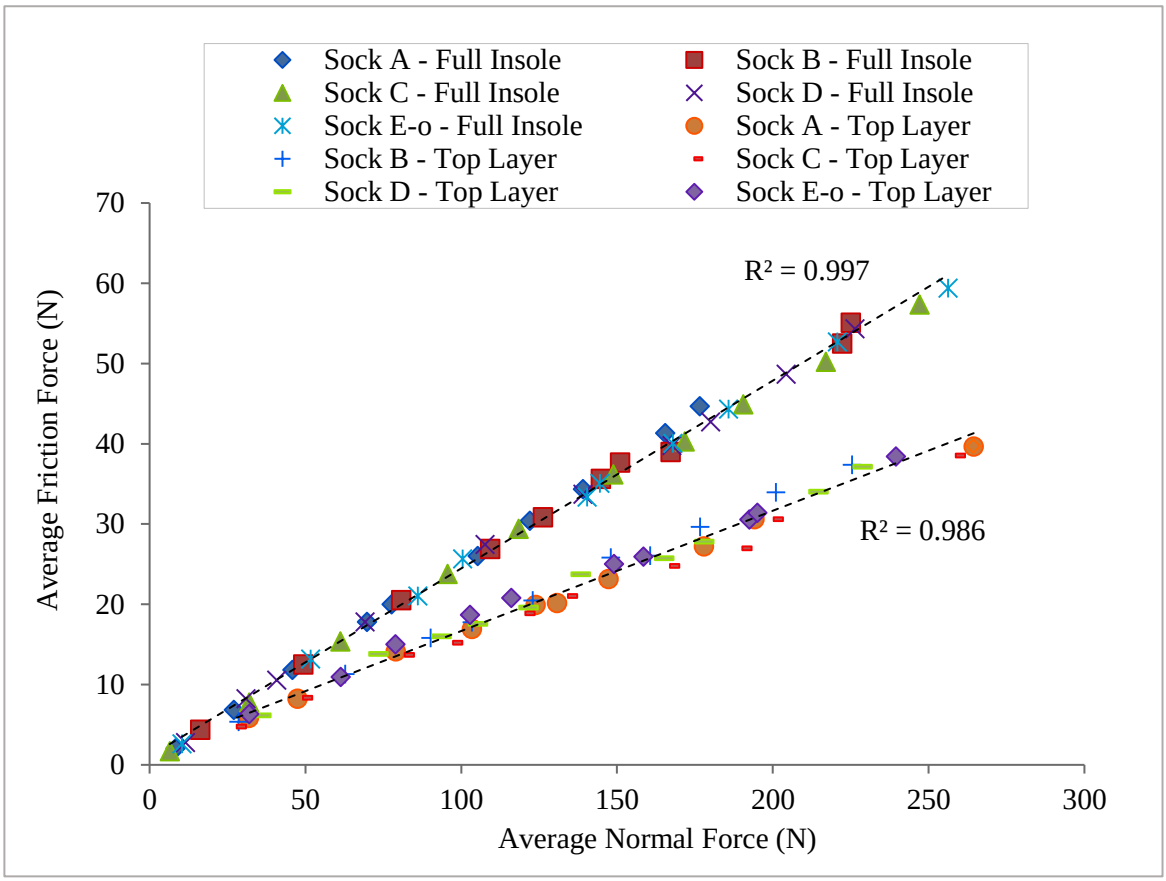

Figure 3.6: The force data show the effects of shoe insole on the average friction force produced.

Figure 3.6 shows the plot of the average friction force data produced from the sock-insole friction experiments against five different sock materials, both with and without the backing foam. Please note that the standard error for each data point was too small and therefore omitted to ensure graphical clarity. It can be seen that for both datasets, the average friction force values increase with increasing ranges of applied normal loading. Two distinct trends, indicated by the two linear fits, were produced. The friction tests using the full insole produced higher dynamic friction values across all sock materials than when using only the textile top layer of the insole. An independent-samples t-test was conducted to compare the dynamic friction coefficients produced by the sock-insole interactions and a statistical

significance difference at a level of $p < 0.05$ was found between the two datasets showed in Figure 3.5; t (98) = 37.2, p = 0.000. The effect size was calculated to be large (eta squared = 0.93), indicating that the results obtained from the tested insoles are indeed very different. This could be attributed to the fact that the backing foam of the insole allows for a much higher deformation of the system to occur, hence contributing to the hysteresis component of friction.

A one-way analysis-of-variance (ANOVA) test was carried out using SPSS 22.0 (Chicago, USA) to assess the statistical differences between the sock materials in both friction experiments. No statistical significance was found between sock materials for the full insole friction tests but two of the sock materials (Socks B and C, Socks E-o and C) showed statistical significant differences at $p < 0.05$ when tested just against the textile top layer of the insole (see Table 3.4 below). This further showed that the friction forces produced by the full insole were dominated by the deformation effect from the backing foam, hence minimising the effect of differences between sock materials.

Although no conclusive results were obtained from this pilot study, the findings provide an insight into the frictional interaction between the shoe insole and sock materials. It would certainly be worthwhile to conduct the same friction experiments in the future using a variety of running shoe insoles and assess the friction effects produced by different insole and backing foam types. This would provide useful information to the shoe manufacturers as well as the shoe buyers who have a high tendency of developing friction blisters. The pilot study also provides a benchmark friction values that can be used when considering the entire foot-sock-shoe insole system.

Table 3.4: Summarised statistical data comparing the frictional effects of the sock materials against a full insole and against textile top layer. The level of significance is indicated by *($p < 0.05$).

Sock type	**Sock type**	***p-values***	
		Full insole	**Top layer only**
Sock A	Sock B	0.878	0.367
	Sock C	0.273	0.669
	Sock D	0.870	0.968
	Sock E-o	0.282	0.198
Sock B	Sock A	0.878	0.367
	Sock C	0.818	0.022*
	Sock D	1.000	0.751
	Sock E-o	0.828	0.996
Sock C	Sock A	0.273	0.669
	Sock B	0.818	0.022*
	Sock D	0.826	0.295
	Sock E-o	1.000	0.008*
Sock D	Sock A	0.870	0.968
	Sock B	1.000	0.751
	Sock C	0.826	0.295
	Sock E-o	0.836	0.527
Sock E-o	Sock A	0.282	0.198
	Sock B	0.828	0.996
	Sock C	1.000	0.008*
	Sock D	0.836	0.527

3.3 Pilot study 3: Investigating the effects of strain on the frictional behaviour of sock fabrics

3.3.1 Introduction

A previous study by Troynikov *et al*. [77] showed that changes in strain present within compression garments may have direct influence on the frictional behaviour between the fabric and skin. This in return will affect the overall physiological comfort of sport apparel including sensorial and tactile components. This can also be applied to all other sport-related fabrics including running socks. The aim of this pilot study was to assess the effect of applied strains on the frictional interaction of the socks against the top layer of the shoe insole.

3.3.2 Tested sock materials and insole

The same varieties of running socks used in the previous pilot study (see Table 3.3 above for the sock compositions and knit patterns) were selected for the purpose of this study. The same insole material was also used for the friction experiments.

3.3.3 Experimental procedure

The insole top layer material was clamped onto the foot friction plate rig as shown in Figure 3.4 and the same friction test protocol was followed. As the MDF carriers produced for the insole analysis did not allow for a larger variance in strain, a different carrier was therefore required. It is important that the shape of the carrier closely-resembles the shape of the previous carrier, in order to simulate the forefoot region of the foot. A climbing shoe with a non-deformable flat sole surface was chosen to be the most suitable sock carrier as it has a relatively larger surface, allowing the sock materials to be mounted and strained at different levels (see Figure 3.7).

The sock material was then adhered to the sock carrier at the intended strain level using double-sided adhesives and bulldog clips to secure the sock to the climbing shoe. All friction tests were only conducted in dry condition and ten values of applied normal load were performed for each strain level. The averages of the friction forces were computed and plotted against the applied normal loads for all sock materials.

Figure 3.7: (left) The carrier used to mount the sock materials at different strain levels; and (right) one of the sock materials mounted onto the carrier.

3.3.4 Results and discussion

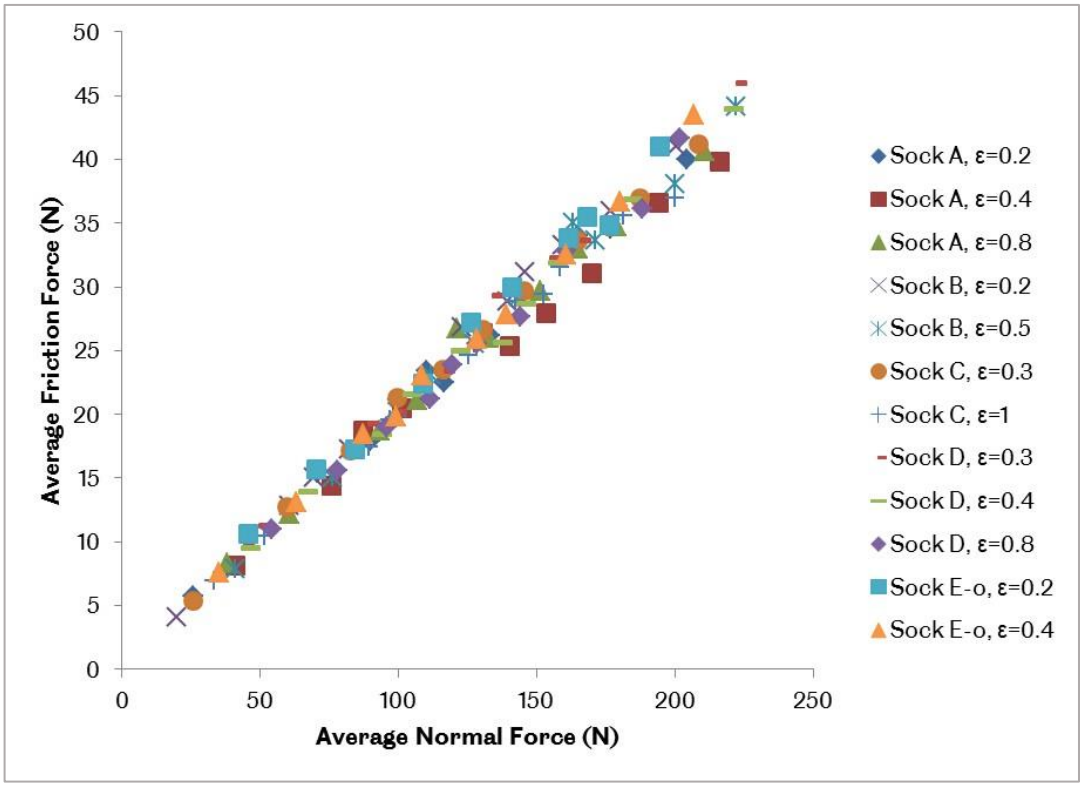

Figure 3.8: The average friction force data plotted against the average normal force across all sock materials at different strain levels.

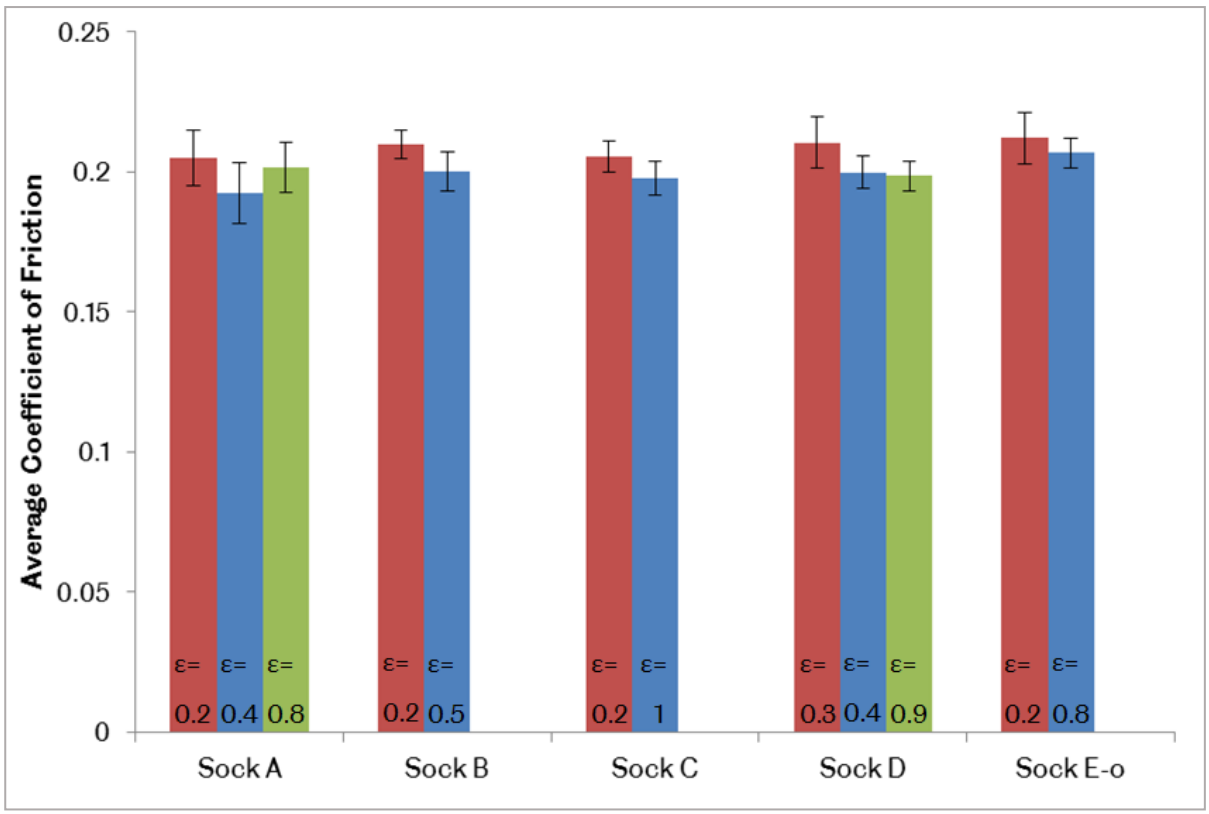

Figure 3.9: The average coefficient of friction values for each sock material, at varying strain levels.

Figure 3.8 shows the average friction force data plotted against the average applied normal load for all sock materials at varying strain levels. Please note that some of the sock materials were only tested at two different strain levels due to the difficulties in counting the number of yarns per 50mm. Only Sock A (a cotton-rich sock) and Sock D (an anti-blister sock) were tested at three different strain levels. A strain level of 0.2 can be translated as 20% strain. Linear fits were applied to all datasets which produced R^2 values of greater than 0.90 across all sock materials at all tested strain levels. All fits showed the same trend where the produced average frictional forces increased with increasing applied normal load. However, very little variance was observed between each sock-strain combination.

The average coefficient of friction values for each sock material at each strain level was then calculated and compared to one another in Figure 3.9. The error bars show the calculated standard deviations obtained from the mean. No significant differences were found

between the sock-strain combination. This finding did not concur with the previous study conducted by Troynikov *et al*. [77], which could be attributed to the small change in fibre deformation between each strain level. In reality, it is nearly impossible to achieve a completely unstrained condition of the sock materials which could be due to the nature of the fibres and the way the yarns were knitted. It is also noted that at the smallest strain level of 20% to 30%, the average coefficient of friction values across all sock materials are all nearly similar. As the level of strain was increased, a slight reduction in the average coefficient of friction values was observed, although no statistical significance was produced ($p > 0.05$). It was difficult to obtain an intermediate strain level for Sock C (a wool-rich sock) due to the 'fluffiness' of the wool fibres.

For all future studies, straining the sock materials at between 20% and 50% was thought to be highly-achievable and easily-reproducible whilst ensuring that the strain is representative of a real-world scenario when the socks are being worn.

3.4 Pilot study 4: Investigating the effects of contact area on the frictional behaviour of sock fabrics against shoe insole in dry condition

3.4.1 Introduction

Determining the real contact area of any given sock fabric can be very challenging. Apparent contact area, however, has been shown by previous studies, as discussed in Chapter 1 and 2, to have direct influence on the frictional interaction of sock fabrics. Investigating the effects of contact area on the frictional interaction between sock materials and shoe insole will provide valuable initial information in understanding the way sock fabrics behave in terms of friction, and aid in future experimental design.

3.4.2 Tested sock materials and insole

For the purpose of this pilot study, only Sock A (a cotton-rich sock) was used for friction testing along with the same insole material used for previous pilot studies. The material composition of Sock A can be found in Table 3.3.

3.4.3 Experimental procedure

The friction experimental setup was similar to the setup used for the previous pilot studies, where the insole was mounted onto the friction plate rig. In order to obtain four different contact areas of sock materials, three larger MDF templates were made similar to the available 5cm^2 template, with surface areas of 10cm^2, 20cm^2, and 40cm^2 as shown in Figure 3.10. The socks were all strained at 20% and the test was only conducted in dry condition. Ten different ranges of normal load were applied and the average frictional forces were computed for further analysis.

Figure 3.10: The four different MDF templates used in the contact area analysis.

3.4.4 Results and discussion

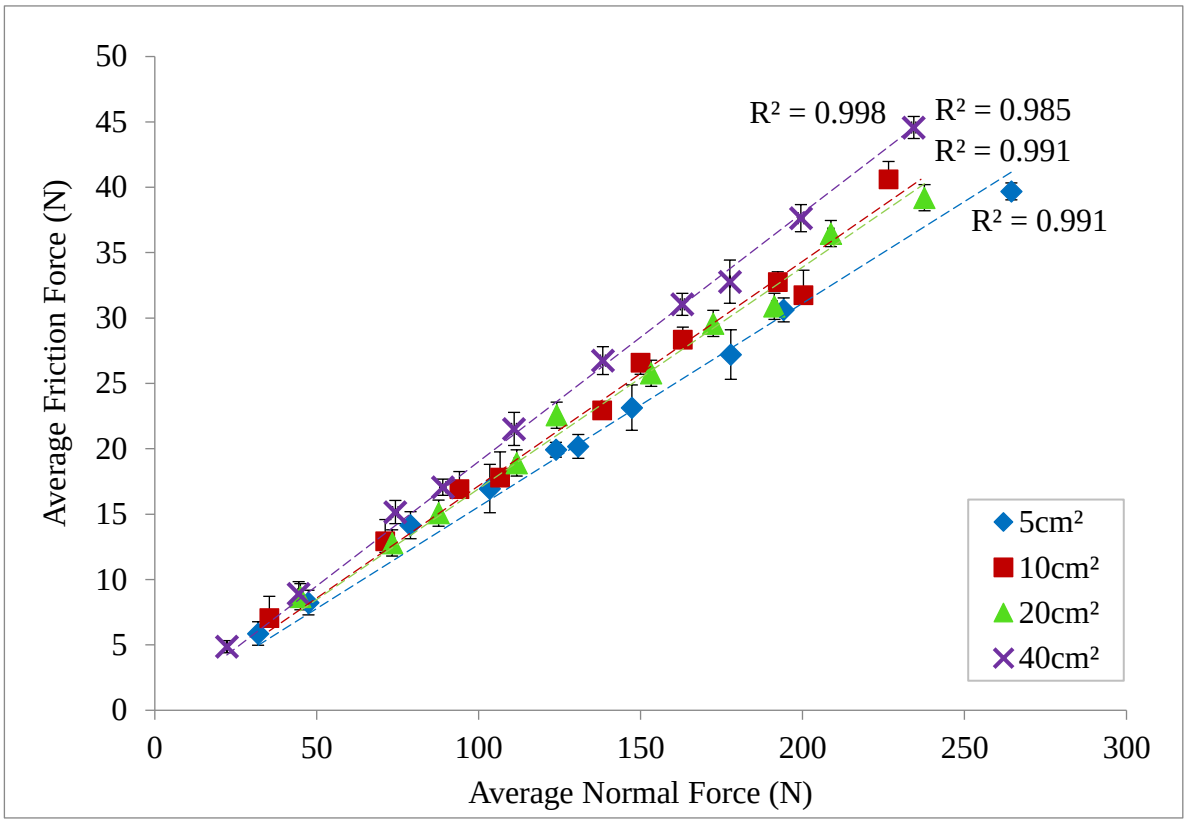

Figure 3.11: shows the average frictional force produced by Sock A against the textile top insole layer in four different contact areas.

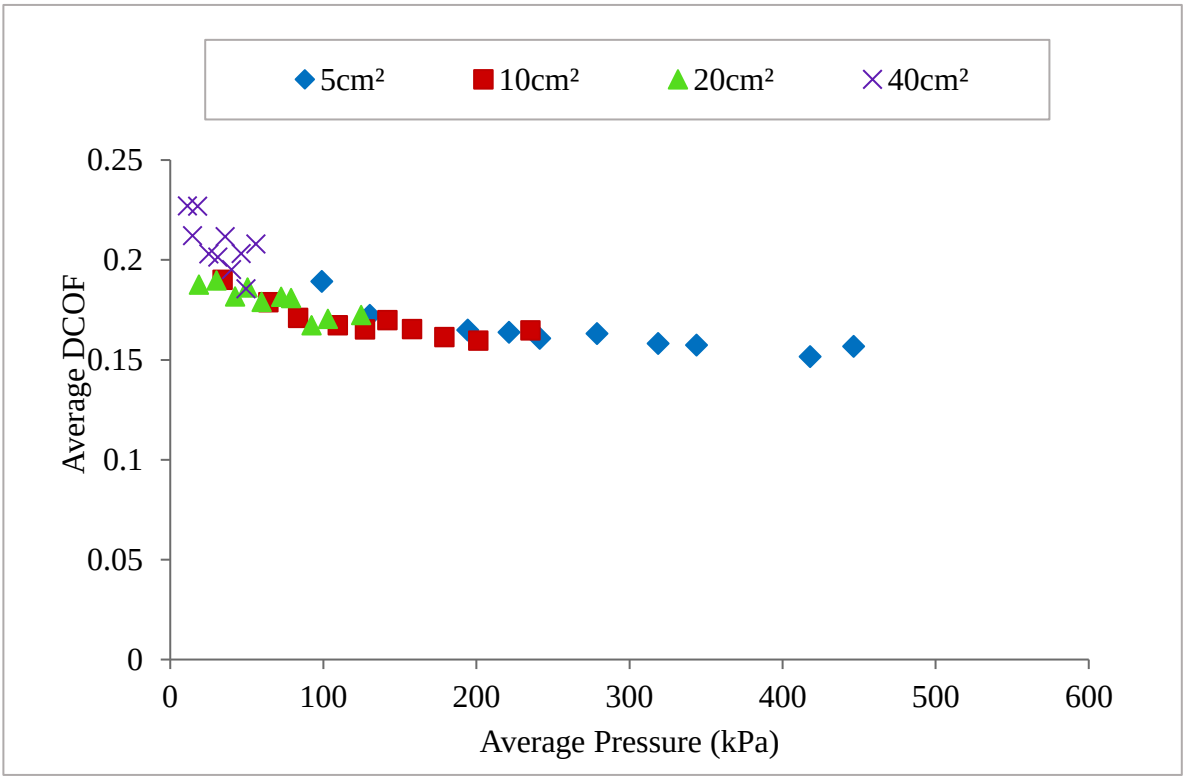

Figure 3.12: shows the comparison of the effects of average pressure on the average coefficient of friction values produced between Sock A and the textile top insole layer in correspondence to the four different contact areas.

The average frictional force produced between Sock A and the shoe insole was plotted against the average applied normal loads in Figure 3.11, with ten data points for each contact area tested. All results show that the average friction force is proportional to the average applied normal loads, similar to results seen in earlier pilot studies. It was found that as the contact area increased, the average frictional force also increased. A one-way ANOVA analysis was carried out and significant differences were found at a level of $p < 0.05$ between the 40cm^2 contact area when compared to all other three contact areas of 5cm^2, 10cm^2 and 20cm^2 [F (3, 36) = 16.61, p = 0.000]. Post-hoc comparisons using the Bonferroni test indicated that the mean DCOF values for 40cm^2 contact area (mean = 0.20, SD = 0.01) was significantly different when compared with all other three contact areas: 5cm^2 (mean = 0.16, SD = 0.01), 10cm^2 (mean = 0.18, SD = 0.01), and 20cm^2 (mean = 0.17, SD = 0.01). The effect size was calculated to be large (eta-squared=0.6), indicating that these differences were

substantial. The increase in average friction forces could be contributed to the increase of the apparent contact area providing greater adhesion component of friction. This demonstrates that, similar to human skin, sock materials do not obey Amonton's Law which states that the friction force is independent of the contact area.

Since the normal loads were applied over specified areas, the data was also represented in terms of the average applied pressure as shown in Figure 3.12. The average coefficient of friction values were found to decrease with average applied pressure, up to a limiting point of approximately 0.16 where the value remained relatively constant.

3.5 Pilot study 5: Investigating the effects of varying moisture conditions on the sock-insole friction behaviour

3.5.1 Introduction

Moisture build-up within a shoe-environment can occur primarily due to high perspiration rate of the feet and warm or humid environment generated within enclosed shoe. Some of the moisture will be transported away from the feet into the external environment whilst some remaining moisture will be absorbed by the sock fabrics and shoe insole. Therefore, this pilot study was carried out to investigate the effects of varying the moisture levels on the sock-insole frictional behaviour.

3.5.2 Tested sock materials and insole

Similar to the skin-insole contact area analysis described above, only Sock A (a cotton-rich sock) was used for friction testing along with the same insole material used for previous pilot studies. The material composition of Sock A can be found in Table 3.3 above.

3.5.3 Experimental procedure

The friction experiments were carried out using the foot friction plate rig. Sock A was mounted on the 5cm^2 template. The top layer of the insole was adhered on to the test plate. Moisture effects were investigated using three conditions: a fully-submerged sock-insole interface, a completely dry sock-insole interface, and a somewhat moist sock-insole interface.

Figure 3.13: shows the fully-submerged friction testing setup.

For the fully submerged test, a modified plastic tank was fixed to the top of the friction plate rig and the entire sock insole interface was fully submerged in water as shown in Figure 3.13. No water was added to both the sock and insole materials for the completely dry sock-insole interface test. The mid-level (i.e. moist) sock-insole interface test was achieved by firstly submerging them both in water and soaking for approximately 5 minutes. Both materials were then removed from the water and placed face down on a layer of absorbent cloth with a 2 kg mass applied to squeeze out some water. The mass was left on both sock and insole materials for 2 minutes before being removed. An alternative method was developed for controlling textile moisture content (see Section 2.7).

3.5.4 Results and discussion

Figure 3.14 presents the results obtained from the sock-insole interface friction tests conducted in three different moisture conditions. Both fully-submerged and mid-level conditions exhibited much higher friction forces than the dry conditions. A one-way ANOVA test was carried out and statistical differences were found at $p < 0.05$ for all three conditions. This was also confirmed by conducting a post-hoc comparisons using the Bonferroni test. The results indicated that the mean DCOF value of each moisture condition: dry (mean = 0.15, SD = 0.01), mid-level (mean = 0.40, SD = 0.01), and submerged (mean = 0.43, SD = 0.01), is considerably different than the other. Presence of water within the sock and insole fabrics increases the adhesion effects of the friction interactions between both materials. This is due to the increase in actual contact area resulting from the swollen fibres with moisture in the contact.

The fully submerged sock-insole interface test was intended to simulate a real-world condition where the in-shoe environment (feet, sock, and insole) was completely soaked with water such as when running in the rain or through puddles (such as in cross-country). The completely dry sock-insole interface test, on the other hand, was intended to simulate a real-world condition opposite to the fully submerged sock-insole interface test. An example of this condition could be for someone who are not susceptible to sweaty feet or when the socks and shoes are worn for a very short period of time. Finally, the mid-level (i.e. moist) sock-insole interface test was intended to simulate real-world conditions that closely-resemble the effects of sweaty feet after a long run and/or in hot environments.

Interestingly, even in the fully-submerged condition, no drop in friction was seen due to a lubricating film of water. It is thought that the textile interface was not capable of setting up a trapped film of water in the same way as a shoe can, for instance, on a hard, smooth floor.

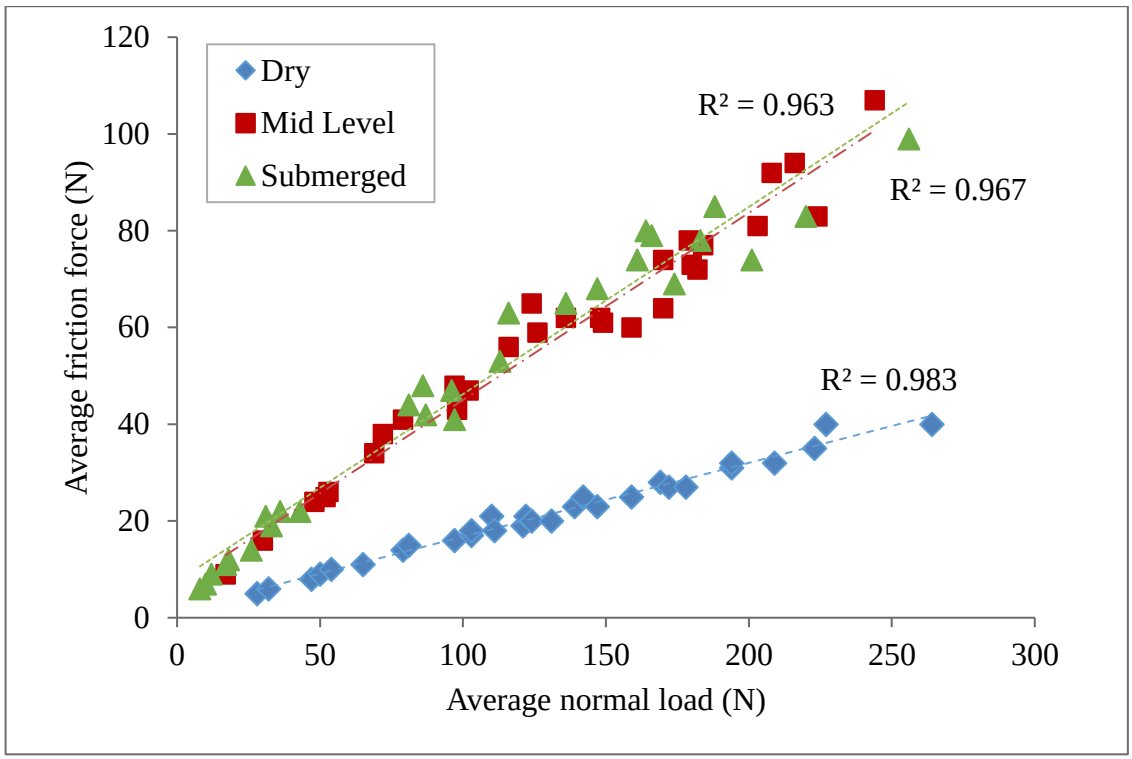

Figure 3.14: shows the average frictional force produced by Sock A against the textile top insole layer in three different moisture conditions.

3.6 Investigating the frictional behaviour of plantar skin against running sock fabrics in dry condition

3.6.1 Introduction

From previous studies on friction blisters, it is known that the moisture content in the stratum corneum [75] and presence of water in the skin-fabric interface could strongly influence the friction of skin. Rubbing wet skin against dry fabrics has been shown to result in a significant increase in friction with larger increases being found for hairy skin compared to glabrous skin [62]. A recent work by Tomlinson *et al.* [34] (not using fabrics), found an increase in skin-surface friction coefficients in a humid environment and attributed them to physical mechanisms including water absorption and capillary adhesion due to meniscus formation. The authors also concluded that there was negligible effect due to the viscous shearing of liquid bridges formed between the skin and the interacting surface. Elevated temperature at the skin surface during rigorous sport activities where the feet are subjected to repeated rubbing could also increase the skin moisture levels through sweating. This is more prominent for shoes with poor air-permeability that represent a barrier to heat transfer. Moisture present in the contact could also increase friction due to changes in the properties of the sock fibres [3].

In this study, the friction coefficients of the plantar skin against five running sock materials were assessed and the foot hydration level was monitored using the established standardised protocol.

3.6.2 Tested sock materials

Five different types of commercially available running socks were selected for this study. Four of these socks (Sock A, B, C, and D) were the same design to the ones used in the previous study. Sock E, however, was a fully nylon sock obtained from the inner sock of the double-layer sock. Table 3.5 below provides the characteristics of all five socks.

Table 3.5: Characteristics of socks used for in this study.

Sock types	Fibre compositions	Knit pattern
Cotton-rich "Sock A"	75% cotton, 17% polyester, 6% nylon, 2% elastane	Terry jersey
100% cotton "Sock B"	100% cotton	Simple jersey
Wool-rich "Sock C"	40% wool, 31% cotton, 19% nylon, 8% elastane	Terry jersey
Anti-blister "Sock D"	99% nylon, 1% elastane	Simple jersey
Double-layer (inner) "Sock E"	100% nylon	Simple jersey

3.6.3 Study participants and test conditions

Twenty-six healthy participants (19 males and 7 females; age: 24.8±4.9 years) were recruited from the University of Sheffield. Ethical approval for this study was obtained from the Ethics Committee at the University of Sheffield. All participants took part voluntarily and provided their written informed consent for the study purpose. Prior to providing their consent, participants were informed of the outlined inclusion and exclusion criteria of the eligibility for the study. The details on these criteria have already been described in section 3.1.2. The participants were also required to undergo the vascular and neuropathy assessments, conducted by the author, at the beginning of the study. All tests took place in a controlled laboratory condition with a temperature of between 20 to 22°C and a relative humidity of 40 to 60%.

3.6.4 Experimental procedure of the foot hydration test

The foot which was to be tested was cleaned with water (at room temperature) to remove any contaminants. Upon removal from the foot bath the foot was dried with paper towels and allowed to acclimatise to the room conditions for 10 minutes.

The hydration level of the plantar skin was monitored throughout testing using a capacitance-based device, the Corneometer® CM 825 (Courage and Khazaka, Germany). Three sets of hydration measurements were taken on each participant: 1) immediately after removing their footwear and before cleaning; 2) after cleaning and acclimatisation, which is also prior to the friction tests and 3) immediately after the friction tests to monitor if any large changes had taken place during testing. Each set of hydration measurements included 18 data: three separate measurements taken at six different plantar regions, as shown in Figure 3.15, to allow for an average hydration value of each region to be calculated.

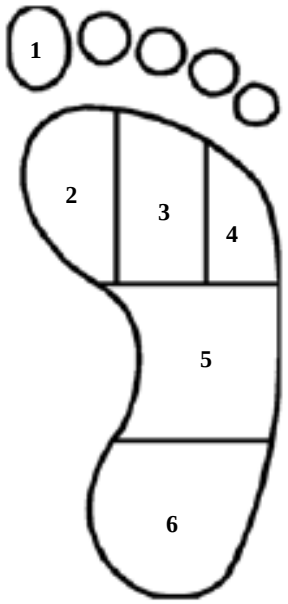

Figure 3.15: Division of plantar regions for hydration testing: 1- hallux; 2- first metatarsal head; 3- between the second and third metatarsal heads; 4- between the fourth and fifth metatarsal heads; 5- arch and 6- heel.

3.6.5 Experimental procedure of the friction test

Friction measurements were conducted in dry condition using a foot friction plate rig. The sock materials were cut into rectangular samples of approximate size 150 mm×400 mm and clamped at either end onto the plate to maintain a consistent level of 50% pre-strain. They were then securely attached to the plate using double-sided adhesive tape to ensure no movement between the sock and the test plate during testing.

Participants were instructed to slide their foot forward against the sock material whilst keeping the sliding velocity fairly consistent by counting to 5 during each test (a protocol adapted from [34]). A range of five different normal loads were applied by the participants for each sock material, starting with the lowest before increasing incrementally. The maximum loads that could be applied by the participants were measured to be as high as 500 N. This is more representative of the real-world foot-loading scenarios, than values used in previous skin research [51, 104, 105]. All five sock materials were tested under dry conditions and the order of testing was randomised for each participant.

3.6.6 Experimental procedure of the contact area test

In order to assess the contact area over which the normal forces were being applied by the participants, the footprint ink method was employed. It is one of the most common methods used in determining the skin contact area when in contact with flat surfaces. An A4 graph paper was attached onto the test plate of the friction rig. Participants were then instructed to press their tested foot on a large inkpad, ensuring that the entire plantar aspect of the foot was covered with a thin film of ink. The stained foot was then pressed onto the graph paper at intended range of normal load. The test was carried out five times to obtain the contact area at five different ranges of normal load up to 500N, starting from the lowest load to the highest.

The imprints obtained were then scanned and saved as digital images for analysis. The contact area was computed using an image processing software, ImageJ where the total number of pixels covered in ink represents the total contact area of the plantar aspect of the foot at a particular applied normal load. The data obtained was then normalised by dividing the contact areas by the measured length and measured width of the participant's foot.

3.6.7 Foot hydration analysis

Figure 3.16 below shows the average hydration values measured across six plantar regions for all twenty-six participants. The hydration values obtained after foot cleaning and acclimatisation were selected as baseline readings. No consistent trend can be seen in the hydration level at different locations. For instance, Participant 23 has a relatively high

moisture level in his forefoot but a slightly drier arch and heel. This demonstrates that unlike the skin on the forearm and cheeks, the plantar skin is less homogenous. This could be attributed to various other participant-specific factors having influence such as gait mechanisms, skin condition, and skin care regimen. A study by Laing *et al.* [106] suggested that the variablity in the skin hydration could be associated with the physical structure of the feet.

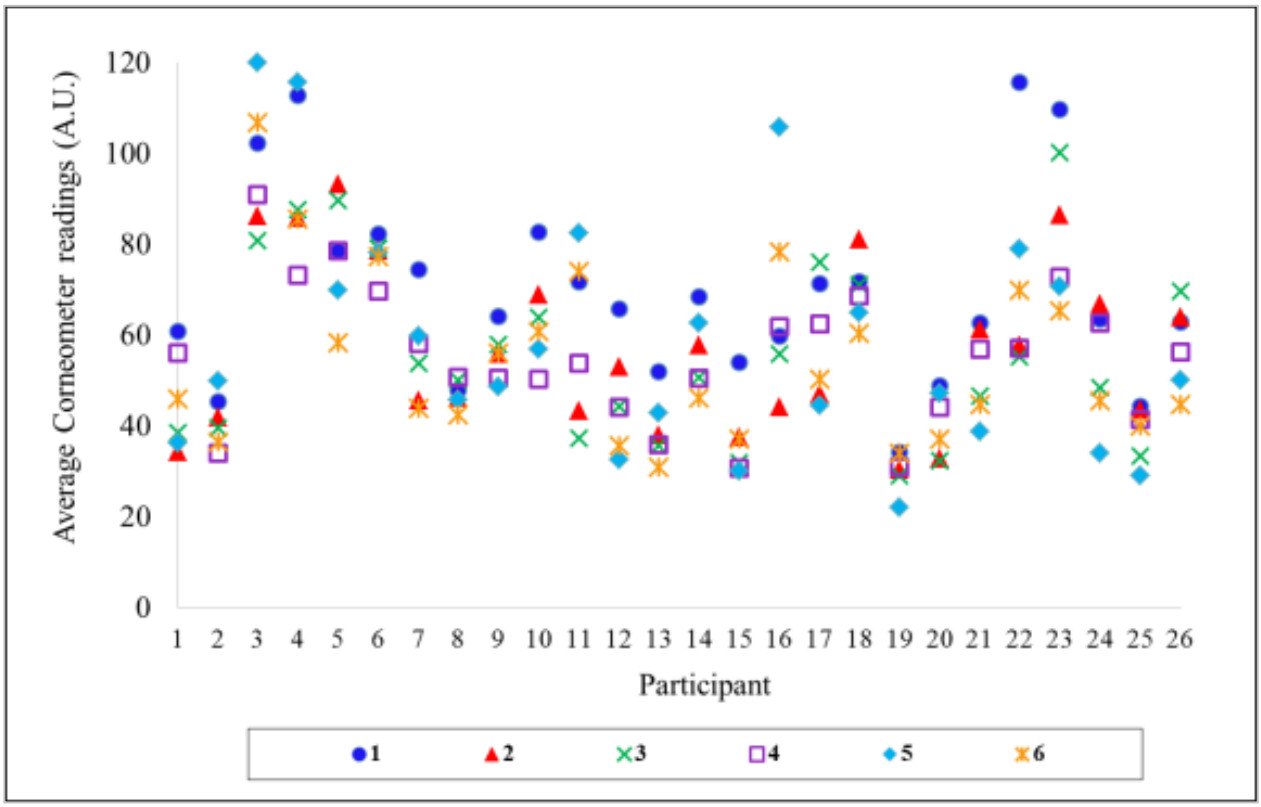

Figure 3.16: The Corneometer readings measured after cleaning and acclimatisation across six plantar regions for all 26 participants: 1- hallux; 2- first metatarsal head; 3- between the second and third metatarsal heads; 4- between the fourth and fifth metatarsal heads; 5- arch and 6- heel.

3.6.8 Evaluating the friction coefficient of the tested sock materials against human plantar skin

Example force data from one participant is shown in Figure 3.17 (a). Similar trends were found for all participants with friction force found to increase linearly with normal force. A value of predicted friction force for a 100 N normal force was then interpolated for each sock material and this data was collated for further analysis.

The friction data obtained from the tests was shown to be widely dispersed across the tested sock materials, as seen in Figure 3.17 (b). No statistically significant differences ($p>0.05$) were found when comparing the differences between the sock materials using the one-way ANOVA test, suggesting that the individual properties of the plantar skin had more of a prominent effect on friction than the knit pattern and composition of sock materials, when tested under dry conditions. This however did not concur with the findings obtained by Baussan *et al.* [105] which showed that the inside of a terry jersey knitted sock had a higher friction coefficient than that of a simple jersey knitted sock.

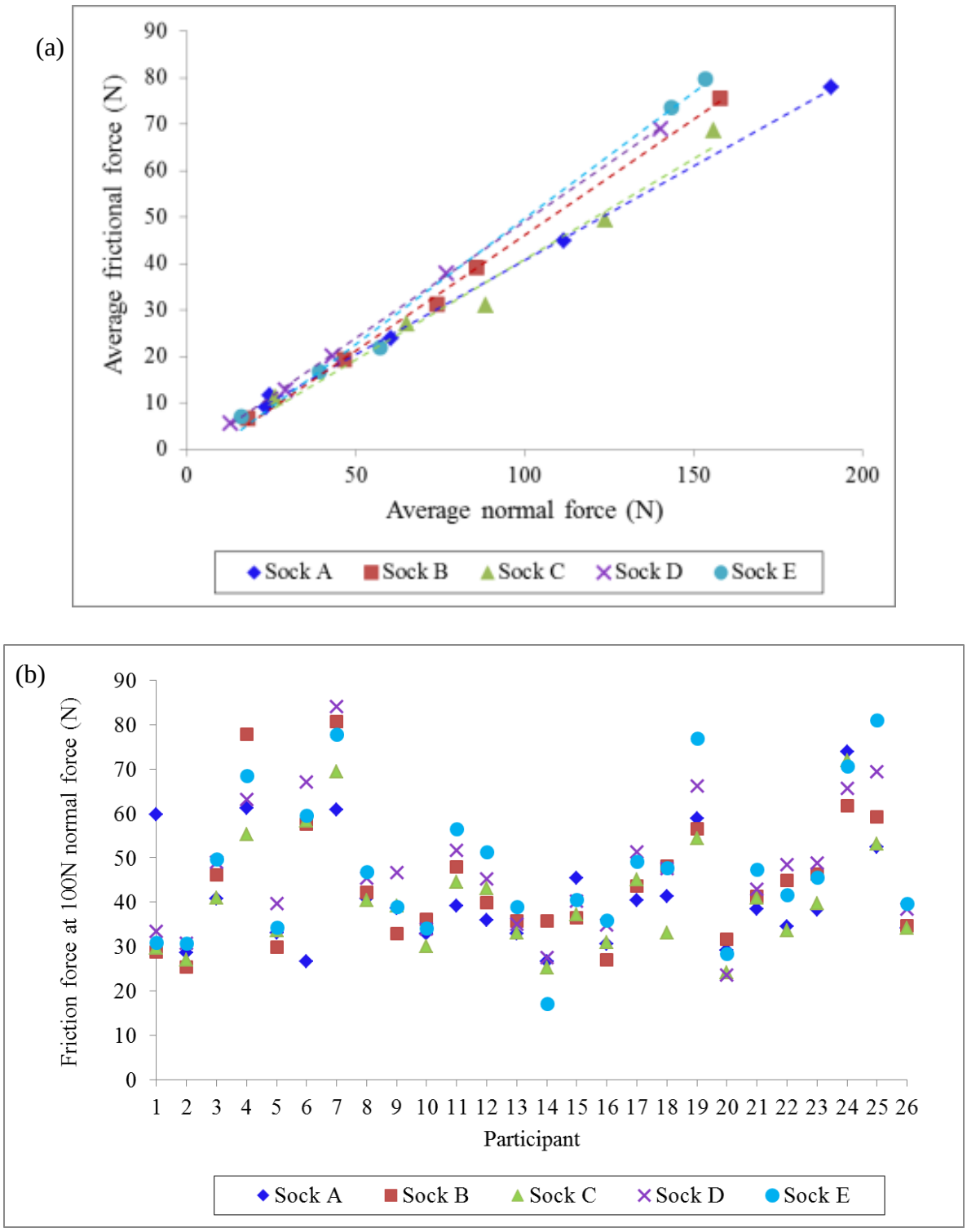

Figure 3.17: (a) Force data for the five sock materials from one of the participants (Subject 6); (b) The friction force produced against five sock materials from all 26 participants.

3.6.9 Evaluating the relationship between friction force and average foot hydration level

In order to analyse the relationship between friction force and foot hydration level, the friction values for the five socks were averaged for each participant and compared with their corresponding average foot hydration level as shown in Figure 3.18. There was a moderate positive correlation between the average friction force and hydration level ($r = 0.661$, $p<0.05$). The error bars show the standard deviations obtained from averaging 18 hydration measurements taken across the plantar region of the foot (x-axis) and from averaging the friction force values at 100N normal force across all five tested sock materials. Higher foot hydration level tended to produce higher friction force when interacted with sock materials. This is in agreement with many previous investigations that showed a similar outcome when moist skin interacts with other surfaces [34]. Other studies reported that skin surface hydration affects the mechanical properties of the skin resulting in a reduced skin tissue elastic modulus [104] which could lead to this trend.

Please note that in this study, the friction tests were carried out in dry condition whilst keeping the foot hydration level fairly similar to the baseline hydration measurements obtained prior to each test. However, this does not eliminate the possibility that the foot hydration level could fluctuate throughout each test run due to perspiration and increased absorption of moisture from high load application. This was reflected in the Corneometer readings taken immediately after friction test where the foot hydration values increased slightly compared to the baselines. In order to acquire good comparisons between the data, it is therefore crucial to consistently monitor the foot hydration level in friction experiments.

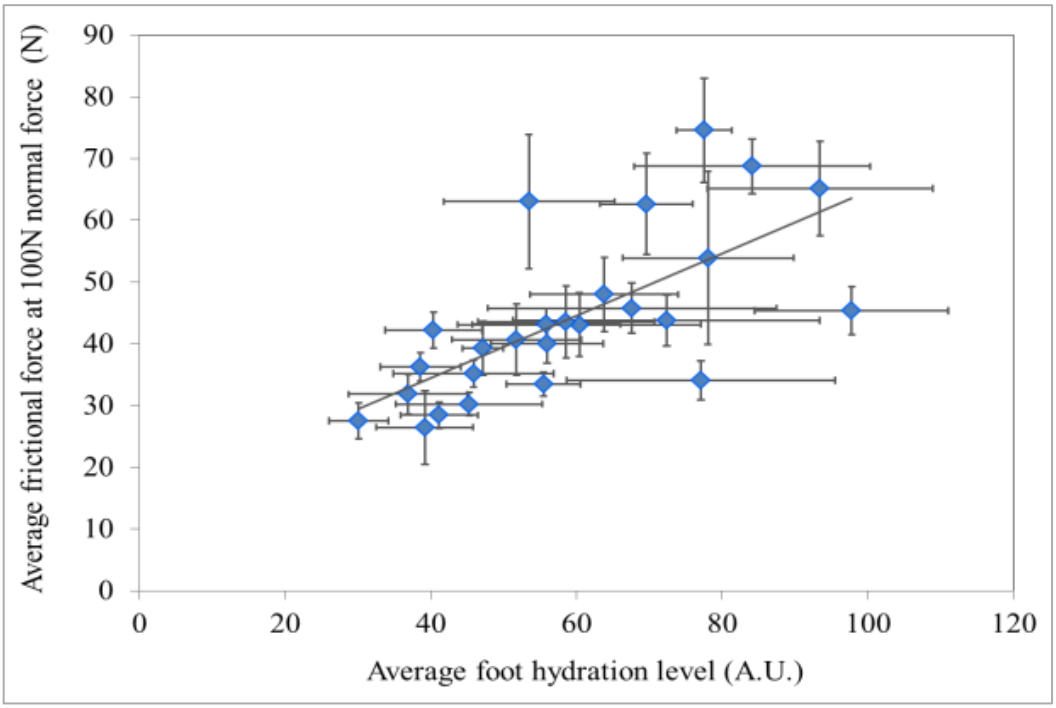

Figure 3.18: Positive correlation between friction force at 100N normal force and varying foot hydration level obtained from 26 participants (r = 0.661, $p < 0.05$).

3.6.10 Evaluating the effect of contact area against the applied normal loading

In this study, the real contact area of the plantar aspect of the foot was assessed against the applied normal loads. Some of the data obtained were not processed due to the false measurements recorded in the applied normal load which exceeded 500N, i.e. the maximum measurable normal load by the foot friction plate rig. A total of 111 data points was processed and normalised by the measured foot length by width, which are presented against their corresponding applied normal load in Figure 3.19.

It can be seen that the increasing trend of the contact area obeys the power law given by the following equation:

$$A \propto {F_N}^c$$

where A is the normalised contact area, F_N is the applied normal load and c is the exponent of F_N. The normalised contact area was shown to depend on the applied normal load to the power of 0.21.

Although no statistical correlation ($p > 0.05$) was found between the participants, a significant moderate correlation was obtained between the normalised contact area and the applied normal loads ($r = 0.450$, $p < 0.05$). Since human skin is considered to be a non-linear, anisotropic, heterogeneous viscoelastic material, its contact area increases as the applied normal load increases. At a lower range of normal load of less than 100N, a relatively steep increase can be seen in the contact area and as the normal load approaches 500N, the increment reaches a plateau at an approximate level of 0.45. This could be attributed to the stress-strain behaviour of the human skin, as discussed earlier in Chapter 1. At lower range of loads, the collagen fibres within the skin dermis lengthen resulting in larger deformations, hence the rapid increment in the contact area. However, as the applied normal load increases, the skin reaches its maximum extensibility resulting in a much stiffer skin surface, and hence only slight increment in contact area. If the applied normal load were to be further increased, it can therefore be concluded that the contact area will either increase very slightly or remain unchanged.

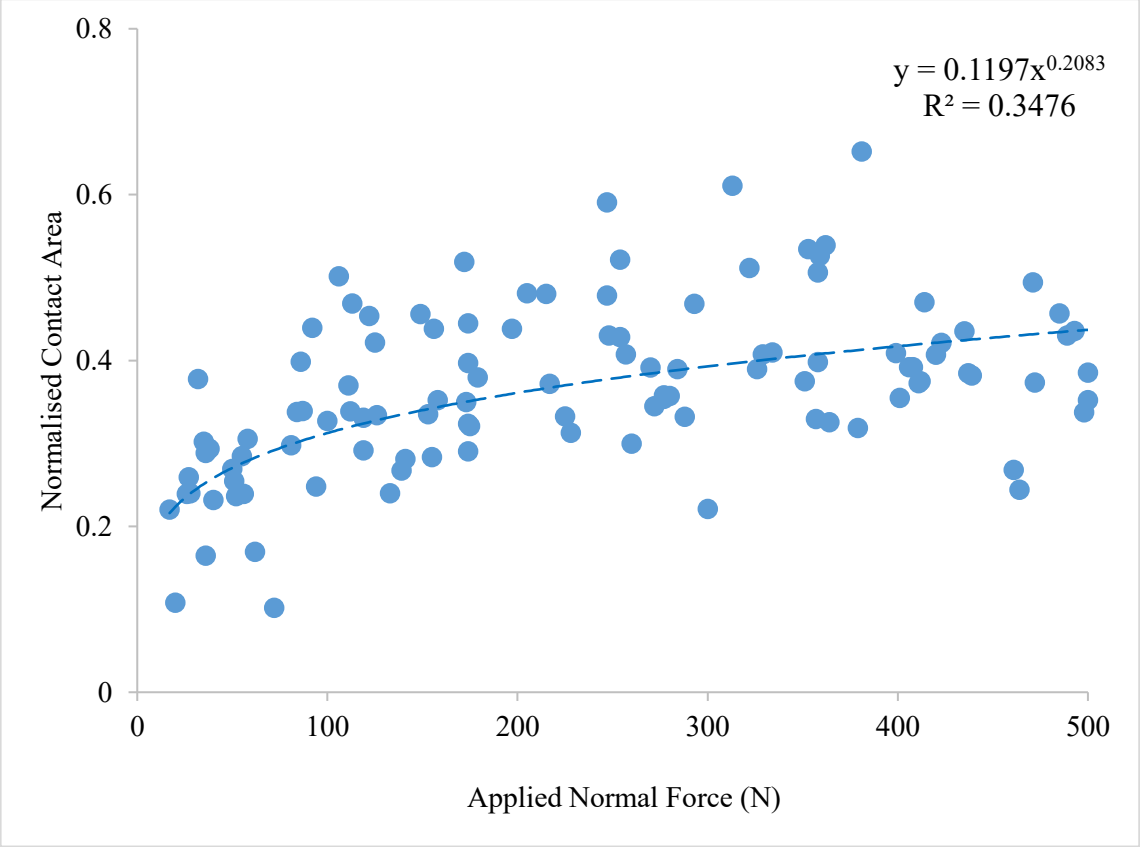

Figure 3.19: Positive correlation between normalized contact area and applied normal load (n = 111, r = 0.450, $p < 0.05$).

3.6.11 Conclusion

This study has established a standard protocol to assess the frictional behaviour of sock materials against human plantar skin in dry conditions. No consistent differences were found between the different socks tested. A relationship was found between friction and foot hydration, indicating that the control of skin moisture levels within the shoe environment could be a key factor to control blisters. It was also found that the contact area of the plantar skin increases with increased applied normal load up to a point of approximately 0.45. Other factors such as the skin roughness may also influence the friction of plantar skin and this warrants further investigation.

3.7 Investigating the frictional behaviour of first metatarsal head (1MTH) against running sock fabrics in different moisture conditions

3.7.1 Introduction

As mentioned in the earlier chapters, the lack of a standard moisture control protocol for fabric experiments means research related to sock moisture can be challenging to carry out and presents difficulties in comparing different studies. Presently, the most commonly used technique in quantifying the change in the amount of moisture within the sock is by weighing them pre- and post-test to compute the weight difference that has taken place. In another study by Van Amber *et al.* [102] the socks were placed in a washing machine and submitted to a time-varying wetting cycle prior to testing to achieve damp socks (i.e. a technique adapted from a study by Laing *et al.* [106]). Although these two methods may have their own practical advantage in studies conducted in a small scale or in accordance to the standard textile testing procedure, they are not considered to be the most time-efficient techniques for human subject testing.

In this current study, the application of the standard moisture control protocol was extended to assess frictional behaviour of the plantar aspect of the first metatarsal head (1MTH), which is one of the most blister-prone areas on the foot [13], against two different types of running socks in three moisture conditions (dry, low moisture, wet). The findings obtained from this study will be used to build on the knowledge from our earlier studies.

3.7.2 Tested sock materials

In this study two types of running socks with different material composition and knit patterns were selected (see Table 3.6).

Table 3.6: Characteristics of the running socks used in this study.

Sock type	Material compositions	Knit pattern	Mean thickness ± SD (mm)
Anti-blister "ABS"	99% nylon and 1% elastane	Simple jersey	1.18 ± 0.04
Cotton-rich "CRS"	70% cotton, 29% nylon, and 1%elastane	Terry jersey	2.62 ± 0.08

Three new sock materials were used for each participant with each new sock corresponding to each tested moisture condition. The order of the tested sock material was counter-balanced for each participant. In order to better reflect the real-world use, all newly-purchased sock materials were hand-washed using water and a mild liquid detergent and left to air-dry at room temperature for at least 72 hours prior to the test. Pre-washing the socks also ensured their dimensional stability and helped to remove any contaminants trapped in the sock fibres.

3.7.3 Study participants and test conditions

Twenty-six healthy participants (18 males and 8 females; average age in years, 25.4 ± 4.3 SD) were recruited from the same institution for the purpose of this study. Approval was obtained from the Ethics Committee at the University of Sheffield. All participants were informed of the entire testing procedure prior to the study and provided their written consent. In addition, they were also informed of the outlined inclusion and exclusion criteria of the eligibility for the study, as outlined earlier in this chapter. The participants were also assessed for their vascular and neuropathy conditions. All testing was performed in a controlled-laboratory setting with a temperature of between 20 to 22ºC and a relative humidity of 40 to 60%.

3.7.4 Experimental procedure of the foot skin characterisation tests: hydration, deformability and temperature

Participants were asked to clean the foot that was to be tested for 1 minute using a room temperature water bath in order to remove any contaminants and sock fibres. The foot was then carefully dried with paper towels and allowed to acclimatise to room conditions for 10 minutes. Hydration measurements were taken on the 1MTH region at intervals similar to the

previous study: 1) prior to cleaning; 2) after cleaning and acclimatisation; 3) prior to friction tests and 4) immediately after each friction test. The hydration measurements taken after cleaning and acclimatisation were considered as the baseline foot hydration level and used for subsequent analysis. Halfway through testing, cleaning and acclimatisation was repeated before changing the sock materials to remove any sweat or contaminant build-up and ensure consistency.

3.7.5 Experimental procedure of the friction test

The foot friction plate friction plate rig was employed for all skin-sock fabric measurements. The sock material was cut along the dorsal line and strained to 50% in both vertical and horizontal directions before being securely adhered to the rig test plate [15]. The sock was placed in such a way that its inside surface facing outwards (i.e. to provide the skin-sock interface for the friction tests). Friction tests were performed on the plantar region of the sock material within the marked area of 102×54 mm. Participants were instructed to press their foot against the sock material and then pushed their foot forward, maintaining the initial level of normal load and a relatively consistent, self-monitored, sliding velocity. Participants were also required to lift their toes throughout sliding to ensure only the 1MTH region was in contact with the sock material during testing, and this was observed and checked throughout.

3.7.6 Moisture application protocol

In order to achieve to achieve three sock moisture conditions that were significantly different from one another: “dry”, “low moisture” and “wet”, the standard moisture control protocol was employed. Water was applied to the targeted region of the sock material using a bottled sprayer, placed 150 mm away from the sock surface. Each spray delivered approximately 1.4 ml of water. After spraying, moisture was left to absorb into the sock for 1 minute before carrying out a set of three Corneometer® measurements, spanning the tested sock region. Spraying and measurements were repeated until the intended level of moisture was reached (see Table 3.7). Sock moisture was also monitored after each test to ensure the intended moisture range was maintained and further sprays were applied if the measurement values

fell lower than the intended range. On the other hand, if the moisture level increased above the intended range, either due to water being squeezed out from the sock fibres or through perspiration, the sock was allowed to dry for a short while before further monitoring. It should be noted that since the maximum reading that the Corneometer® was capable of was 120 AU, some of the "wet" condition samples found at this level may have had slightly higher actual amount of moisture present than indicated.

Table 3.7: Corneometer® measurements defined for each moisture condition.

Moisture condition	**Intended Corneometer range (AU)**	**Measured Corneometer reading ± SD (AU)**	
		ABS socks	**CRS socks**
Dry	15-17	15.81 ± 0.27	15.98 ± 0.19
Low Moisture, "LMo"	40-50	46.70 ± 4.39	46.13 ± 5.04
Wet	110-120	119.35 ± 1.66	118.64 ± 1.76

For all participants, the order of testing was kept the same, starting with "dry" condition followed by "low moisture" and finally "wet". Tests were carried out five times at a range of applied normal loads, for each moisture condition. After each set of tests, an 8-minute rest period was given to the participants to ensure that the hydration level of the 1MTH returned to its baseline. The rest period was also included to allow the investigators to run a quick check on the sock materials, ensuring that it was still securely adhered to the test plate as well as to prevent the participants from being fatigued. Subsequent data analysis and an interpolation protocol was used to calculate the friction force that would be required to slide the foot for each fabric-moisture combination, when pressed against the sock with 100 N normal force.

3.7.7 Statistical analysis

All statistical analyses were performed using SPSS 22.0 (Chicago, USA). The Shapiro-Wilk test was used to confirm that any data sets were normally distributed (at significance level $p > 0.05$) prior to performing the one-way analysis of variance (ANOVA) and Pearson's correlation coefficients among assessed variables.

3.7.8 Investigating the effects of sock moisture level variation on 1MTH friction

One-way ANOVA tests revealed that when moisture data for both sock materials at the same intended moisture condition was compared, no statistical differences could be found at the level $p < 0.05$. This demonstrates the ability of the monitoring and control protocol in being able to maintain appropriate levels of moisture condition in the sock textiles.

The friction force data (corresponding to a normal load of 100 N) plotted against sock moisture level was presented in both Figures 3.20 (a) and 3.20 (b), for tests on the anti-blister and cotton-rich socks, respectively. It can be clearly seen that the three moisture conditions, "Dry", "LMo" and "Wet" are distinctively differentiated by the intended range of Corneometer® readings (see Table 3.7 above). A number of the "Wet" data can be seen to be at the maximum measurement level of 120 AU, meaning they could have been slightly wetter than indicated by this value. One-way ANOVA (independent variable: defined moisture condition; dependent variable: sock moisture level measured using the Corneometer®) was performed to compare the moisture data for each moisture condition. The results confirmed statistically significant differences at the level $p < 0.05$ for tests on both sock materials.

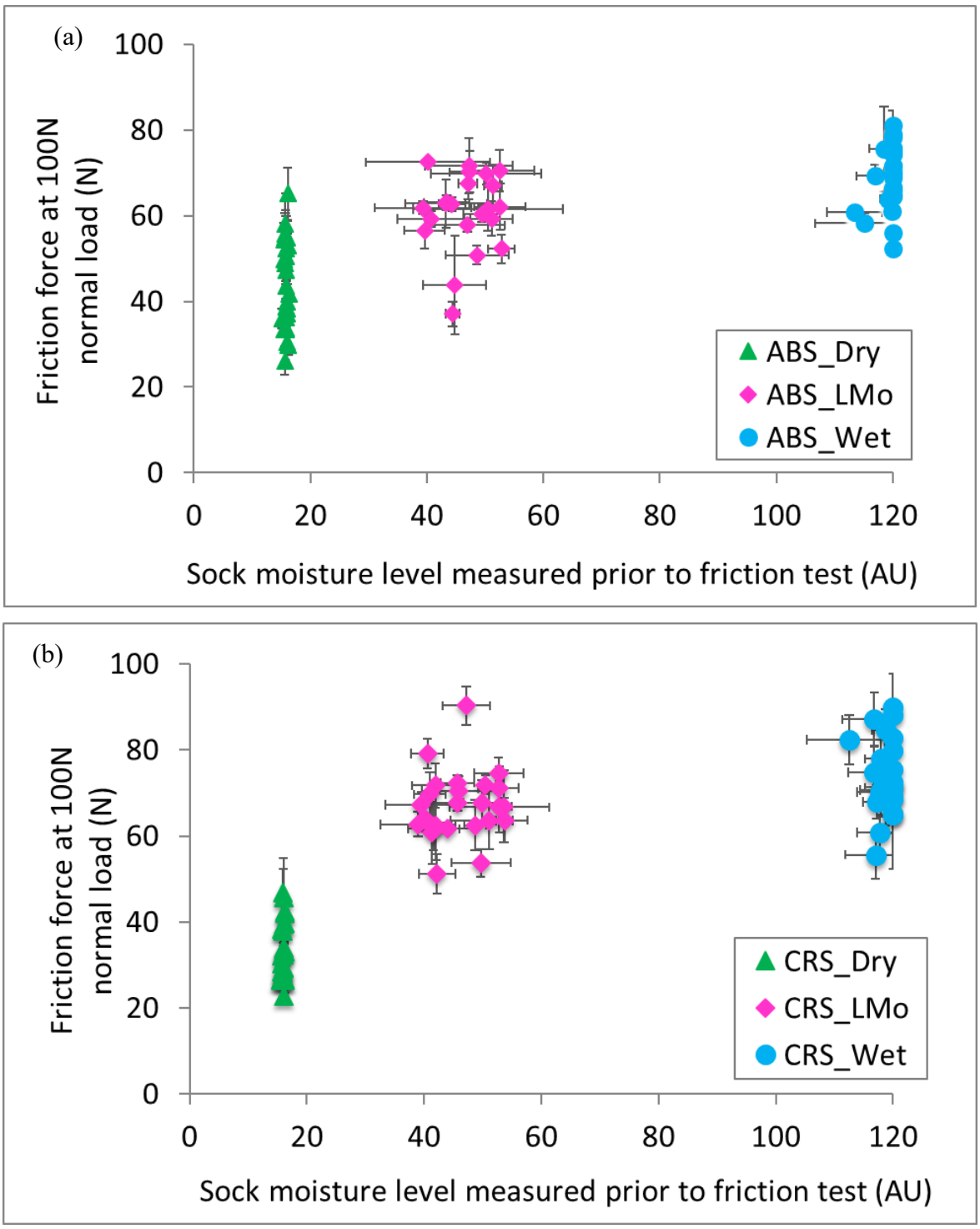

Figure 3.20: Sliding fiction force data plotted against sock moisture level for each participant tested wit (a) the anti-blister sock; (b) the cotton-rich sock (n = 26 for each sock/moisture combination)

A noticeable increase can be seen in the level of friction forces, necessary for sliding, as the sock moisture increases above the dry condition. This was validated by the statistically significant differences ($p < 0.05$) produced by the one-way ANOVA test (independent variable: defined moisture condition; dependent variable: friction force at 100N normal load). When comparing "wet" with "low moisture" condition data, the slight increase in friction of approximately 10% may be due to an increase in contact area between the 1MTH and sock surface due to swelling of sock fibres [9] following water absorption. Cotton fibres that make up 70% of the cotton-rich sock are more hydrophilic than the nylon fibres that make up 99% of the anti-blister sock [9]. This is most likely why a greater effect due to moisture is seen in Figure 3.20 (b), compared to Figure 3.20 (a). As mentioned earlier, it should be noted that even though the three moisture conditions were found to be statistically different with ANOVA, the "wet" condition tests could have included moisture readings somewhat higher than the maximum measurable value of 120 AU.

3.7.9 Investigating the effects of foot hydration level on friction

The relationships between the measured 1MTH moisture prior to friction tests and the sliding friction at 100N normal loading, for each textile-moisture combination are presented in Figure 3.21. No significant relationships could be found at the level ($p < 0.05$), for any of the textile-moisture combinations. This did not concur with a previous study [12] that found a moderate positive correlation between foot moisture and friction. However, in the previous study [12], the skin hydration level was averaged over the entire plantar area as opposed to being localised in the 1MTH region, as in the current study. A high variation of skin hydration level can be seen even within the same individual [16] and the lack of a measurable effect of foot moisture in the current study could be attributed to participant-specific factors such as skin condition, pressure distribution and foot anatomy.

It should be noted that the study did not aim to achieve a high range of foot moisture. The fact that the foot was well ventilated (not being inside a shoe) and participants were not undergoing exertion, meant that higher hydration levels may be found in real-world sports scenarios. In addition, although the feet were acclimatised in-between the friction testing, some of the water may still be absorbed by the 1MTH skin when it was in contact with the

"low moisture" and "wet" fabrics during sliding. This could increase the area of contact between the skin and the sock fabric due to increased skin tissue flexibility, as seen in previous studies [34, 104]. By monitoring the foot hydration level at specific intervals in accordance to the established test protocol ensured that this effect could be considerably minimised.

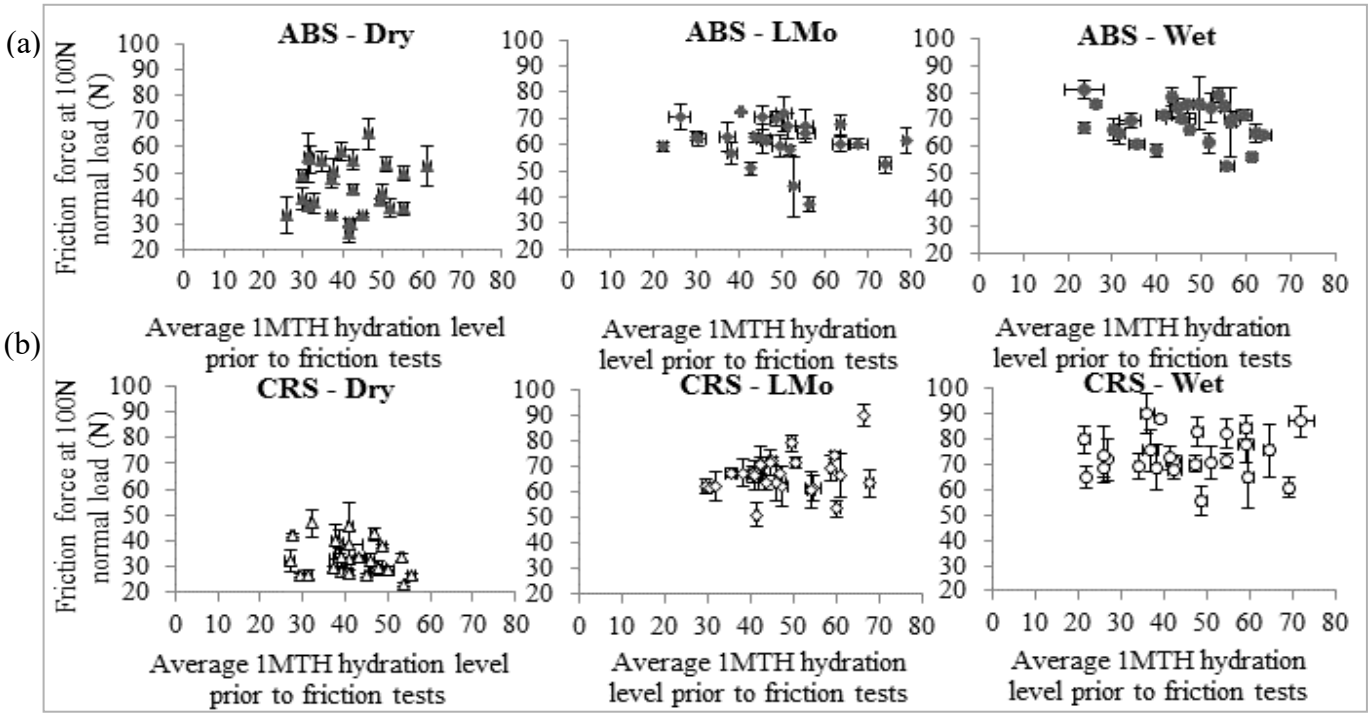

Figure 3.21: Sliding friction force data plotted against the measured 1MTH moisture level prior to friction tests for each participant, separated by sock moisture condition, tested with (a) the anti-blister sock; (b) the cotton-rich sock (n = 26 for each sock/moisture combination)

3.7.10 Comparisons of the sock frictional performance across moisture conditions

The sliding friction force data for both sock materials was converted to dynamic coefficients of friction (DCOF) by dividing by the 100 N normal load, on which the data was based. This data was plotted in Figure 3.22, with each moisture condition indicated. The effect of moisture on increasing friction can be seen but a line of gradient 1 allowed comparison between socks. In dry conditions, the anti-blister sock produced higher sliding friction than

the cotton-rich sock. However, when moisture was present, the opposite effect was observed All six textile-moisture combinations were also compared in Table 3.8 which presents the highest friction sock for each comparison, along with the level of significance from a one-way ANOVA test (independent variable: sock textile-moisture combination; dependent variable: DCOF). All comparisons showed statistically significant differences at the level $p < 0.05$ [F (5, 150) = 99.03, p= 0.000] apart from when comparing the low moisture cotton-rich sock with the wet anti-blister sock. Post hoc comparisons using the Bonferroni test indicated that the DCOF values for each sock textile-moisture combination are significantly different than the other. The effect size was calculated to be large (eta squared = 0.77), indicating the differences were indeed substantial.

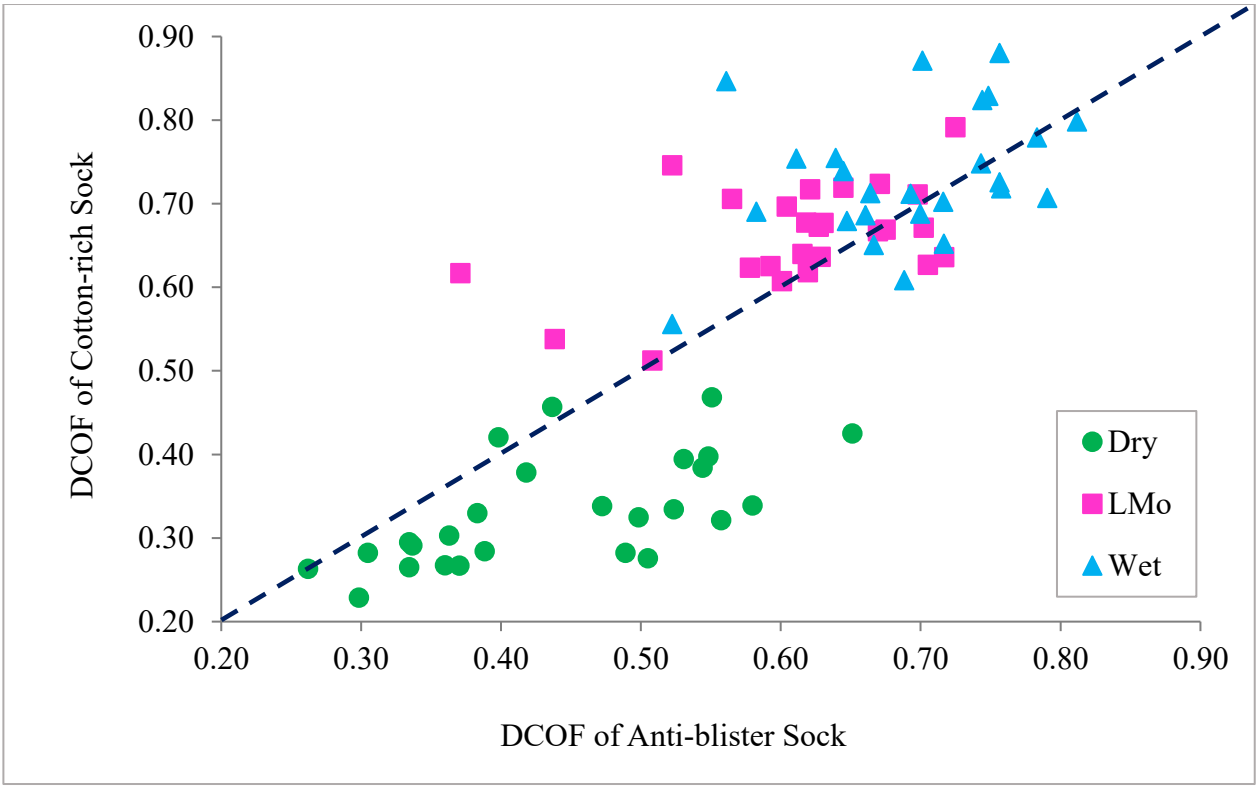

Figure 3.22: Dynamic coefficient of friction data for both sock materials, plotted against one another for comparison.

Table 3.8: Comparisons of sock frictional performance in different moisture conditions including the values of mean DCOF±**SD** (▲: highest DCOF;; ═: similar DCOF level). The level of significance is indicated by * ($p < 0.05$).

	ABS_Dry (DCOF = 0.44 ± 0.10)	**ABS_LMo (DCOF = 0.61 ± 0.08)**	**ABS_Wet (DCOF = 0.69 ± 0.07)**
CRS_Dry (DCOF = 0.33 ± 0.07)	ABS (▲) p=0.000*	ABS (▲) p=0.000*	ABS (▲) p=0.000*
CRS_LMo (DCOF = 0.67 ± 0.08)	CRS (▲) p=0.000*	CRS (▲) p=0.011*	ABS ═ CRS p=0.448
CRS_Wet (DCOF = 0.74 ± 0.08)	CRS (▲) p=0.000*	CRS (▲) p=0.000*	CRS (▲) p=0.028*

In a real-life scenario it is reasonable to expect some degree of moisture in the foot-sock contact due to perspiration, so comparing the sock frictional performance in "low-moisture" or "wet" conditions seems to be most appropriate. Based on this assumption, the anti-blister sock can be considered as the sock which would have least friction. However, if athletes find that they experience drier feet when using a cotton-rich sock, then a real-world comparison may be different (i.e. "ABS LMo" vs "CRS Dry" in Table 3.8). There could be many reasons why the socks perform differently, as the jersey pattern (simple vs terry) had been found in a previous study to have an effect [2] and the different sock fibres (cotton vs nylon) will have different tribological properties and hydrophobicity [17]. Further work is required to study the separate and combined effects of these factors.

3.7.11 Conclusions

This study demonstrated the extended application of a moisture control protocol and an experimental approach capable of assessing skin-sock friction at appropriate levels of loading in the 1MTH region. The desired moisture levels were found to be controllable to a high level of repeatability. It was found that by increasing sock moisture above the dry condition will increase the foot-sock sliding friction for both sock materials tested. However, no significant correlation ($p > 0.05$) was seen between foot hydration level and sliding friction over the hydration range tested. In comparing both socks tested, the anti-blister sock is expected to

provide lower friction during intensive athletic events where moisture is present due to perspiration.

3.8 Monitoring skin morphological parameters of the 1MTH using an Optical Coherence Tomography (OCT) in a skin-fabric friction study

3.8.1 Introduction

Few studies were conducted to assess changes in skin morphology during tribological measurements. The purpose of this study is to monitor skin morphology in the first metatarsal head (1MTH) region using optical coherence tomography (OCT) during a skin–sock textile friction study.

3.8.2 Experimental method

Data from twelve male participants (average age, 26.2 years ± 4.7 SD) obtained from the 1MTH friction study were analysed using the analysis algorithm described in Chapter 2. Participants tested with an anti-blister sock first were categorised as Group A whereas those tested with a cotton-rich sock first were categorised as Group B. Sub-surface OCT images of the 1MTH region (see examples in Figure 3.23) were obtained using a VivoSight system (Michelson Diagnostics) before and after friction measurements. The stratum corneum (SC) thickness and roughness of the outermost skin layer and the SC junction were then analysed and compared for any changes before and after friction tests.

3.8.3 Results and discussion

As seen in Figure 3.24, participants were found to have different SC thickness measurements from one another, but monitoring showed no individual SC thickness changes during the friction study. This indicates no measurable effects on SC due to the testing, either due to moisture absorption or abrasion. In Figure 3.25, friction was found to be affected by moisture condition, but correlations between the friction force at 100N normal load and the measured 1MTH morphological parameters for the subjects were not found to be significant at level (p

< 0.05). This suggests that friction behaviour could be dominated by other factors such as individuals' skin mechanical properties.

In conclusion, OCT can be used as a technique to continuously monitor skin property changes during friction studies which is not only limited to the skin thickness but also the skin roughness.

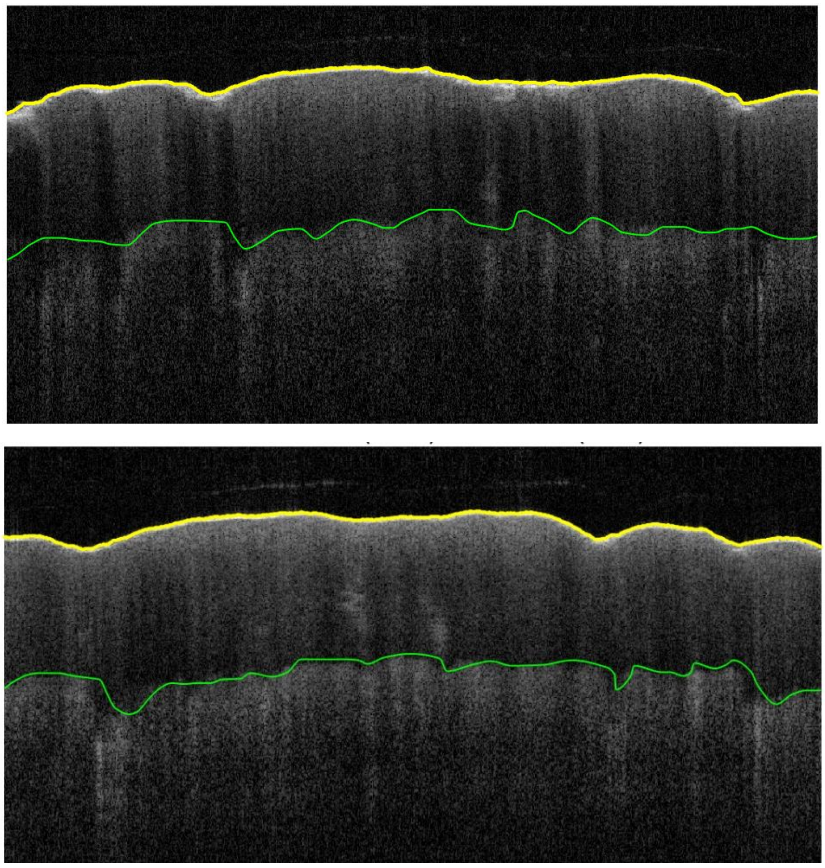

Figure 3.23: The above images show the SC layer taken from subject SA01 (left) before the friction test in dry condition and (right) after the friction test in dry condition. The yellow curve indicates the outermost SC layer whereas the green curve indicates the SC junction detected by the skin layer detection algorithms.

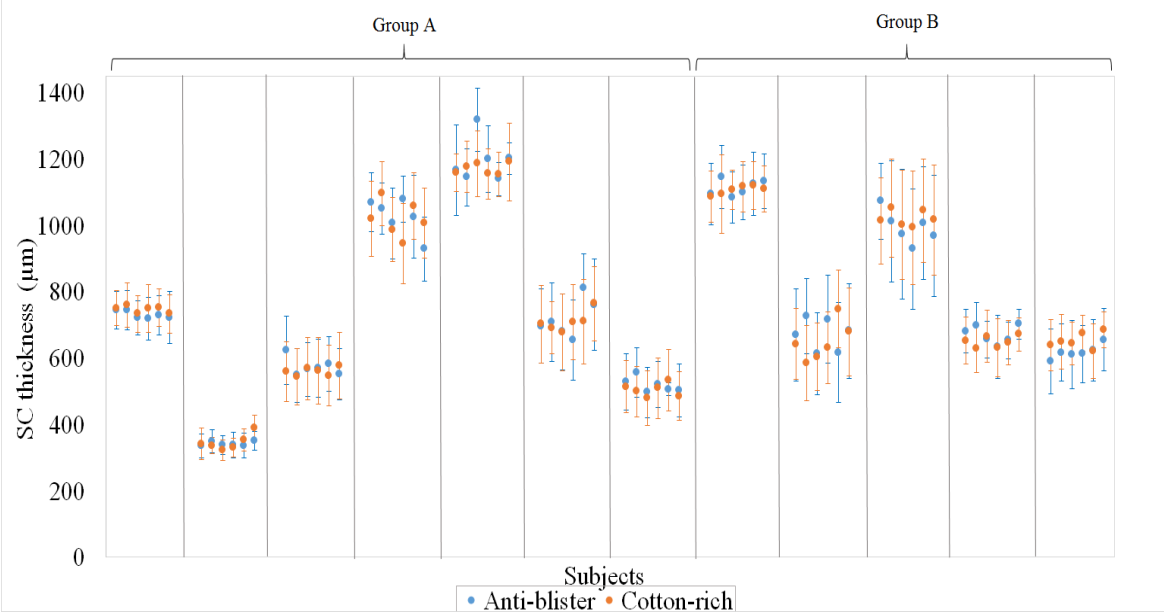

Figure 3.24: The diagram shows the SC thickness measured across all participants. Group A participants were tested with an anti-blister sock first whereas Group B participants were tested with a cotton-rich sock first. From left to right each epidermal thickness value corresponds to: (i) before friction test in dry condition; (ii) after friction test in dry condition; (iii) before friction test in low moisture condition; (iv) after friction test in low moisture condition; (v) before friction test in wet condition; (vi) after friction test in wet condition. The error bars indicate the standard errors of the thickness measurements taken over the 1MTH region.

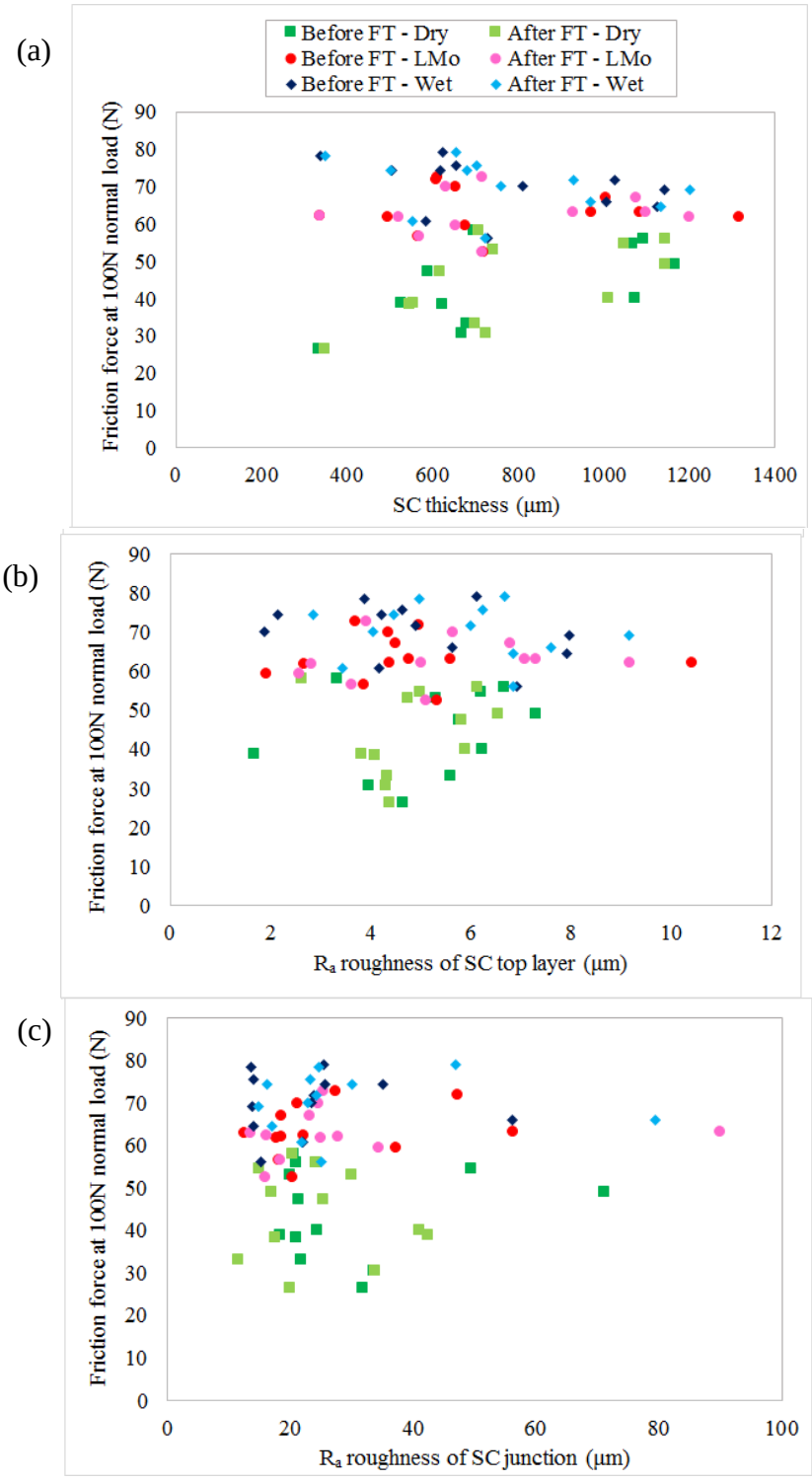

Figure 3.25: The diagram above shows the friction force at 100N normal load plotted against the (a) SC thickness; (b) R_a roughness of the SC top layer; and (c) R_a roughness of the detected SC junction for both before and after friction tests across all moisture conditions.

Chapter 4

Development of biofidelic test-beds

4.1 Introduction

Synthetic skin models made of polymeric materials have been proposed and described in a number of previous studies for their applications in skin and textile research. In friction blister studies, utilising synthetic skin test-beds provide numerous advantages in comparison to conducting the research on human participants or animal test subjects. For instance, they allow friction tests to be carried out at much higher ranges of applied normal load. This produces frictional data that are more comparable to that experienced by human skin in daily life. In addition, the test-beds can also be made to be attachable to measurement instrumentation, enabling more controlled loading to be achieved thus increasing the reproducibility factor of the study. It can also be assumed that since synthetic test-beds do not require any special surface preparation prior to testing, unlike human skin, the testing can therefore be carried out in a more time-efficient manner. Additionally, the versatility of polymeric materials allows a range of synthetic test-beds to be fabricated in order to represent a variation of human skin characteristics (such as thick, thin, young and old skin) as well as specific skin conditions (such as callused and dehydrated skin).

However, there remain challenges in developing test-beds that closely resemble human skin still remains. This could partly be attributed to the difficulties in selecting the most appropriate type of polymers to represent the different skin layers. To date, there has been an increasing amount of research being carried out to address this particular issue although no conclusive results have been published. It should also be noted that the

complexity in developing the synthetic test-beds extends when taking their deformation and frictional properties into account. More often some compromise has to be made in the test-bed design. This is one of the main reasons why most existing synthetic test-beds are 'simplified' to represent just the basic structure of skin layers (epidermis, dermis and hypodermis), without including the muscles, tendons and nerve tissues. A hard-backed material may be included in the test-bed to represent the bone, which also functions to hold the different polymeric layers together as a solid structure [82, 83].

This chapter is dedicated to the development of biofidelic test-beds using a novel method. The term 'biofidelic' simply refers to the close resemblance to pertinent human physical characteristics such as the geometry, size, and stiffness. The 1MTH was chosen to be the simulated skin area which allows comparisons to be made with the 1MTH-sock fabric friction results obtained from the wider study (please refer to Chapter 3). The stages involved in the fabrication of the biofidelic test-beds are described along with the equipment, testing procedure and materials used. To the author's knowledge, no previous attempt has been made in simulating the 1MTH using polymeric materials. The results obtained from the deformation and frictional tests will be included and further discussed in the following Chapter 5.

4.2 Design Stage 1: Geometry of biofidelic test-beds

As discussed earlier in Chapter 1, the basic structure of skin comprises the epidermis (outermost skin layer), followed by the dermis which is anchored to the deeper layer of the subcutaneous tissue (hypodermis). Both dermis and subcutaneous tissue constitute the soft tissue of the skin structure. In order to closely simulate the human 1MTH in terms of its deformation and friction behaviours, it is firstly important that the geometry of the test-bed closely resembles the intended anatomy. Therefore, in the first design stage, a thorough review was conducted to obtain data and information from previous literatures on the thickness of the different 1MTH skin layers and their Young's modulus properties, as well as the geometry and dimensions of the 1MTH bone. The results from the review were tabulated in Table 4.1 below.

Table 4.1: The characteristics of the different layers in human first metatarsal head.

Layer	The characteristics of each respective layer obtained from previous studies		
	Thickness (mm)	**Young's Modulus (kPa)**	**Poisson's ratio**
Epidermis	0.55 ± 0.19 [107]	136 [108]	0.48 [108]
Dermis	3.00 [109]	80 [108]	0.48 [108]
Epidermis and soft tissue	9.43 ± 1.88 [107]	-	-
Fat pad	6.00 ± 1.20 [6]	34 [108]	0.48 [108]
1MTH	AP- 60.70 ± 3.86 ML– 20.66 ± 1.99 [110]	1500×10^{6} [108]	0.48 [108]

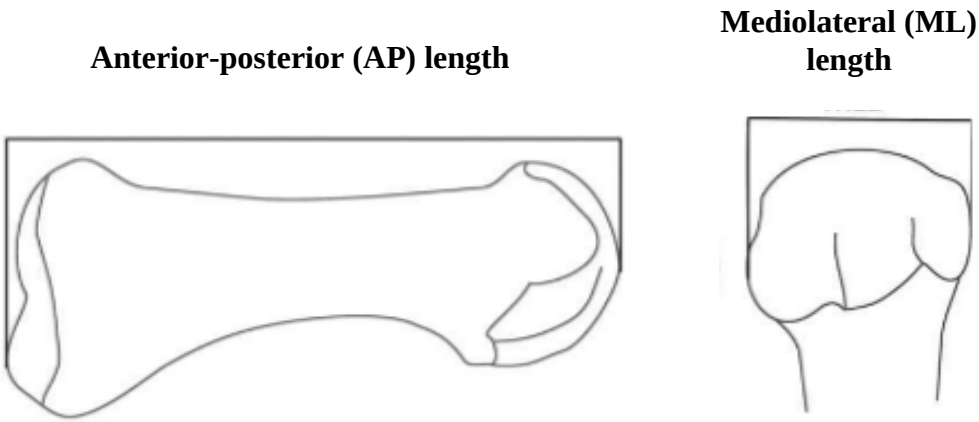

Figure 4.1: The anterior-posterior and mediolateral dimensions of the 1MTH bone as reported in a study by De Groote *et. al* [110] (the image was adapted from the same study).

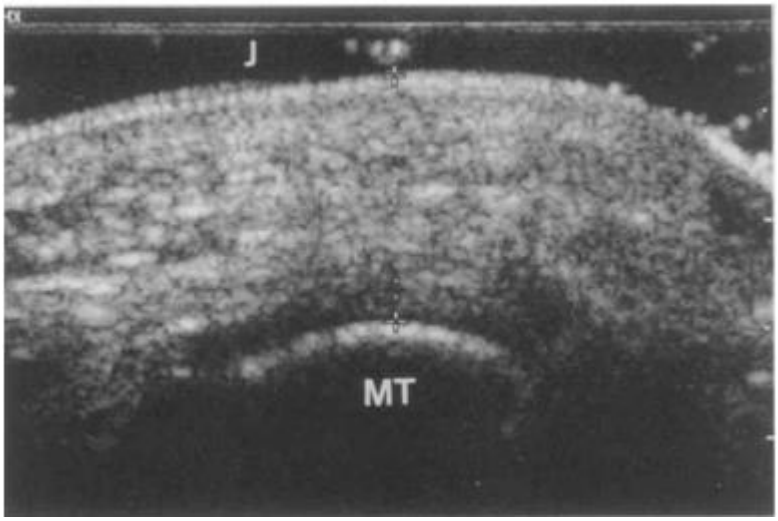

Figure 4.2: A cross-section of the 1MTH and the soft tissue; MT- metatarsal head (image reproduced from [111].

A cross-section of the 1MTH obtained from a study carried out by Wang et. al [111] was used as a reference shape for the biofidelic test-beds.

4.2.1 Selecting the geometry of the prototype test-beds

After collating the required data and information on the geometry of the human 1MTH, a decision has to be made in terms of the number of layers that need to be incorporated into the test-bed design. As the skin is a non-linear material, simulating all three skin layers in a test-bed may increase the complexities in controlling desired parameters which will lead to considerable inconsistencies during deformation and friction tests. By simplifying the three-layer physical skin model into a two-layer system, with the first layer simulating the combined 1MTH epidermal dermal tissues and the second layer representing the combined 1MTH dermal and subcutaneous tissues, these issues can be greatly reduced. Besides, in order to develop a set of prototype test-beds which vary from one another, it is more important that the dimensions and mechanical properties of the layers can easily be manipulated to achieve the desired mechanical and frictional behaviours.

Figure 4.3 shows the two-layer skin model which is equivalent to the three-layer human 1MTH skin. The equivalent thickness, L_{eq} and Young's moduli, E_{eq} of the two-layer model were then evaluated using the data obtained in Table 4.1.

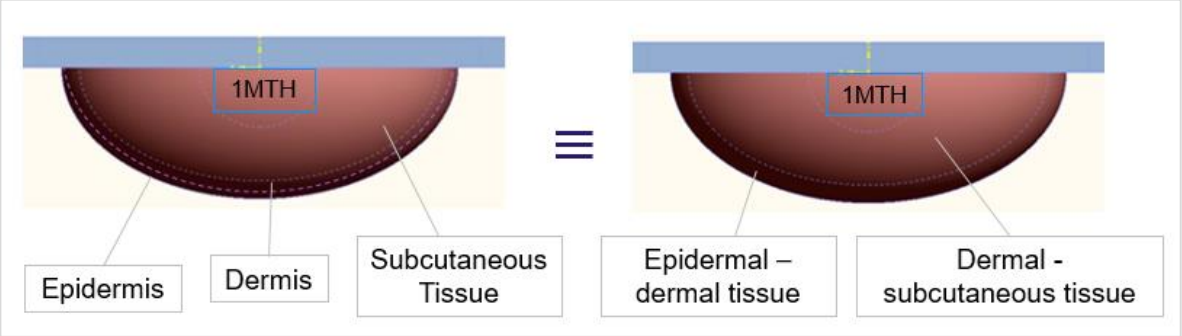

Figure 4.3: The equivalent two-layer model for the prototype test-beds with its respective combined layers.

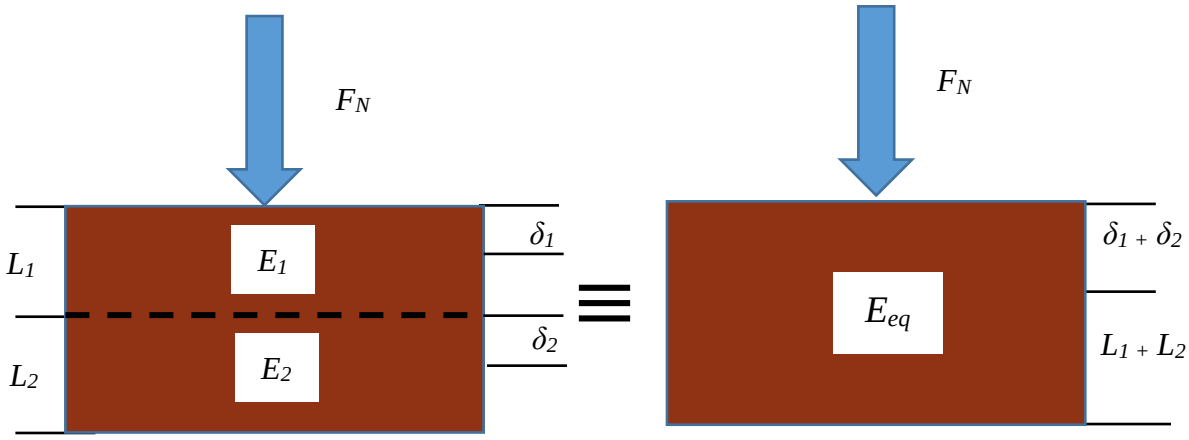

Figure 4.4: The free-body diagram used to evaluate the equivalent thickness and Young's moduli of the two-layer model for the prototype test-bed.

Both layer 1 and layer 2 of the test-bed are assumed to have the same cross-sectional area and are subjected to equal normal force.

$$A_1 = A_2 = A$$

$$F_1 = F_2 = F_N$$

The Young's modulus, E is stress, σ divided by strain, ε. Stress is normal force divided by the cross-sectional area, A and strain is the change in length, δ divided by the original length, L.

$$E = \frac{F_N/A}{\delta/L} = \frac{F_N . L}{A . \delta}$$

Therefore,

$$\delta_1 = \frac{F_N . L_1}{A . E_1}$$

$$\delta_2 = \frac{F_N . L_2}{A . E_2}$$

For the equivalent two-layer test-bed,

$$(\delta_1 + \delta_2) = \frac{F_N}{A}\left(\frac{L_1}{E_1} + \frac{L_2}{E_2}\right) = \frac{F_N}{A}\frac{(L_1 + L_2)}{E_{eq}}$$

The equivalent Young's modulus value can then be obtained from the following equation:

$$E_{eq} = \frac{(L_1 + L_2)}{\left(\frac{L_1}{E_1} + \frac{L_2}{E_2}\right)}$$

Table 4.2 presents the calculated equivalent thickness and Young's modulus values for each combined layer of the two-layer test-bed. Note that the dimension of the bone was estimated based on the data reported in the previous literature. These values will be used as reference values during the fabrication of the prototype test-beds in design stage 3.

Table 4.2: The equivalent thickness and Young's modulus values for the simulated combined layer of the two-layer skin model

Simulated combined layer	**Equivalent thickness (mm)**	**Equivalent Young's modulus (kPa)**
Epidermal - dermal tissue	3.43	85.7
Dermal - subcutaneous tissue	8.88	41.8
1MTH bone	10.00	1500×10^6

In general, the biofidelic prototype test-bed will have an axisymmetric shape resembling the cross-section of the 1MTH shown in Figure 4.2 and comprises two simulated combined layers, with the outer layer representing the epidermal-dermal tissues and the inner layer representing the dermal-subcutaneous tissues. A material of a hemisphere shape will also be incorporated into the test-bed to simulate the 1MTH bone. Figure 4.5 shows the schematic drawing of the prototype biofidelic test-bed with the dimensions for each respective layer. Note that in the schematic drawing, the biofidelic test-bed was attached to a flat plate which provides a firm base for the test-bed. A constraint plate was also included in the design of the prototype test-bed to securely hold the test-bed during manual handling and testing.

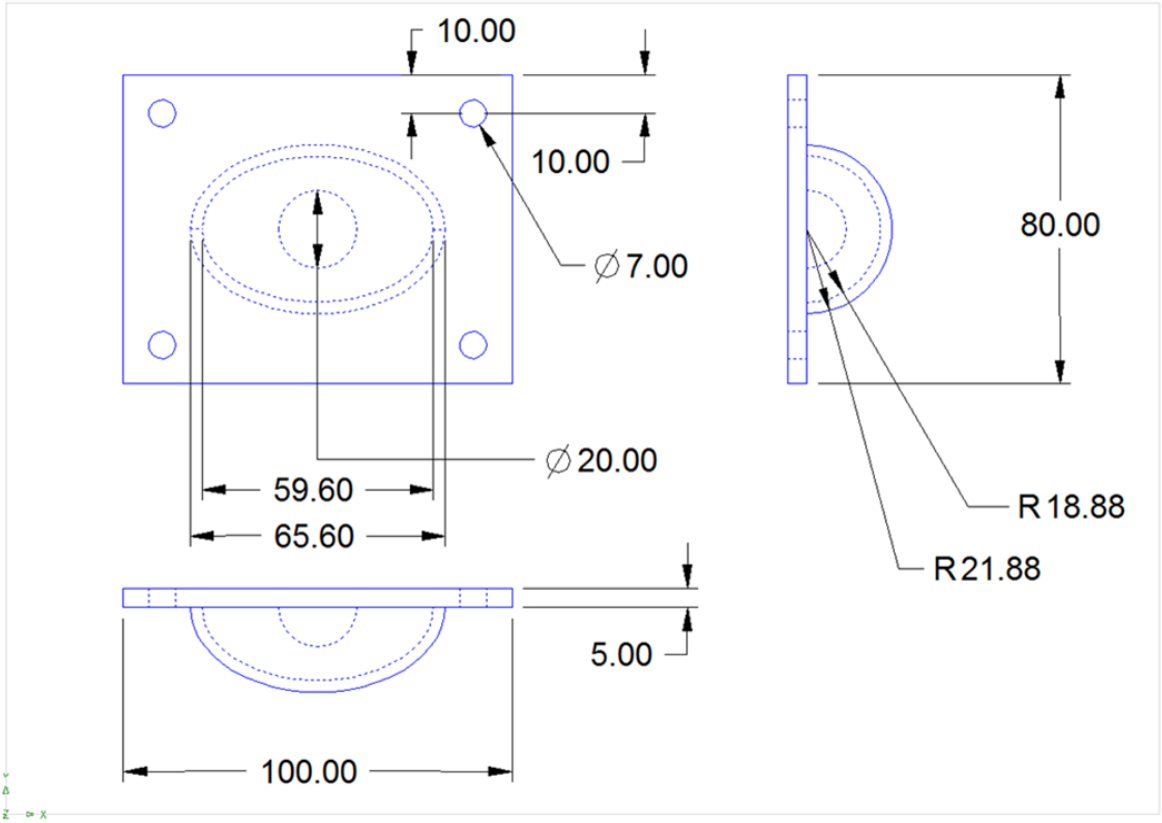

Figure 4.5: The schematic drawing of the biofidelic test-bed with the dimensions for each respective layer.

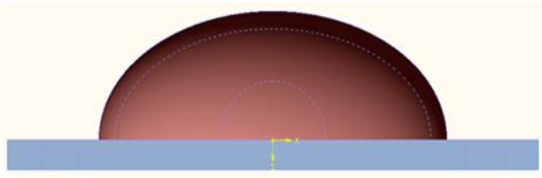

Antero-posterior projection of the test-bed on a flat base

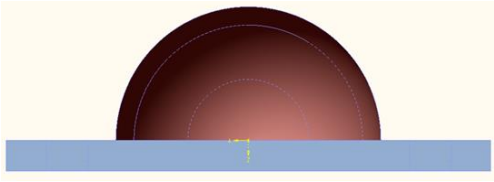

Medio-lateral projection of the test-bed on a flat base

Assembled prototype biofidelic test-bed with a constraint plate

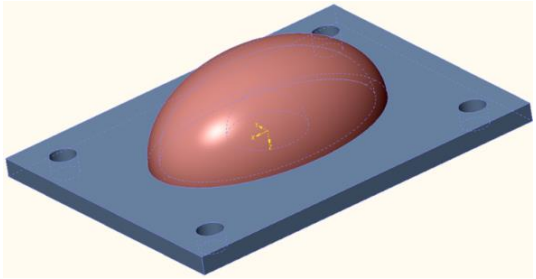

Figure 4.6: The mechanical sketches of the prototype biofidelic test-bed with a flat base and a constraint plate.

4.3 Design Stage 2: Material selection for the biofidelic test-beds

4.3.1 Selection of candidate materials

A number of potential candidate materials were identified and tested to be used to simulate the combined layer of the biofidelic test-beds, as summarised in Table 4.3. The materials were shortlisted from a wide range of polymers which have been commonly used to simulate human skin. All materials were subjected to Dynamic Mechanical Analysis (DMA) tests, which will be described in the following section. The test results obtained from the DMA tests helped to inform the mechanical properties of each material in varying compositions.

The following factors were taken into consideration during the material selection process:

1) Availability of the material
2) Versatility of the material
3) Shelf-life / durability of the material
4) Ease of use in terms of its working and curing time
5) Cost of the material
6) Material storage

Table 4.3: A summary of the potential candidate materials for each layer of the prototype biofidelic test-beds. **E-D** denotes the epidermal-dermal tissues whereas **D-SC** denotes the dermal-subcutaneous tissues

Simulated layer	Candidate material	Material description
E-D	Liquid latex (Polycraft)	This is an extremely versatile material which is often used in a wide range of manufacturing industries and film industries. It cures at room temperature within 30 to 60 minutes, depending on the thickness of the layer.
E-D **D-SC**	Pro-Gel 10 (PS Composites)	A two-part silicone consisting of part A (base) and part B (catalyst). This type of silicone quickly cures at room temperature within 20 minutes with a mixing ratio of 1:1. A softener may be added to reduce the elastic modulus.
D-SC	Silskin 10 (Polycraft)	A two-part room temperature vulcanising silicone consisting of part A (base) and part B (catalyst). It cures at room temperature in 60 minutes. Silicone softener can be added to the mixture to soften the material but only up to a maximum of 40% of the total base and softener mixture. It has a shelf-life of 18 months.
D-SC	Magic Power Gel (Raytech)	A two-part polyorganosiloxanes silicone consisting of part A (base) and part B (softener). It has a 10-minute working time and cures relatively quickly at room temperature. It does not have a shelf-life.
D-SC	S-10 RTV (Polycraft)	A two-part silicone consisting of part A (base) and part B (catalyst). It cures at room temperature and has the longest curingtime of up to 7 days, depending on the size of the sample. Silicone softener can be also added to the mixture to reduce the elastic modulus.
1MTH bone	Stainless steel	Hemisphere of steel used to represent the hard bone layer.

4.3.2 Dynamic Mechanical Analysis (DMA) of candidate materials

Dynamic Mechanical Analysis (DMA) is a widely-used technique to characterise polymers in terms of their viscoelastic behaviour. Prior to the DMA tests, the polymer samples were moulded into cylindrical shapes using syringes and left to cure at room temperature for 24 hours. Each sample was 20.0mm in length and approximately 12.4mm in diameter.

Two different types of material tests were performed using a Viscoanalyseur Metravib VA2000 which are: 1) strain sweep and 2) temperature sweep tests. In the strain sweep test, the samples were sinusoidally loaded at 1Hz with an applied dynamic strain in the range of 0 to 0.010, with a gradual increment of 0.0001. The Young's modulus and loss factor (tan delta) results were then recorded in the functions of the experimental dynamic strain. Prior to the temperature sweep test, the polymer samples were cooled to 0^0C using liquid nitrogen before being subjected to a temperature change up to 40 ^{0}C, with a gradual increment of 1^0C per minute. Similar to the strain sweep test, the Young's modulus and loss factor (tan delta) results were obtained as functions of the test temperature. The results of the DMA testing were then compared among the samples for the purpose of material selection. Both sweep and temperature sweep tests were carried out by technician, Les Morton, and the results obtained were fully processed and analysed by the author of this thesis.

Figure 4.7: The Viscoanalyseur used for the Dynamic Mechanical Analysis (DMA) testing.

4.3.3 Material selection and determination of material composition for the prototype test-beds

It was noted that the results obtained from both strain and temperature sweep tests across all tested materials were very comparable. Therefore, for purposes of clarity, only sweep test results for each material will be presented in this thesis. The results obtained were plotted in terms of their Young's modulus, as shown in Figures 4.8 - 4.11.

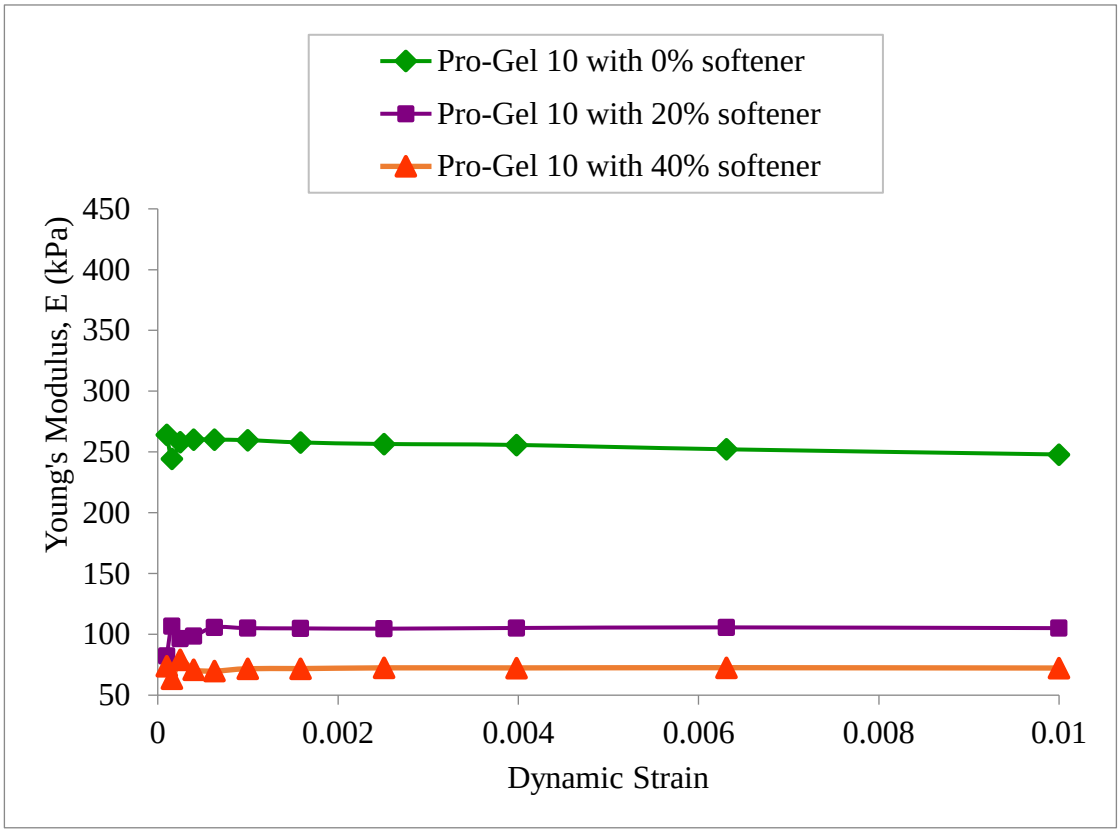

Figure 4.8: The strain sweep test results obtained for the Pro-Gel 10 at three different percentages of softener.

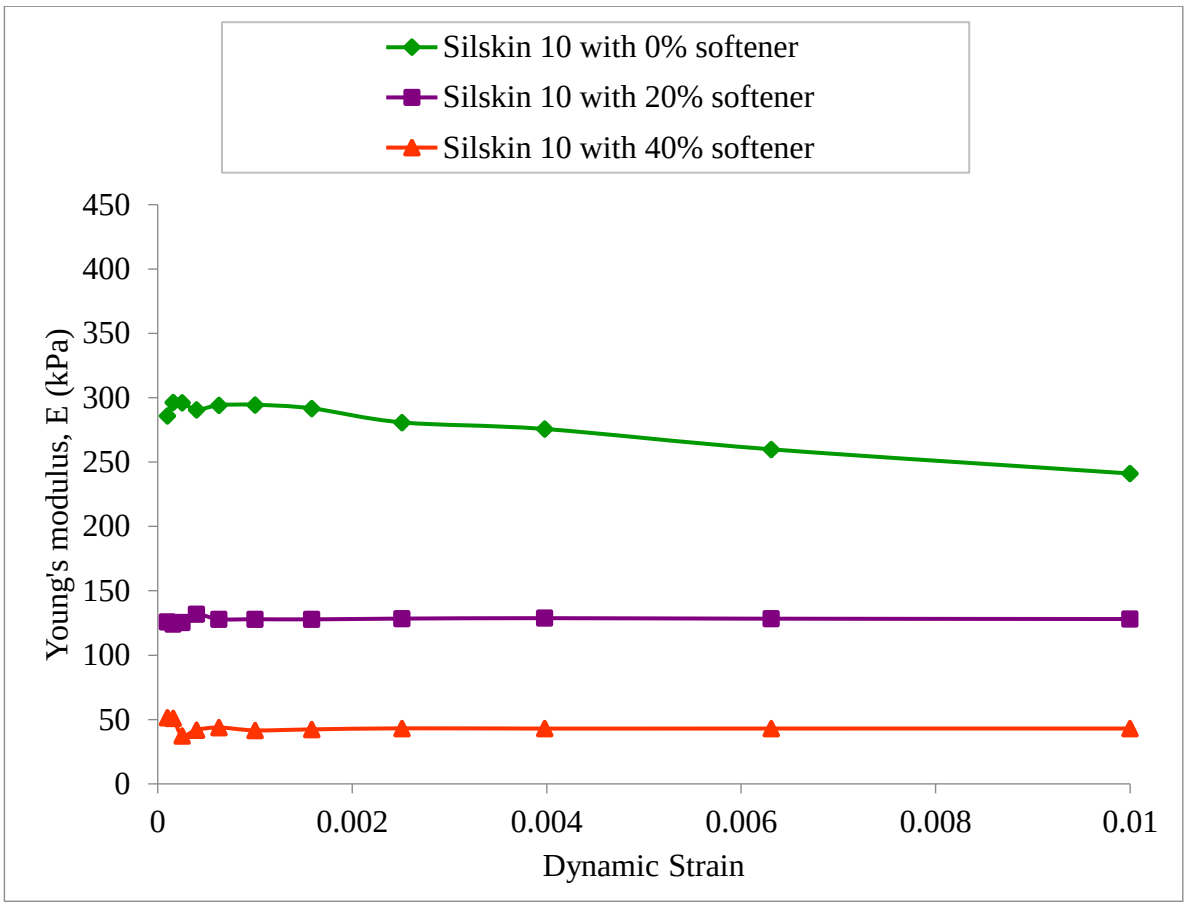

Figure 4.9: The strain sweep test results obtained for the Silskin 10 at three different percentages of softener.

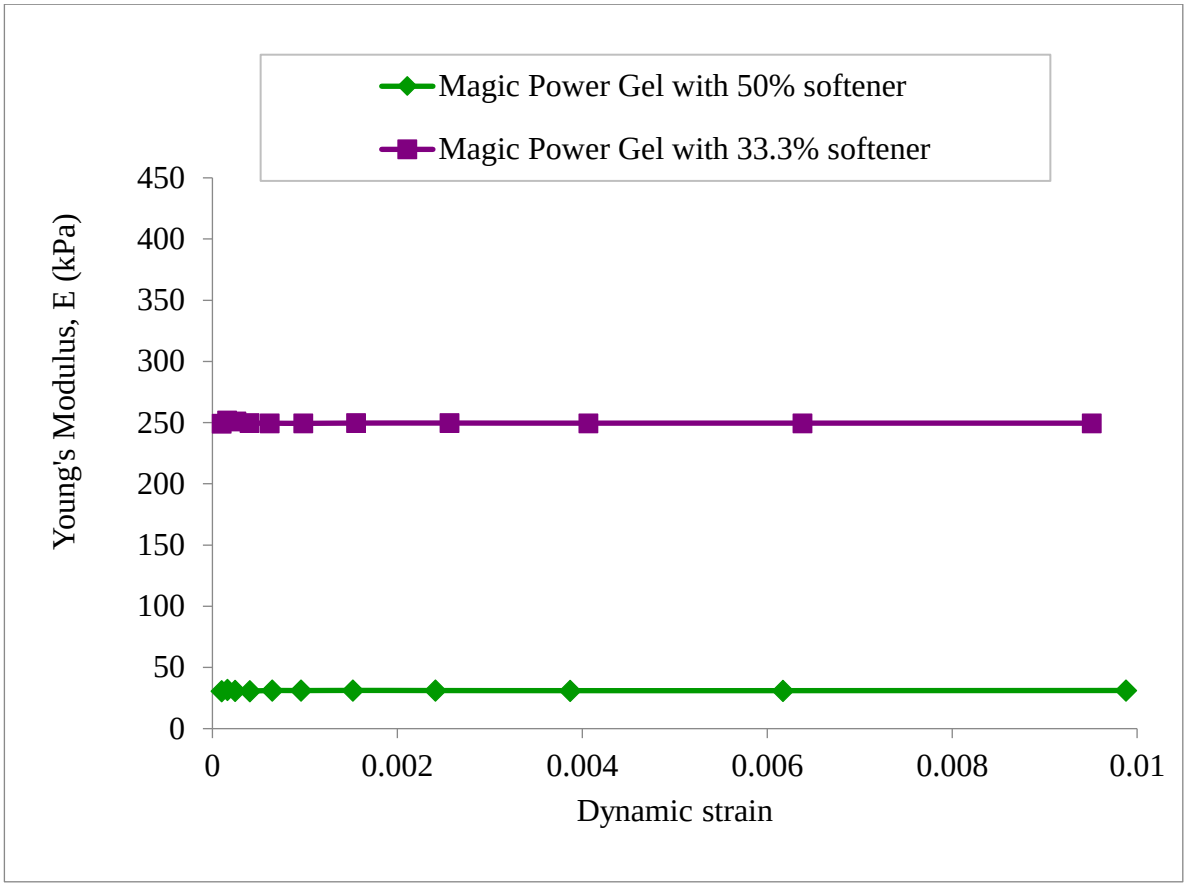

Figure 4.10: The strain sweep test results obtained for the Magic Power Gel at two different percentages of softener

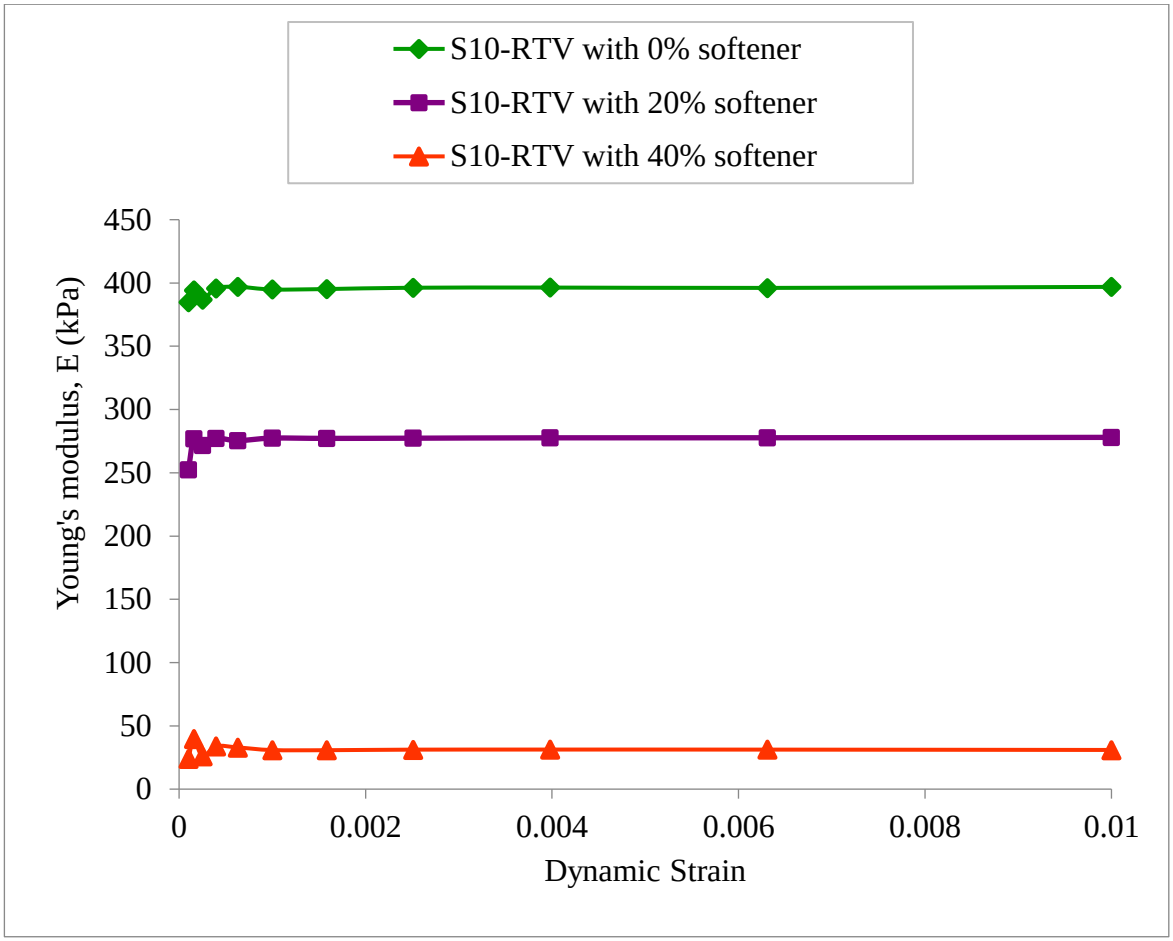

Figure 4.11: The strain sweep test results obtained for the S10-RTV silicone at three different percentages of softener.

The average Young's moduli across all materials were then evaluated and included in Table 4.4.

Table 4.4: The calculated averaged Young's modulus values for the tested polymer materials.

Tested material	Young's modulus, E (kPa)				
	0% softener	20% softener	33.3% softener	40% softener	50% softener
Pro-Gel 10	256.14	231.4	-	71.95	-
Silskin 10	394.02	101.92	-	31.16	-
S-10 RTV	282.48	127.68	-	43.82	-
Magic Power Gel	-	-	31.09	-	249.9

Two weeks following the strain sweep tests, it was noticed that for the samples made with Pro-Gel 10, Silskin 10 and S-10 RTV silicone materials became considerably stiffer than when they were first made. This is due to the ongoing cross-linking process at the molecular level between the base and the softener. Interestingly, the sample made using the polyorganosiloxanes silicone (Magic Power Gel) remained unchanged. The samples made with Pro-Gel 10, Silskin 10 and S-10 RTV silicones were submitted to another two strain sweep test at two-week interval after that and the Young's moduli for all samples changed quite considerably. This effect was even more pronounced in samples made with the highest percentages of softener since the high amount of softener increases the cross-linking rates. Therefore, based on these results, the polyorganosiloxanes silicone was selected to be the best polymer material to simulate the inner layer of the biofidelic test-beds.

The strain sweep test results of the Magic Power Gel were then extrapolated (see Figure 4.12) to obtain an estimate of a Young's modulus value comparable to human 1MTH. A range of intended Young's moduli values were used to obtain the percentages of softener required for the inner dermal-subcutaneous tissues of the test-beds (see Figure 4.12).

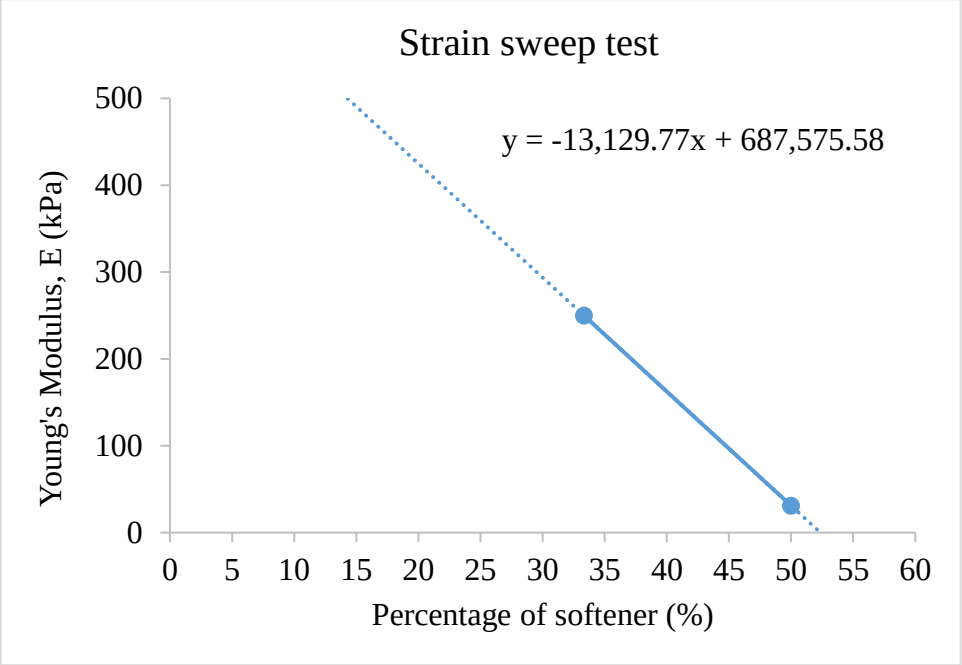

Figure 4.12: The extrapolated results obtained from the sweep test for Magic Power Gel.

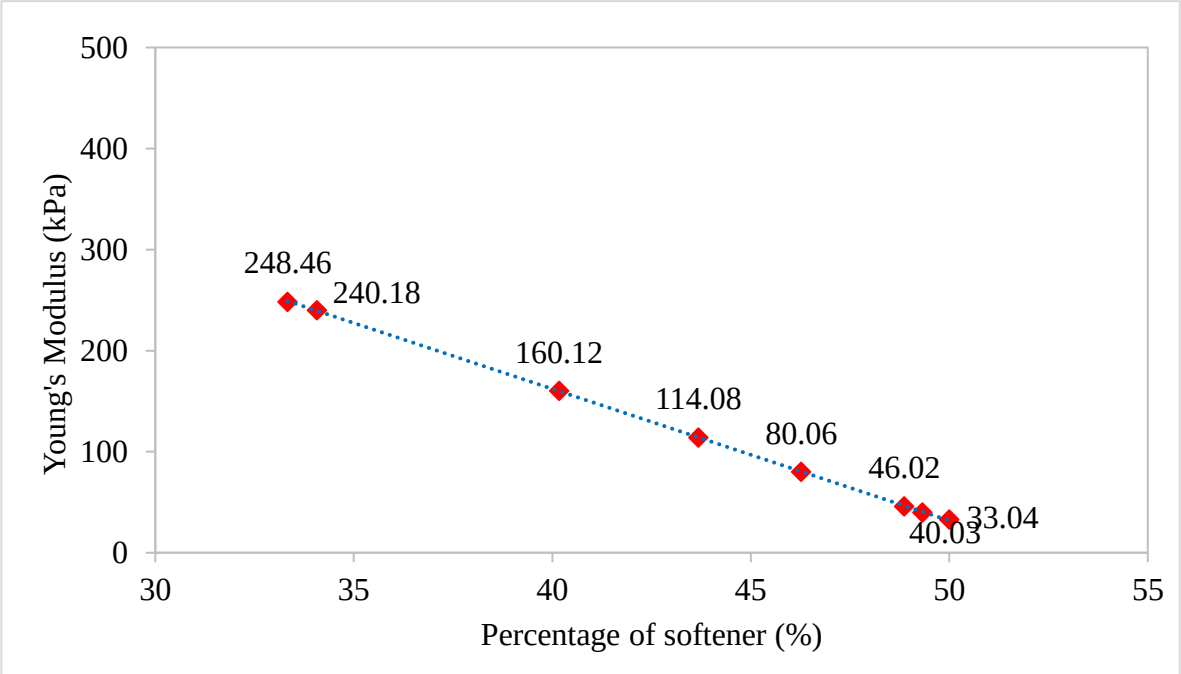

Figure 4.13: The extrapolated results obtained from the sweep test for Magic Power Gel.

Initially, both liquid latex and Pro-Gel 10 silicone were considered for the epidermal-dermal layer of the test-bed. However, from the pilot study, it was found that Pro-Gel 10 did not produce a robust surface for the outer layer of test-bed, in addition to being highly adhesive. The surface was easily damaged when subjected to low load friction test of less than 50N. Latex was therefore chosen to be the best material to simulate the outer layer of the biofidelic test-beds mainly due to its high durability. The liquid latex was also found to be highly versatile as it can be used to obtain surface textures from human foot.

4.4. Design Stage 3: Fabrication of the prototype biofidelic test-beds

4.4.1 Manufacture of textured surface layer

In order to obtain the plantar surface impression from a participant's foot for the manufacture of the latex outer skin, a number of approaches using different materials were attempted.

Chromatic Alginate (Polycraft)

Chromatic alginate is a skin-safe, non-allergenic moulding impression compound that is widely-popular among professional modellers and craft-makers. It is made of a type of seaweed and is even widely used in dentistry to take dental mouldings. It is easy to use and due to its relatively slow setting time, it allows the mixing to be made thoroughly. However, the mould could only last for a maximum 7 days before it becomes watery and mouldy. In addition, due to its slippery finished surface, liquid latex painting was extremely challenging and did not produce the desired outcome.

Plaster of Paris (Polycraft)

Similar to the Chromatic alginate, Plaster of Paris is a skin-safe, non-allergenic moulding impression compound that is frequently used in life-casting human body parts. It can be easily mixed with water and it has a much slower setting time compared with the alginate. Once the foot was removed from the mould, the imprint was clearly visible with a dry finished surface. Latex can be painted on the mould and easily removed once dried. However, some fine debris

was left attached to the textured latex and could not be fully removed. Cracks could occur in the mould over time as the plaster becomes drier.

Figure 4.14: The latex was painted on the foot impression made using the Plaster of Paris.

SILFLO (J & S Davis)

SILFLO is another type of impression polymer which is frequently used in dentistry and dermatology. It comes with a base material and a catalyst which helps to accelerates the setting process. It can be easily mixed without added water and self-dries within 5 to 10 minutes. The base and catalyst were mixed at a 1:2 before applying it onto a participant's skin. The skin was cleaned and acclimatised according to the acclimatisation protocol described in Chapter 2. Once it had dried and been removed from the skin, it was placed on a solid platform and secured using adhesive tape at its perimeter. The finished surface was clearly visible, enabling for the anterior and posterior of the 1MTH to be identified and marked prior to latex painting. No air bubbles were seen on the imprint and latex could easily be painted onto the surface. It was also noted that, unlike chromatic alginate and Plaster of Paris, the impression mould did not shrink in size over time and it was therefore selected as the best material to be used for obtaining the foot imprint. As with all polymer materials, SILFLO was kept away from direct sunlight and extreme humidity.

Figure 4.15: SILFLO used to obtain a negative impression of a participant's plantar skin (Subject S08).

4.4.2 Developing the test-bed mould

The next stage in fabricating the biofidelic test-beds is the development of the mould with the intended dimensions as shown in Figure 4.16. The mould was made of stainless steel.

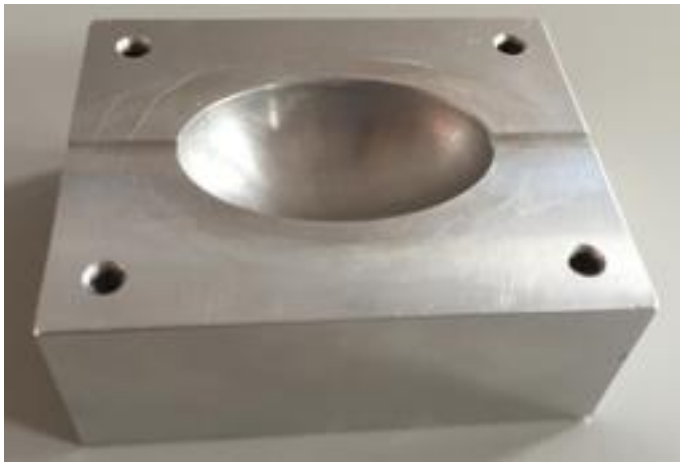

Figure 4.16: The manufactured biofidelic mould made of stainless steel.

4.4.3 Degassing vacuum chamber for mixture preparation

A degassing vacuum chamber allows the removal of air bubbles trapped within the polymeric mixture whilst setting, which could otherwise influence the deformation behaviour of the test-beds. The degassing chamber was self-assembled in collaboration with another PhD student, Almaky Almagirby. The equipment comprises a vacuum pump, a pressure gauge, a degassing bowl (chamber), a thick acrylic sheet and an air hose. The transparent acrylic sheet allows the polymeric mixture to be observed throughout the degassing procedure to ensure that all bubbles are degassed before removing it from the chamber.

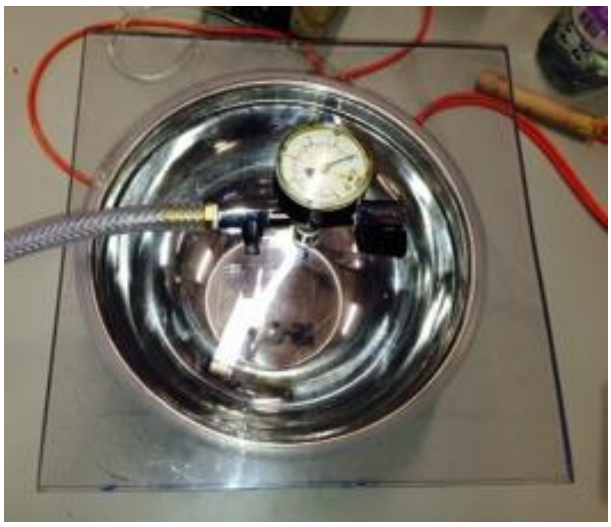

Figure 4.17: The self-assembled degassing chamber.

4.4.4 Summarised fabrication process for the biofidelic test-beds

The different steps involved in the fabrication of the biofidelic test-beds can be summarised as follows and are shown in Figure 4.18.

Step 1: Initially, a thin layer of liquid latex was evenly painted in the biofidelic mould and was left to dry at room condition for at least an hour before painting on another thin layer. Extra care was taken during this process to avoid the latex from clumping and air bubbles from forming. The latex was painted until the desired thickness was achieved.

Step 2: The Magic Power Gel was then mixed at the intended ratio and placed in the degassing chamber to remove the trapped air bubbles. The mixture was then carefully poured into the painted biofidelic mould with the latex layer already in. The stainless steel hemisphere, representing the 1MTH bone, was attached to a steel plate which allowed it to be suspended in the polymeric mixture during the curing process. The duration of the curing process is highly dependent on the amount of softener added into the silicone mixture. A higher percentage of softener will lengthen the curing process.

Step 3: For textured test-beds, the latex texture could be prepared while waiting for the sample to be fully cured. Similar to Step 1, a thin layer of liquid latex was evenly painted on the surface of the SILFLO foot imprint and was left to dry between 30 and 60 minutes before painting another layer. This process was repeated until the desired texture thickness was achieved.

Step 4: Once the sample was fully-cured, it was carefully removed from the mould and the latex texture was then placed on top of the sample, ensuring that no crinkles were formed on its surface and around its structure. The texture was then clamped using a plate to allow the latex texture to bond with the latex surface of the sample. This process could take up to 2 days to ensure that the texture is inseparable from the test-bed.

Initially eight prototype biofidelic test-beds were developed with four having textured surface and the remaining four non-textured. The thickness of each layer was then measured to ensure that the targeted thickness (please refer to Table 4.2) for each simulated combined layer was achieved. Table 4.5 below summarises the measured thickness and the material composition of the prototype biofidelic test-beds.

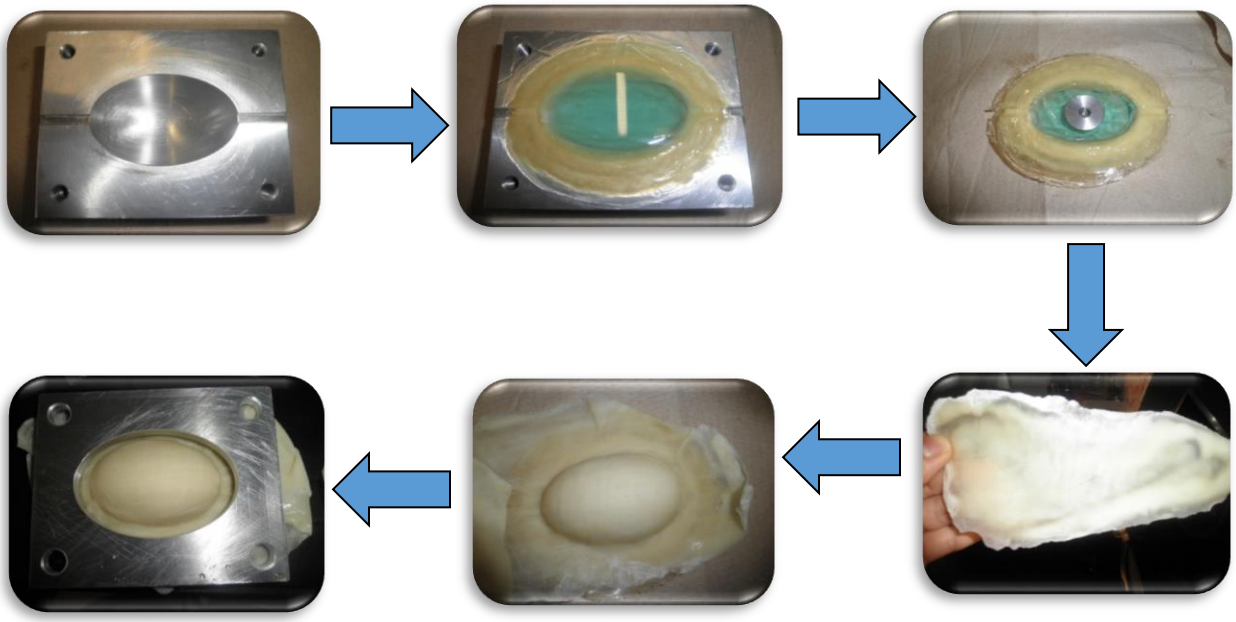

Figure 4.18: The various different steps involved in the fabrication of the biofidelic test-beds.

Table 4.5: Summarised material composition and respective layer thickness for all eight prototype biofidelic test-beds.

Test-bed	Combined epidermal-dermal tissues (Material: Latex rubber)			Combined dermal – subcutaneous tissues (Material: MagicPower Gel)		Total thickness of outer layer + inner layer + bone (mm)
	Non-textured (NT) or Textured (T)	Total thickness (mm)	Thickness of texture (mm)	Percentage of softener (%)	E (kPa)	
BFA	NT	2.95	-	49.46	40.03	20.66
BFB	NT	3.26	-	46.36	80.06	21.21
BFC	NT	2.82	-	40.17	160.12	20.79
BFD	NT	3.05	-	33.97	240.18	21.68
BFE	T	3.42	0.45	49.46	40.03	21.03
BFF	T	3.47	0.46	46.36	80.06	21.05
BFG	T	3.44	0.47	40.17	160.12	21.50
BFH	T	3.49	0.48	33.97	240.18	21.01

4.5 Design Stage 4: Testing prototype biofidelic test-beds

All biofidelic test-beds were submitted to deformation test prior to the friction test in order to assess their stiffness and Young's modulus values. For both indenter and flat plate deformation tests, the applied load was limited to 30N in order to prevent the test-beds from being damaged under high loads, but still sufficient to provide an insight into their behaviour under loading. Also, for the same reason, each test-bed was only tested once to minimise the risk of permanent deformation, which will adversely affect the friction tests.

4.5.1 Deformation tests using an indenter and a flat plate

The deformation test of the biofidelic test-beds was conducted using an indentation device equipped with a basic force gauge mounted on a manual test stand and a linear variable differential transformer (LVDT). An indenter with a diameter of 20mm and a flat plate with a thickness of 17mm were used to evaluate the deformation behaviour of the biofidelic test-beds. The indentation test was conducted in accordance to the Brinell indentation hardness principle (ASTM E10-12). The contact between the samples and the indenter and flat plate was fully lubricated with water-based lubricant to eliminate the influence of friction on the samples' deformation behaviour. This is also one of the assumptions provided by the Hertz theory of elastic contact, which is one of the classical solutions used by researchers to study non-adhesive elastic contact. The indentation device was manually operated to apply the intended normal load on the test-bed. Both the force gauge and LVDT was connected to a written LabView programme where the load-displacement plot obtained from each test-bed could be recorded for further analysis using an Oliver and Pharr approach which will be described further in the result section.

Figure 4.19: The flat plate and indenter used for the deformation tests, both manufactured from stainless steel.

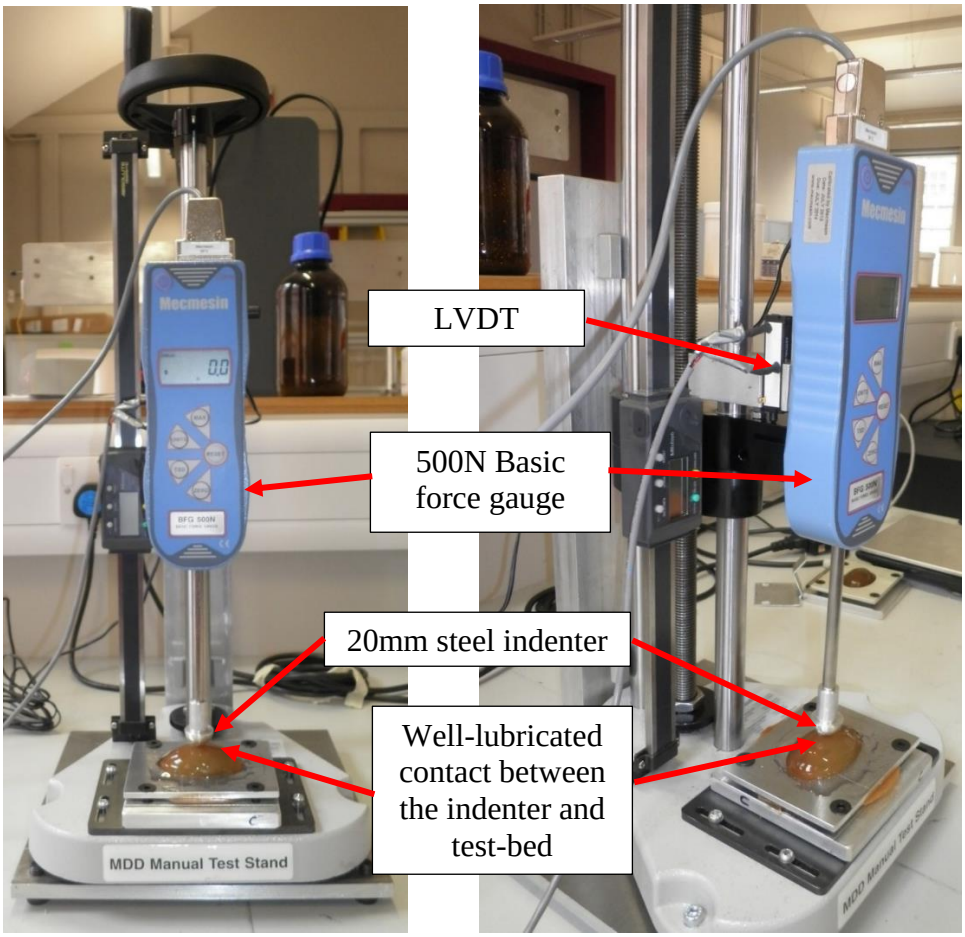

Figure 4.20: The indentation device used for the deformation test.

4.5.2 Friction tests using a dynamic friction rig

As mentioned earlier in this chapter, one of the main purposes to develop biofidelic test-beds is to be able to carry out the friction tests with more controlled high normal loads. In order to achieve this purpose, a dynamic friction rig was developed.

The foot friction plate rig used in the earlier skin-sock studies was incorporated into a dynamic rig, which consists of a movable carrier attached to a linear sliding stage (see Figures 4.21 and 4.22). The carrier has a weight holder on its top and a slot was incorporated to hold the test-bed during the friction test. The foot friction plate rig was positioned at the front of the dynamic rig as shown in Figure 4.23 to ensure that the testing took place on the plantar region of the sock, similar to the test protocol on human foot. A holder was attached to the weight holder to pull the carrier forward, simulating the forward sliding of human foot in the earlier studies. In the absence of added weights, the carrier weighs approximately 10kg. Therefore, the lowest amount of normal load that could be applied on the test-bed is ≈100N.

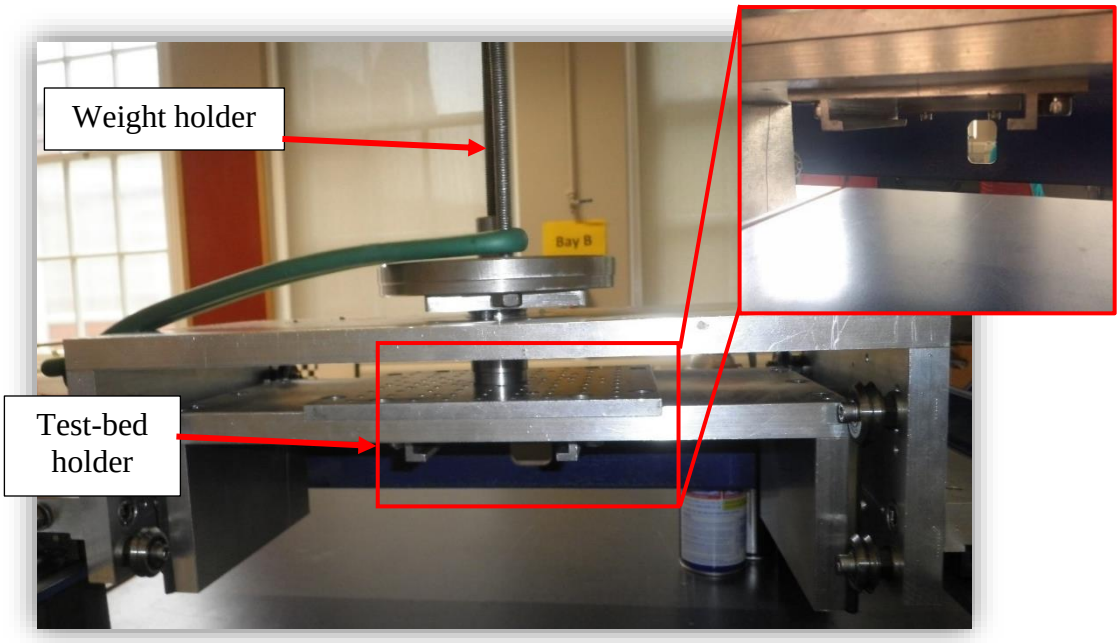

Figure 4.21: The developed carrier system with a weight holder and a slot to hold the tested test-bed.

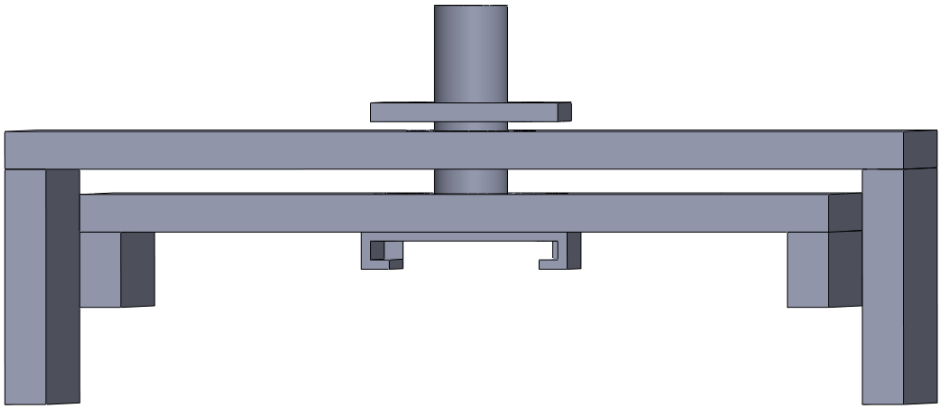

Figure 4.22: A schematic illustration of the carrier system

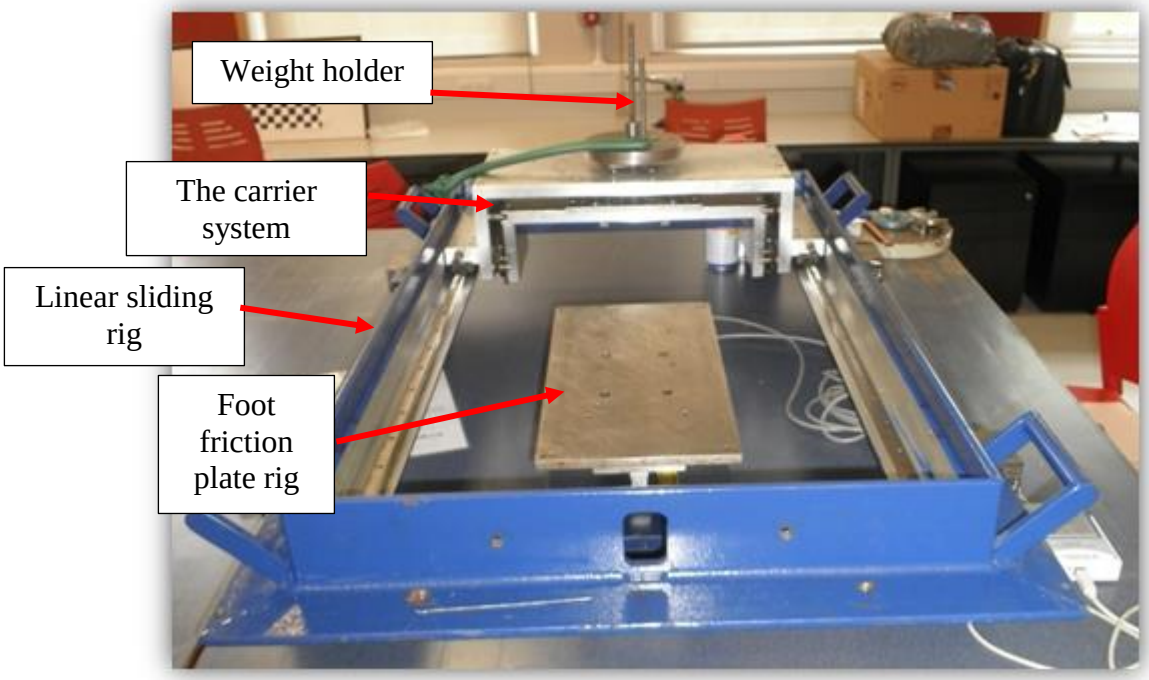

Figure 4.23: The set-up of the dynamic friction rig.

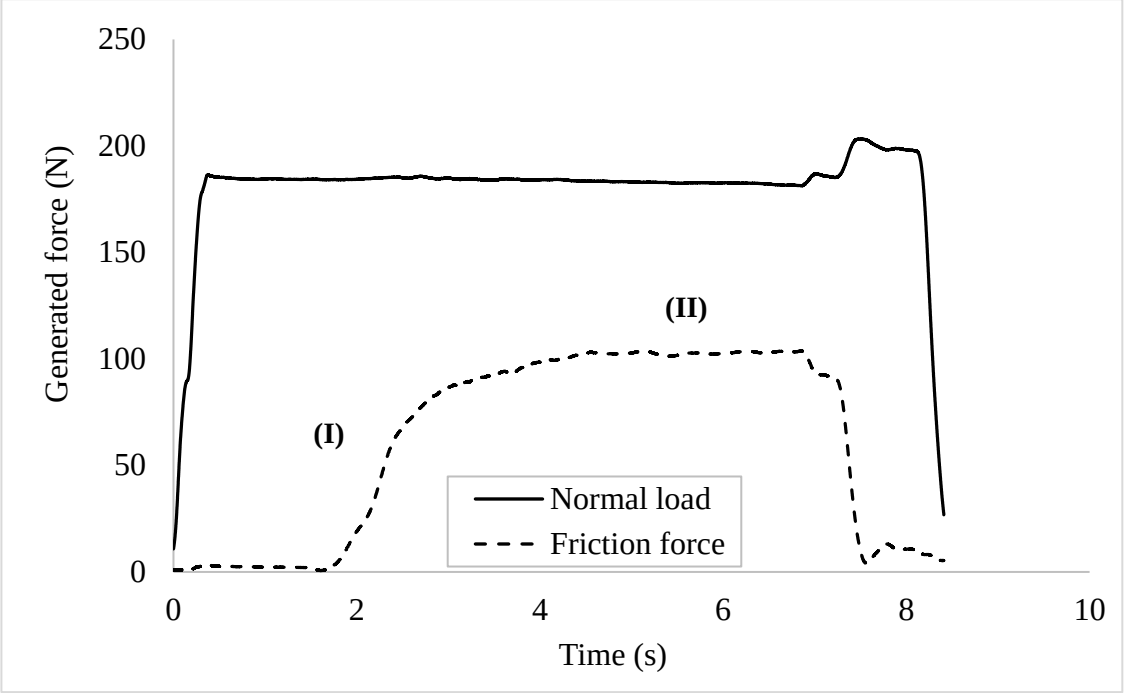

Figure 4.24: The force-time plot obtained from the LabView programme.

An example of the force-time plot obtained from the dynamic friction rig is shown in Figure 4.24. Note the similarity of this plot with the one obtained from the two friction methodologies comparative study described earlier in Chapter 2. The dynamic region, denoted by (II) in Figure 4.23, was selected for analysis. The movement of the biofidelic test-bed relative to the sock fabric occurred at the beginning of this dynamic region. The main improvement from using this equipment can be seen in the consistent level of the applied normal load. The friction test was conducted at 5 different ranges of applied normal loads which are: 100 - 120N, 121 - 140N, 141 - 160N, 161 – 180N and 181 – 200N. Each selected test-bed was tested twice for each sock-moisture condition and the averaged friction and normal forces were used for further analysis. Similar to the protocol used to assess the frictional behaviour of the human plantar and 1MTH, dry condition was tested first and later followed by the low moisture and wet conditions. A new washed sock was used for each moisture condition and the order of the sock was randomised.

Chapter 5

Deformation and frictional properties of the biofidelic test-beds

5.1 Introduction

This chapter presents the results and analysis obtained from the both deformation and frictional tests carried out on the biofidelic test-beds using the experimental protocols explained in Chapter 4. Comparisons to the human 1MTH data obtained from earlier studies are also included in the hope to provide a better overall insight to the performance of the biofidelic test-beds, and consider the best way forward for future development.

5.2 Estimating the Young's modulus of the biofidelic test-beds using an analytical approach

An example of the force-displacement plot obtained from the indentation tests on biofidelic test-bed A (BFA) is shown in Figure 5.1 below. It can be seen that the result shows a non-linear deformation behaviour which does not conform to Hooke's Law. Therefore, in order to estimate the Young's modulus values of the test-beds, the experimental force-displacement curves were analysed using the Oliver and Pharr approach [112], which had also been thoroughly reviewed by Herbert et. al. [113].

A polynomial curve of 4th order was fitted to the loading data which allows the displacement to be interpolated at two different applied load values which are 20N and 30N. The

experimentally measured stiffness, *S* can then be evaluated by calculating the gradient of the loading curve at the intended applied loads, which in this case at 20N and 30N.

$$S = \frac{Applied\ normal\ force, dF}{Displacement, d\delta}$$

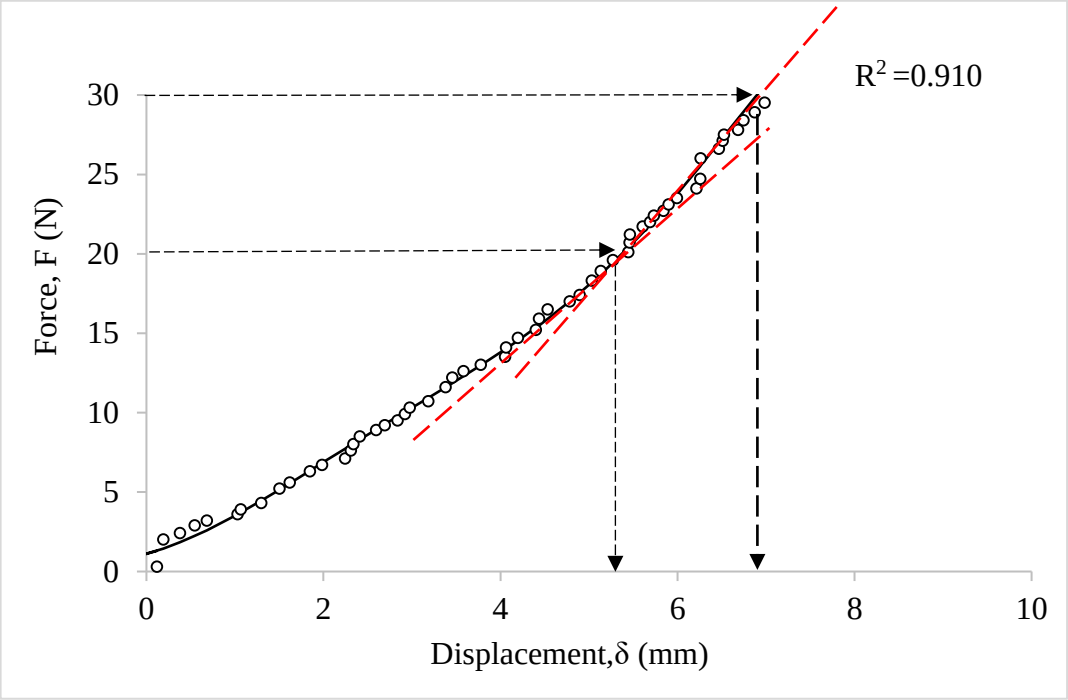

Figure 5.1: The loading segment of the force-displacement data obtained from biofidelic sample A (BFA).

By assuming the indented sample as an elastic half-space loaded over a small region, its reduced Young's modulus, *E** was then obtained by utilising the Oliver and Pharr equation:

$$E^* = \frac{\sqrt{\pi}}{2}\frac{S}{\sqrt{A}}$$

where A is the contact area between the indenter tip and the test-bed. However, in practice, the test-bed surface can either pile-up or sink-in which effectively means that the displacement is not equal to the contact depth. Therefore, the contact area, *A* is substituted by the projected contact area, *Ap,* which can be evaluated using the following equation:

$$Ap = \pi a^2$$

where *a* is the contact radius and is related to the displacement by following equation:

$$a = \sqrt{R\delta}$$

where R is the radius of the indenter.

The reduced Young's modulus, *E** is also related to the elastic modulus of the indented test-beds according to the following expression:

$$E^* = \left[\frac{1 - {v_i}^2}{Ei} + \frac{1 - {v_s}^2}{Es}\right]^{-1}$$

where subscripts i and s respectively refer to the indenter and the indented sample (i.e. in this case either test-bed or human skin). The Poisson's ratio is denoted by *v*. Since the elastic modulus of the indenter, *Ei* >> the elastic modulus of the indented sample, *Es* it can therefore be assumed that the reduced elastic modulus, *E** of the indented sample can be evaluated using the following equation:

$$\frac{1}{E^*} \approx \frac{(1 - {v_s}^2)}{Es}$$

Since accurate Poisson's ratio values for human skin and many viscoelastic materials are unknown, the value of 0.495 was used for analysis in this case study.

As mentioned earlier in Chapter 4, all indentation and flat plate tests carried out in this study was considered frictionless as the contact between the indenter and the indented sample (both test-beds and human 1MTH skin) was fully-lubricated using non-toxic, skin-safe water-based lubricant. The main rationale for this is to minimise the effect of surface friction on the deformation results.

5.3 Analysis of the indentation force-displacement curves

The raw force-displacement data obtained from the indentation tests conducted on all eight biofidelic test-beds were plotted together with the indentation results obtained from the 1MTH of six male participants, SIT001 to SIT006, (26.3 years ± 3.6 SD) for comparison, as shown in Figure 5.2.

Recall that test-beds A, B, C and D are 'non-textured' test-beds whereas test-beds D, E, F and G are 'textured' test-beds. The average total thickness of the outer latex layer across all eight test-beds was measured at 3.24mm ± 0.26 SD whereas the average total thickness of all eight test-beds measured at its centre of symmetry was 21.12mm ± 0.34 SD. The inner layer of both biofidelic test-beds A and D were made with the highest amount of silicone softener (i.e. approximately 50%). This was followed by test-beds B and F with approximately 46%, test-beds C and G with about 40% and finally test-beds D and H which were made with the least amount of softener (i.e. approximately 34%) (please refer to Table 4.5 for more details).

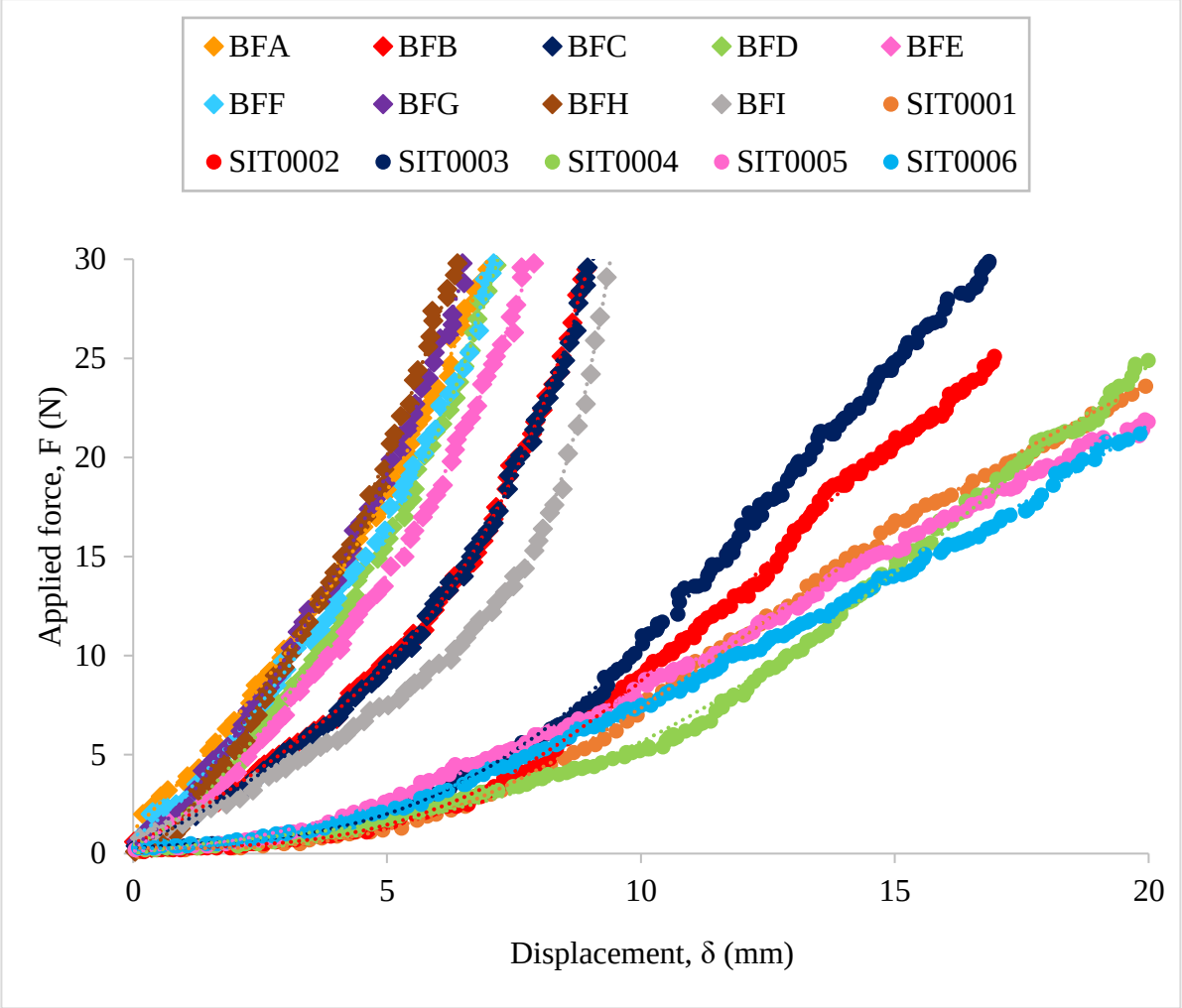

Figure 5.2. The raw force-displacement data obtained from the indentation tests carried out on all biofidelic test-beds (n=8) and human 1MTH (n=6).

In general, all results in Figure 5.2 show an increase in the displacement as the applied force increased during the indentation deformation. It is also noted that all results exhibit a non-linear force-displacement relationship. No measurable deformation remained on the indented surfaces post-testing and therefore plastic behaviour was not observed. Hence, within the tested load range, the test-beds and human skin can be considered to be mainly an elastic material.

However, a clear variation can be seen between the test-beds and the human 1MTH data. The test-beds results are all clustered at the lower end of the force-displacement range

whilst exhibiting much steeper initial gradients in comparison to the human 1MTH data. This effect is even more prominent at low applied load of less and equal to 5N where the human 1MTH skin deformed at a much larger magnitude than the test-beds. This trend continued throughout the tested load range and generally suggests that the test-beds are much stiffer than the human 1MTH skin. The maximum deformation exhibited by the test-bed ranges between 6.38 and 9.39 mm (mean = 7.75 mm, SD = 1.15 mm) whereas that of the human 1MTH ranges between 16.96 and 20.36 mm (mean = 19.07 mm, SD = 1.61 mm). In order to gain better insight on the deformation behaviour of the test-beds and the human 1MTH, the reduced Young's modulus values, E^* were evaluated at two chosen applied indentation loads: 20N and 30N, using gradients from fitted polynomials (see the example provided in Figure 5.1). These loads were selected for simple comparison with human data.

5.4 Comparisons of the deformation behaviour of the biofidelic test-beds

Figure 5.3 illustrates the variations of the calculated reduced Young's modulus, E^* values across all biofidelic test-beds and the average Young's modulus, E^* value of the tested participants (n=6) obtained from the indentation test results at both 20N and 30N applied indentation force.

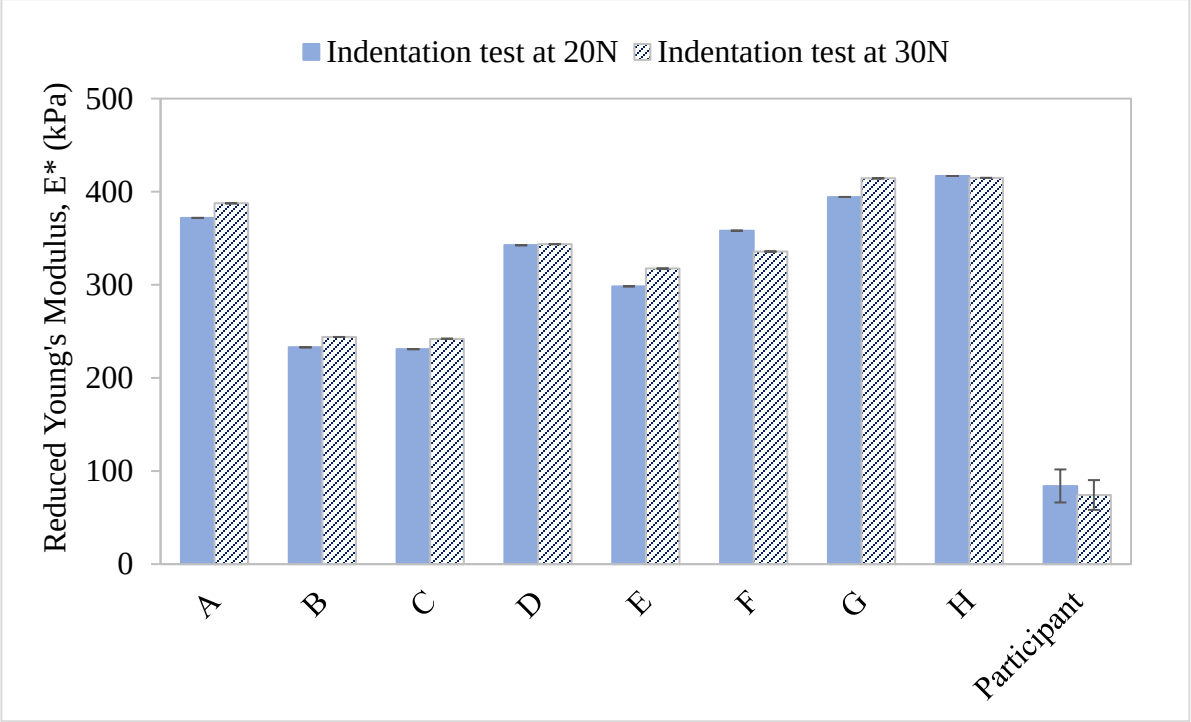

Figure 5.3: The reduced Young's Modulus, *E** values obtained from the indentation tests for the biofidelic samples A – H, compared to that of the 1MTH obtained from the participants' 1MTH at two different applied forces: 20 N and 30N.

A large variation can be seen between the human 1MTH and all eight biofidelic test-beds, with the percentage difference ranging from about 63% to 82%. Results from the one-way ANOVA further provides a significant difference at $p < 0.05$. As discussed earlier, at the same applied indentation load, the test-beds exhibited much lower indentation displacement in comparison to the human 1MTH. This is reflected in the results presented in Figure 5.3, where the reduced Young's moduli calculated for the biofidelic test-beds were of much larger magnitude than the human 1MTH. This could be attributed to the boundary effects provided by the constraint plate that was used to securely hold the test-bed in place, thus increasing the local stiffness where the indentation load was applied. It was observed that in test-bed A, F and H that the reduced Young's moduli at 30N indentation testing were slightly higher than that at 20N. This could be due to a slight reduction in the elastic energy dissipated during the further increment of the indentation load to 30N, which causes the test-bed to resist the deformation load. It was also thought that the boundary effects resulted from

the constraint plate may have influenced the localised contact stress which in return influence the deformation.

Figure 5.4 presents the variations of the calculated reduced Young's modulus, E^* values across all biofidelic test-beds obtained from the interpolating the flat plate test results at both 20N and 30N applied indentation force. Please note that since the flat plate test was not conducted on the human 1MTH skin, no direct comparisons can therefore be made. However, the results from this test still provide valuable information of the deformation behaviour of the biofidelic test-beds when in loaded with a rigid flat plate body.

Based on the data in Figure 5.4, it can be seen that the results obtained are relatively comparable for all biofidelic test-beds, therefore increasing the confidence level of the previously obtained Young's moduli. It can also be safely assumed that the flat plate test results were also much stiffer than the indentation results obtained on human 1MTH. However, in contrast to contact area experienced by the biofidelic test-beds during the indentation test, the contact area experienced during the flat plate test was larger due to the larger surface area covered by the flat plate. Pile-up or sink-in effects were not observed throughout the test across all eight biofidelic test-beds although the boundary effects may still be present.

Figure 5.4: The reduced Young's Modulus, *E** values of the biofidelic samples A – H obtained from the flat plate tests obtained at two different applied forces: 20 N and 30N.

5.5 Comparison of modulus data for the prototype

Another important comparison that could be made using the calculated Young's moduli from both indentation and flat plate tests is to determine whether the developed 'non-textured' biofidelic test-beds A, B, C and D are similar to their counterpart 'textured' biofidelic test-beds E, F, G and H. By theory, it was expected that each 'non'textured' test-bed would be similar to its counterpart 'textured' test-bed, since the inner layer of both test-beds were made of the same percentage of softener, despite the presence of the 'textured' layer. Therefore, any differences would be due to variation in thickness of the outer layer. In order to evaluate this, post-hoc Benferroni's test was conducted post one-way ANOVA test. A summary of the results is tabulated in Table 5.1 for the indentation test and Table 5.2 for the flat plate test.

Table 5.1: Summarised p-values obtained from the post-hoc Bonferroni's test comparing the reduced Young's modulus, E* obtained from the indentation tests. Top row – indentation test at 20N; bottom row – indentation test at 30N. The level of significance is marked by * ($p < 0.05$).

Test-bed	A	B	C	D	E	F	G	H
A		0.000*	0.000*	0.756	0.003*	1.000	1.000	0.804
		0.000*	0.000*	1.000	0.015*	1.000	1.000	0.000*
B			1.000	0.000*	0.005*	0.000*	0.000*	0.000*
			1.000	0.000*	0.021*	0.000*	0.000*	0.000*
C				0.000*	0.003*	0.000*	0.000*	0.000*
				0.000*	0.016*	0.000*	0.000*	0.000*
D					0.926	1.000	0.017*	0.003*
					1.000	1.000	0.067	0.013*
E						0.527	0.000*	0.000*
						1.000	0.000*	0.000*
F							0.031*	0.005*
							0.114	0.023*
G								1.000
								1.000
H								

The statistical results obtained from the indentation tests showed that test-bed A was significantly different ($p < 0.05$) from test-beds B and C which was expected since the inner layer of these test-beds were all made with different percentage of softener. However, no significant difference between A and D ($p > 0.05$), which means that both test-beds are indeed very similar despite test-bed A having more percentage of softener than test-bed D. Test-bed E was tested significantly different than test-beds G and H ($p < 0.05$) similarly to test-bed F and H ($p < 0.05$). No significant difference was obtained between test-beds G and H ($p > 0.05$).

When comparing non-textured test-beds (A, B, C, and D) to their counterpart textured test-beds (E, F, G and H), significant differences were obtained ($p < 0.05$), indicating that despite the same percentage of softener used for the inner layer, the reduced Young's modulus values produced were in fact different.

Table 5.2: Summarised p-values obtained from the post-hoc Bonferroni's test comparing the reduced Young's modulus, E* obtained from the flat plate tests. Top row – flat plate test at 20N; bottom row – flat plate test at 30N. The level of significance is marked by * ($p < 0.05$).

Test-bed	A	B	C	D	E	F	G	H
A		1.000	1.000	1.000	1.000	1.000	1.000	0.296
		1.000	1.000	1.000	1.000	1.000	1.000	1.000
B			1.000	1.000	1.000	1.000	1.000	1.000
			1.000	1.000	1.000	1.000	1.000	0.234
C				1.000	1.000	1.000	1.000	1.000
				1.000	1.000	1.000	1.000	0.437
D					1.000	1.000	1.000	1.000
					1.000	1.000	1.000	1.000
E						1.000	1.000	1.000
						1.000	1.000	1.000
F							1.000	1.000
							1.000	1.000
G								1.000
								1.000
H								

The statistical results obtained from the flat plate tests, on the other hand found no statistical difference ($p > 0.05$) at all when comparing all test-beds, which indicates that all test-beds behave similarly when deformed under flat plate loading.

Each test-bed comprises two different layers with the outer latex layer having much higher Young's modulus than the inner silicone layer. Based on the observations made during both indentation and flat plate testing, it could be hypothesised that the latex outer layer has considerable effect on the overall deformation behaviour of the test-beds. This effect was greatly enhanced by the boundary effect resulted from the constraint plate. When compared to the experimental design developed for the human indentation testing, where the boundary effect from the constraining plate was not present, this would certainly lead to discrepancy in the results obtained. Since the test-beds were developed manually in the laboratory, slight variations in outer layer thickness were expected although the consequence resulting from it was unforeseen.

5.6 Investigating the deformation behaviour of a test-bed with reduced overall outer latex layer thickness

Based on the results obtained from the indentation and flat plate test, it was proposed that perhaps by reducing the overall thickness of the outer latex layer would slightly improve the reduced Young's modulus, by minimising the dominant effect of the much stiff latex. Another test-bed of similar inner layer composition to test-bed C was developed to investigate this hypothesis. The overall outer latex layer thickness was reduced by approximately 50%, from 3. 24mm to 1.67mm. All geometrical dimensions were kept the same as the previous test-beds. The results obtained from the indentation and flat plate tests are presented in Figures 5.5 and 5.6 respectively.

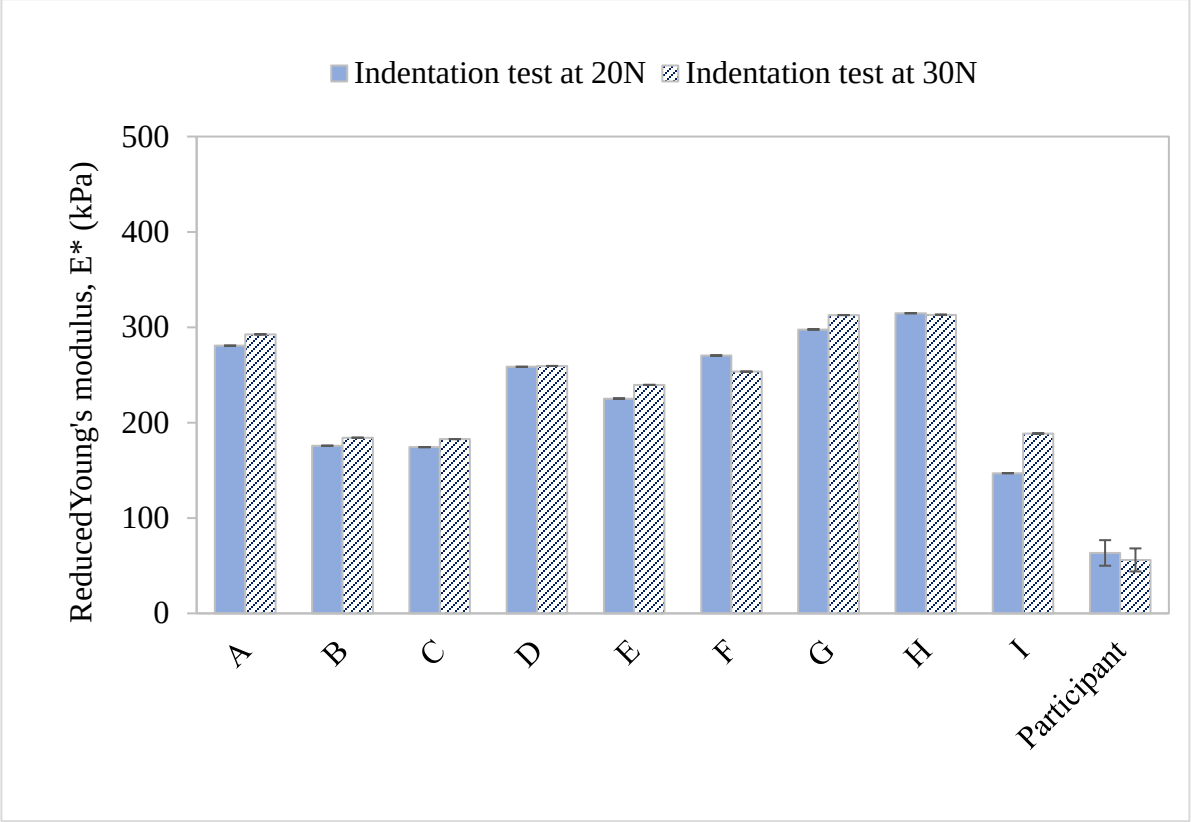

Figure 5.5: The reduced Young's Modulus, E* values of the biofidelic test-bed I (BFI) obtained from the indentation tests at two different applied forces: 20 N and 30N, in comparison to other test-beds.

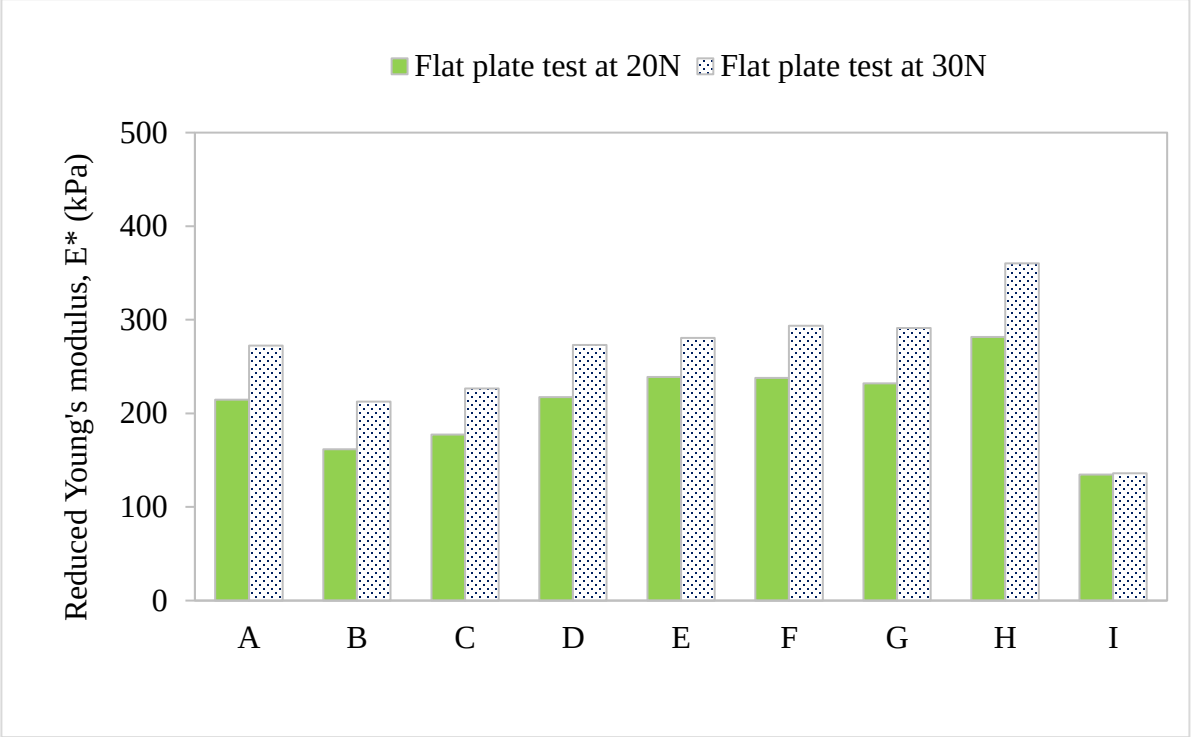

Figure 5.6: The reduced Young's Modulus, E* values of the biofidelic test-bed I (BFI) obtained from the flat plate tests at two different applied forces: 20 N and 30N, in comparison to other test-beds.

Differences can be seen in the results obtained from carrying out the deformation tests on test-bed I which has half the original overall thickness of the outer latex layer of the other test-beds. From the indentation test at 20N and 30N, the calculated Young's moduli were reduced to 194.74 kPa and 249.84 kPa respectively whereas from the flat plate test at 20N and 30N, the calculated Young's moduli were reduced to 178.56 kPa and 180.13 kPa. These results were supported by the results obtained from the post-hoc Bonferroni statistical test where significant differences can be seen between test-bed I when compared with test-beds A, D, E, F, G and H ($p < 0.05$). No significant difference was found when comparing test-bed I to test-beds B and C, further confirming that the reduction seen in the calculated Young's modulus values could be attributed to the reduction in the outer latex layer thickness. This result provides a clear justification to the dominant effect exhibited by the thick latex layer thickness during the indentation tests.

5.7 Investigating the frictional behaviour of the biofidelic test-beds in comparison to the human testing

Following the deformation tests, the biofidelic test-beds were then subjected to a series of friction tests against the anti-blister and cotton-rich socks in three different moisture conditions. The protocol of the test was similar to the one previously conducted on 26 participants to assess the frictional behaviour of the human 1MTH. It was initially thought that all test-beds would be subjected to the friction tests. However, test-beds A, E, F, and I were excluded after running a quick trial run in dry conditions at 100N normal load due to the fact that some of the inner silicone material was squeezed out of the test-beds upon sliding against the tested sock fabrics. These low modulus test-beds were found to not be robust enough for further testing. The friction test was therefore carried out on the remaining test-beds B, C, D (non-textured test-beds) as well as G and H (textured test-beds).

Similarly, to the friction tests conducted on the human 1MTH, the order of the tested sock was randomised. Test-beds B, D, and G were tested with cotton-rich sock first whereas test-beds C and H were tested with anti-blister sock first. The moisture condition of the sock fabrics was also monitored throughout using the Corneometer® device. Since the outer latex layer of the biofidelic test-beds is considered waterproof, moisture from the sock fabrics was not be absorbed and retained in the outer layer. However, the moisture level of the test-beds was still monitored throughout the friction tests to ensure consistency. The friction tests were carried out twice for each sock-moisture condition combination. Figures 5.7 - 5.9 illustrate the average friction force at 150N normal load of the biofidelic test-beds in comparison to the frictional data obtained from the previous human 1MTH study. In addition, the results were also compared with Subject S08 since the textured layers of the test-beds E, F, G and H were obtained from a negative impression of the subject's tested foot. Please note that in these figures, the error bars of the biofidelic test-beds represent the standard deviation between two repetitions of the friction tests, whereas the error bars presented for Subject S08 data represent the standard deviations of the averaged friction force data at each normal load range. The error bars of the "human feet" data represent the standard deviations obtained across all 26 participants from 1MTH friction study.

The statistical data obtained by the paired t-test were also provided in Table 5.3 for the anti-blister sock and in Table 5.4 for the cotton-rich sock.

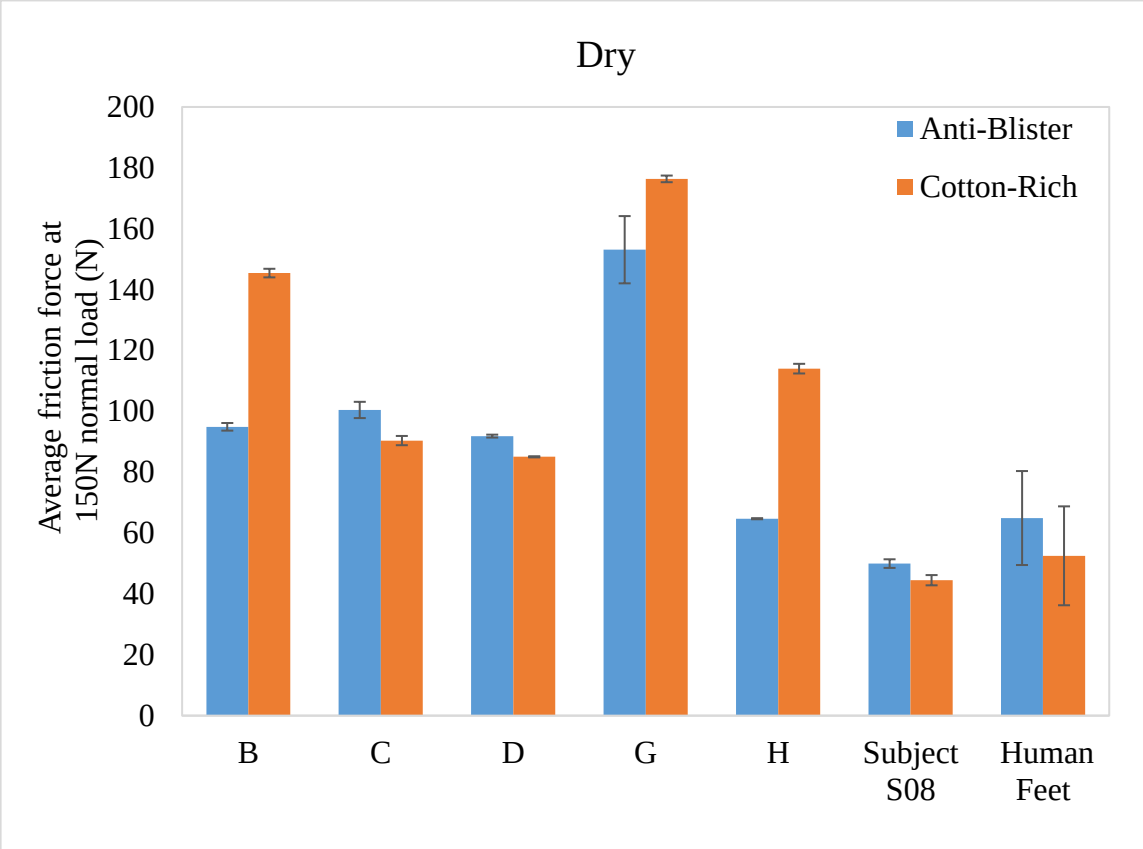

Figure 5.7: Averaged friction force at 150N normal load for the biofidelic test-beds in comparison with the human friction data in dry conditions.

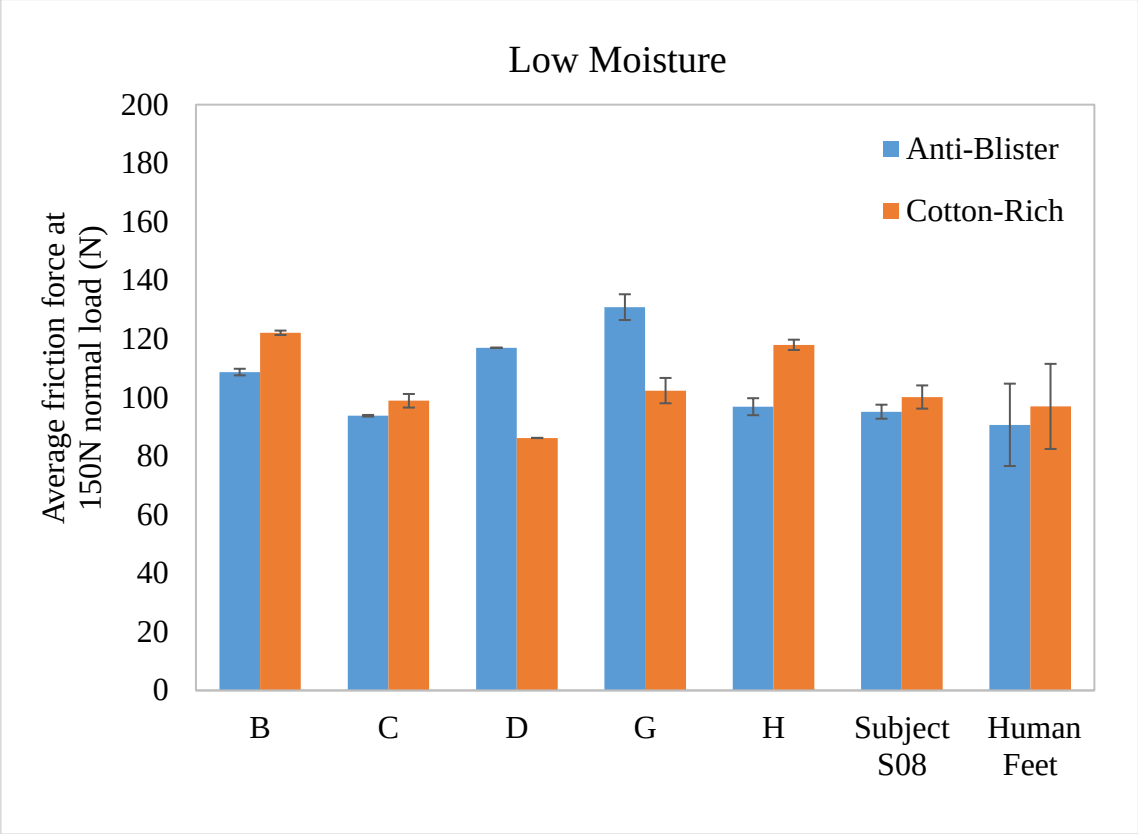

Figure 5.8: The variations of the averaged friction force at 150N normal load of the biofidelic test-beds in comparison to the human friction data in low moisture conditions.

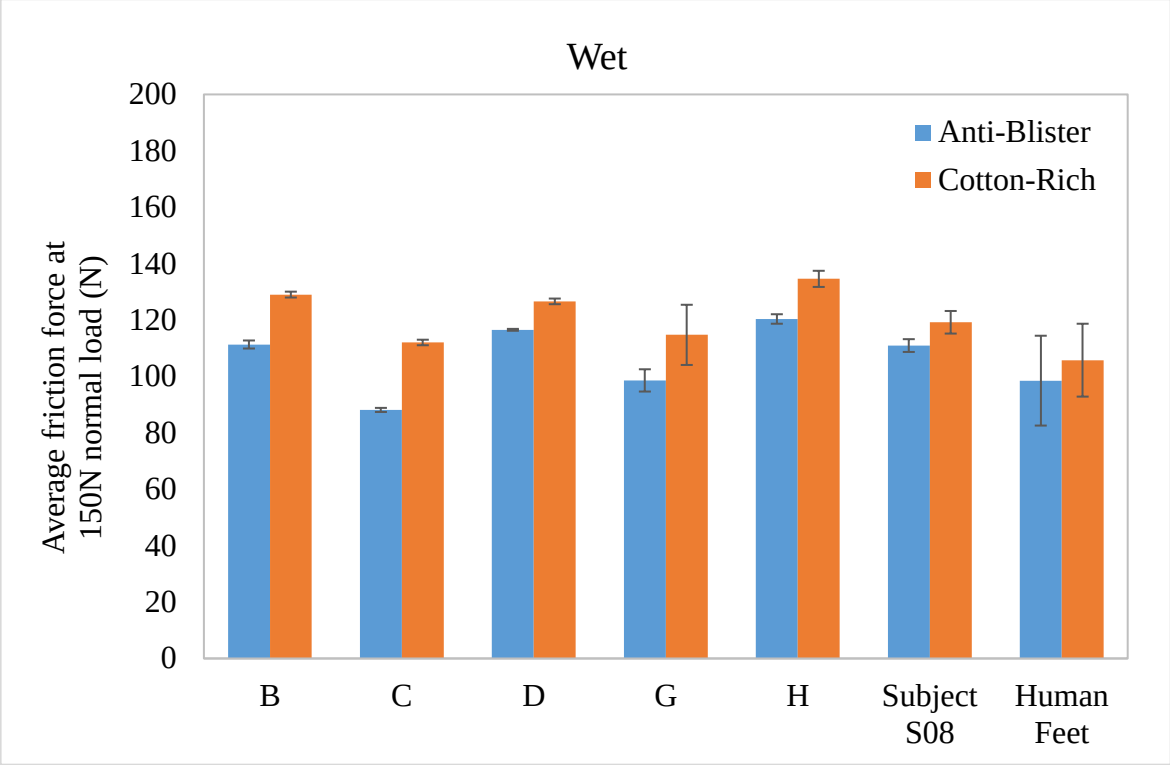

Figure 5.9: The variations of the averaged friction force at 150N normal load of the biofidelic test-beds in comparison to the human friction data in wet conditions.

Table 5.3: Summarised average friction force values at 150N normal load for anti-blister sock, percentage differences in comparison to subject S08 and human feet (n=26) and statistical values obtained from the paired t-test.

The level of significance is set at ($p < 0.05$) *

Sock condition	Tested sample	Average friction force at 150N normal load for anti-blister (N)	DCOF	Percentage (%) difference of average friction force in comparison to subject S08	p-value	Percentage (%) difference of average friction force in comparison to human feet (n=26)	p-value
Dry	BFB	88.37	0.59	76.88	0.000*	36.10	0.168
	BFC	100.44	0.67	101.05	0.000*	54.70	0.067
	BFD	91.85	0.61	83.85	0.000*	41.47	0.079
	BFG	153.10	1.02	206.45	0.000*	135.80	0.000*
	BFH	64.70	0.43	29.52	0.080	-0.34	1.000
	Subject S08	49.96	0.33				
	Human feet	64.93	0.43				
Low moisture	BFB	108.70	0.72	14.22	0.014*	19.86	0.462
	BFC	93.78	0.63	-1.46	0.367	3.41	1.000
	BFD	116.99	0.78	22.93	0.002*	29.01	0.047*
	BFG	130.88	0.87	37.52	0.000*	44.32	0.001*
	BFH	96.88	0.65	1.80	0.167	6.83	1.000
	Subject S08	95.17	0.63				
	Human feet	90.69	0.60				
Wet	BFB	111.34	0.74	0.34	0.018*	14.81	1.000
	BFC	88.13	0.59	-20.57	1.000	-9.13	1.000
	BFD	116.53	0.78	5.03	0.008*	20.16	0.596
	BFG	98.59	0.66	-11.14	0.036*	1.67	1.000
	BFH	120.38	0.80	8.49	0.003*	24.13	0.187
	Subject S08	110.95	0.74				
	Human feet	96.98	0.65				

Table 5.4: Summarised average friction force values at 150N normal load for cotton-rich sock, percentage differences in comparison to subject S08 and human feet (n=26) and statistical values obtained from the paired t-test. The level of significance is indicated by * ($p < 0.05$).

Sock condition	Tested sample	Average friction force at 150N normal load for cotton-rich (N)	DCOF	Percentage (%) difference of average friction force in comparison to subject S08	p-value	Percentage (%) difference of average friction force in comparison to human feet (n=26)	p-value
Dry	BFB	145.42	0.97	226.76	0.000*	176.91	0.000*
	BFC	90.38	0.60	103.08	0.001*	72.09	0.001*
	BFD	85.04	0.57	91.09	0.004*	61.94	0.012*
	BFG	176.37	1.18	296.31	0.000*	235.85	0.000*
	BFH	114.01	0.76	156.19	0.000*	117.11	0.000*
	Subject S08	44.50	0.30				
	Human Feet	52.52	0.35				
Low moisture	BFB	122.11	0.81	21.89	0.026*	23.95	0.062
	BFC	98.90	0.66	-1.28	1.000	0.39	1.000
	BFD	86.21	0.57	-13.94	1.000	-12.49	1.000
	BFG	102.37	0.68	2.18	0.162	3.91	0.667
	BFH	118.00	0.79	17.79	0.057	19.78	0.176
	Subject S08	100.18	0.67				
	Human Feet	98.51	0.66				
Wet	BFB	129.03	0.86	8.24	0.086	21.99	0.223
	BFC	112.05	0.75	-6.01	1.000	5.93	1.000
	BFD	126.62	0.84	6.22	0.125	19.71	0.365
	BFG	114.75	0.76	-3.74	0.380	8.48	1.000
	BFH	134.60	0.90	12.92	0.017*	27.26	0.025*
	Subject S08	119.21	0.79				
	Human Feet	105.77	0.71				

Figure 5.7 shows the average friction force values interpolated at 150N normal force for both tested sock materials when tested in dry condition. Compared to the results obtained from the previous dry human 1MTH-sock fabric study, the anti-blister sock exhibited significantly higher average frictional force of 64.93 ± 15.44N (DCOF:0.43) than that of the cotton-rich sock, 52.52 ± 16.25N (DCOF:0.35). It can be seen that the prototype test-beds generated much higher average frictional forces than the human readings for both types of socks, which could be associated to the high adhesion force produced by the outer latex layer during the dry sliding. Test-beds B, C, D, and H produced comparable average frictional forces to the human 1MTH for the anti-blister sock as indicated by the lack of significant differences when comparing each test-bed with the human 1MTH data ($p > 0.05$) (please refer to Table 5.4 for this). However, none of the tested test-beds produced comparable frictional behaviour to the human 1MTH when tested with the cotton-rich sock ($p < 0.05$). For the anti-blister sock, it was also found that the textured test-bed H produced the exact same DCOF of 0.43 ($p > 0.05$) as the human 1MTH, which is also very close to the Subject S08's DCOF of 0.33 ($p > 0.05$).

The frictional behaviour of the test-beds against both sock fabrics in low moisture condition is presented in Figure 5.8. In the previous low moisture human 1MTH-sock fabric study, the cotton-rich sock produced significantly higher average frictional force of 98.51 ± 15.93N (DCOF:0.66) than that of the anti-blister sock, 90.69 ± 14.06N (DCOF:0.60). Comparable results were obtained from test-beds B, C and H for both sock fabrics ($p > 0.05$). In addition, when compared with Subject S08's frictional data, textured test-bed H gave comparable results for both sock fabrics ($p > 0.05$). Despite not producing comparable frictional results for the anti-blister sock, both test-beds D and G were found to generate similar frictional behaviour to the human 1MTH ($p > 0.05$) when tested with the cotton-rich sock.

The frictional results obtained from the wet condition for both sock materials are plotted in Figure 5.9. The previous wet human 1MTH-sock fabric friction study showed that the cotton-rich sock exhibited significantly higher average frictional force of 105.77 ± 12.92N (DCOF:0.71) than that of the anti-blister sock, 96.98 ± 14.53N (DCOF:0.65).

Interestingly, for the anti-blister sock, all prototype test-beds produced comparable results to that of the human 1MTH ($p > 0.05$). Except for test-bed H, all other four test-beds were found to compare quite well to the human frictional data obtained with the cotton-rich sock ($p > 0.05$). When compared with Subject S08's data, the textured test-bed G was found to compare well when tested with the cotton-rich sock ($p > 0.05$) but not when tested with the anti-blister sock ($p < 0.05$).

5.8 Conclusions

Based on these results, it was found that the frictional performance of the non-textured test-bed C was found to be very comparable to the human 1MTH for both sock fabrics ($p > 0.05$), whilst generating the same frictional trends seen in the study. In dry condition, the outer latex layer was seen to exhibit high adhesion force when slid against the sock fabrics due to its highly-adhesive surface. This effect, however, was observed to be less prominent in both low moisture and wet conditions where moisture was presence in the interface contact between the test-beds and the sock fabrics. The adhesion effect was more pronounced when tested with the terry-jersey knitted cotton-rich sock in comparison to the simple jersey anti-blister sock. The furry surface of the cotton-rich sock effectively increases the real contact area between the test-beds and the sock, leading to an increase in the adhesion force and hence the generated frictional force. Similar adhesive effect was seen in the study conducted by Shao *et al.* [114] on a polymer-based finger-tips. The authors suggested that controlling the degree of the adhesive shear in frictional test is important although it is one of the most challenging tasks in developing artificial test-beds.

Despite being stiffer than a human 1MTH, test-bed C was found to compare well with the human 1MTH deformation data. This could be due to the fact that the test-bed has the lowest reduced modulus value compared with the other test-beds (except test-bed I). Test-bed I, which has lower outer latex layer thickness than test-bed C, was found to have lower elastic modulus values, approaching the human 1MTH. This suggests that by reducing the thickness of the outer latex layer, a test-bed with much closer elastic modulus with human 1MTH could be produced. However, decreasing the thickness further in order to achieve close deformation behaviour with human data was found to have reduced robustness for

friction testing, as seen in test-beds of lower modulus. Therefore, in manufacturing the test-beds, a compromise has to be made between the thickness of the outer layer and having adequate robustness for friction testing.

Another important aspect that was discovered from this study is that adding texture surface which closely resembles human 1MTH imprint did not always results in comparable frictional behaviour with human 1MTH. It can be deduced that it is more important to match the mechanical properties of the test—bed as a whole to the mechanical properties of the human 1MTH.

Chapter 6

Conclusions and future work

This final chapter outlines the conclusions from this study in reference to the established objectives highlighted in Chapter 1. It includes a complete summary of the main results and findings obtained from the study as well as some recommendations of future work for further research into the topic of plantar skin friction.

6.1 Conclusions

At the beginning of this thesis, two different packages of work were described by the two-fold aims of the study. The first package of work was carried out to gain a better understanding of the friction interactions between the plantar skin and selected sock fabrics which include the complex interplay of contact and moisture parameters. It is acknowledged from previous skin-fabric studies that these parameters are the primary contributors in friction blisters development. Despite the on-going extensive research in skin tribology, very little is known regarding the effect of plantar skin properties on friction. One of the reasons for the lack of research on the plantar skin friction was found to be due to the absence of a standard friction testing methodology. The initial stage of the first work package was dedicated to address this issue. Two different methodologies in measuring foot skin-sock friction were investigated and compared. The first methodology utilised a foot friction plate rig that requires the participants to slide their foot against the sock material which is secured on the plate rig. This second approach, on the other hand, utilised a foot loading device with an instrumented probe that slides on the participant's foot. Both methodologies produced similar findings, but the first methodology was found to be capable of measuring higher normal loading conditions and was therefore selected for use in the remaining foot-skin friction studies. A novel moisture control and management protocol was also developed using

a commercially-available Corneometer® CM825 device. This protocol provides a quick and easy way to monitor the level of moisture on both skin and sock materials during moisture application and at specific intervals during the friction test.

As part of the first work package, a series of pilot studies was carried out on the sock-insole interface to investigate how the frictional behaviour of the socks was affected by the contact area, strain and the different level of moisture presence. It was found that the sock materials do not obey Amonton's Laws as the friction force was found to be dependent of the contact area. The pilot test on the effect of strain in sock fabrics showed that different level of strain has no significant effect on the sock friction. A strain level between 20 to 50% was thought to be achievable and representative of the strain experienced in a real-world scenario when the sock is being worn, and hence was used in the remainder of the studies. It was found that varying the moisture levels at the sock-insole interfaces influences the sock-insole friction behaviour. In dry conditions, the socks produced relatively low friction force in comparison to the low moisture and wet conditions. Overall, the findings from the pilot studies provided valuable information that was later fed into the human participant studies.

Comprehensive studies were then conducted on healthy human participants starting with the entire region of plantar skin in dry condition. It was found that there was a large variability in the average foot hydration level due to the low homogeneity of the plantar skin. Other participant-specific factors such as gait mechanisms, skin condition, physical structure of feet and skin care regimen were also thought to have influence this aspect. Nonetheless, a positive correlation was obtained between the average foot hydration level and the friction force at 100N normal force. This finding is in agreement with many earlier studies that found a similar outcome when moist skin comes in contact with other surfaces. The contact area of the foot was also found to plateau at high normal loads due to the skin becoming stiffer as it reaches its maximum extensibility, and the contact area not changing significantly.

Two sock materials were then selected for the further friction test on the plantar aspect of the first metatarsal head (1MTH) which are the predominantly nylon anti-blister sock and the cotton-rich sock. These two socks were made of different material compositions and knit

patterns. The 1MTH was chosen due to the fact that it is the region of the foot that experiences the highest normal load during running and that it is located in the forefoot region where majority of blister incidences were reported to occur. The frictional behaviour of the 1MTH was assessed using the friction methodology in three significantly different moisture conditions namely dry, low moisture and wet. When studying the effect of average 1MTH hydration level on friction, no significant relationships could be found for all sock-moisture combinations. This is in contrast to the findings obtained from the plantar skin-sock friction. The high variation of 1MTH skin hydration level within the same individual was suggested to be the reason for the lack of a measurable effect of 1MTH moisture. The frictional performance of both anti-blister and cotton-rich socks was also compared against one another across all three moisture conditions. It was found that that in dry conditions, the anti-blister sock gave higher sliding friction than the cotton-rich sock. On the other hand, in both low moisture and wet conditions, the cotton rich sock gave higher sliding friction than the anti-blister sock. This could be attributed to the fact that cotton fibres, which are hydrophilic in nature, make up 70% of the cotton-rich material composition. These results were also related to the thermophysiological characteristics of the socks which was investigated in collaboration with Siti Hana Nasir and Professor Olga Troynikov at the RMIT University (please refer to Appendix 10). They found that the cotton-rich sock fabric has a lower absorption rate on both its top and bottom surfaces due to its relatively thicker fabric. In addition, the cotton-rich sock exhibited lower accumulative one-way transport index (AOTI) than the anti-blister sock which means that the anti-blister sock is capable of transporting sweat away from the skin surface much quicker than the cotton-rich sock. The anti-blister sock fabric was also found to have a better score of the overall moisture management capacity (OMMC) than the cotton-rich sock which helps to explain why in the presence of moisture, the anti-blister socks produced lower sliding friction than the cotton-rich sock. This indicates that the anti-blister sock has better wicking properties than the cotton-rich sock and is better at keeping the feet dry within a shoe environment.

The second package of work involved in the study was to design and develop prototype biofidelic test-beds that closely match the mechanical and frictional properties of the plantar aspect of the 1MTH. These test-beds are basically two-layer physical models with

similar geometry and dimensions to the human 1MTH and made of polymer-based materials. Extensive studies were carried out prior to selecting the best combinations of materials to be used for the test-beds. Nine different test-beds were developed. Test-beds A, B, C, D and I were non-textured whereas test-beds E, F, G, and H were textured. The outer layer of the test-bed represents the epidermis and dermis layers of the 1MTH skin whereas the inner layer of the test-beds represents the dermis and subcutaneous tissue layers of human 1MTH. The outer latex layer was made using liquid latex whereas the inner layer was made with a silicone-based material, Magic Power Gel (Raytech), with four different variations of Young's modulus ranging from 40kPa to 240kPa. A steel hemisphere was also included as part of the test-bed design to represent the 1MTH bone.

Deformation tests using a 20mm diameter indenter and a flat plate were carried out on all nine test-beds prior to the friction test. The reduced Young's moduli for the test-beds were calculated using the stiffness values extracted from the force-displacement data obtained from the indentation tests. It was found that all test-beds produced higher reduced Young's moduli in comparison to the human 1MTH. This was thought to be attributed by the boundary effects resulted from the constraint plate used to hold the test-beds in place. A dynamic friction rig was also developed in order to carry out friction tests in controlled normal loading, ranging from 100N to 200N. The same friction methodology used to test human plantar skin was utilised for the friction test on the biofidelic test-beds against the anti-blister and cotton-rich socks. Test-beds A, E, F, and I were not included in the friction test due to their low robustness. The friction results obtained were then compared with the human 1MTH-sock friction data. It was found that test-bed C exhibited the mechanical and frictional properties closest to the human 1MTH data.

6.2 Contributions of the thesis

The main contributions of this thesis are as follows:

- Two different methodologies in measuring foot skin – sock friction were investigated and compared. The use of foot friction rig was found to be appropriate for testing involving higher ranges of applied normal loads.

- A novel moisture control and management protocol was devised using a commercially-available device, Corneometer® CM825 device. This protocol provides an efficient way of monitoring the level of moisture on both human skin and sock materials during friction testing.
- A friction protocol to evaluate the frictional behaviour of the skin – sock interface was developed. Using the same friction protocol in all friction studies ensures repeatability in the procedures involved in friction testing, allowing the results to be compared systematically.
- The friction interaction between the plantar skin and five different sock materials in dry condition has been investigated at higher ranges of applied normal loads (i.e. up to 500N).
- The friction interaction between the human 1MTH and two commercially-available running socks, the anti-blister and cotton-rich, has been assessed in three different moisture conditions: dry, low moisture and wet.
- A range of biofidelic test-bed prototypes has been designed and developed to closely-resemble the mechanical and frictional properties of the plantar aspect of the 1MTH.
- The friction between the biofidelic test-bed and two selected sock fabrics, the anti-blister and cotton-rich, has been evaluated in three different moisture conditions: dry, low moisture and wet.
- The results obtained from the friction testing of the biofidelic test-beds were validated using the human 1MTH friction data.

6.3 Suggested future work

This study has addressed several aspects of plantar skin-sock friction with the aim to close the gaps in the existing knowledge on this topic. However, several questions have arisen during the course of the study which were not covered within the scope of the research conducted. This provides possibilities to venture in other research directions which would further the understanding of plantar skin-sock friction in relation to foot friction blisters.

6.3.1 Plantar skin properties

As mentioned earlier in this chapter, the existing data on the plantar skin properties is still very limited in comparison to the other parts of human skin and therefore still poorly understood. Even with the existing data, comparisons have been proven to be challenging due to the variety of measurement techniques used. Establishing a standard mechanical testing protocol to precisely measure the Young's modulus of the plantar skin would certainly allow better measurements and comparisons to be made hence contributing to the further understanding of the plantar skin properties.

6.3.2 Testing other running sock materials

The friction and moisture protocols developed in this study can be extended to study the friction interaction between the plantar skin and other running sock materials that are frequently used by long-distance runners. The data obtained from the further work can then be used to build on the existing plantar skin-sock fabric database allowing better comparisons to be made in terms of the socks frictional performance.

6.3.3 Measurements of area of contact during the friction experiments

Further work needs to be carried out on the effects of contact area during the dynamic friction test. As discussed earlier in Chapter 3, plantar skin does not obey Amonton's Laws and the frictional force is not independent of the contact area. This would provide better insight on how varying the contact area would influence the plantar skin-sock fabric friction. The skin contact area results can then be associated to the hydration level and mechanical properties of the plantar skin to study the extent of its variability.

6.3.4 Reinforcing the robustness of the biofidelic test-beds

A novel approach used to fabricate the biofidelic test-beds is now developed into a protocol that can be used to produce new test-beds that more closely match the human mechanical and frictional properties. However, the robustness of the test-beds need to be further improved. In Chapter 5, the friction test was not able to be conducted on test-beds A, E, F and I due to the low robustness of the test-bed design. More improvement is therefore required to enhance

the durability and robustness of the test-beds so that they are capable to withstand the high normal and shear loads that occur during testing and the surfaces can be improved in terms of wear resistance.

6.3.5 Extending results of friction studies to blister formation

Another important aspect that could be explored is to extend results of friction studies to enhance understanding in blister formation. In the current friction studies, plantar skin-sock interface was investigated separately to the sock-insole interface to gain better understanding of how plantar sock interacts with sock fabrics. The friction protocols developed in this study could be applied to study the foot-sock-insole interactions as a whole, including how the normal and shear loads are distributed within the shoe.

Cited references

1. Guerra C, Schwartz CJ. Development of a synthetic skin simulant platform for the investigation of dermal blistering mechanics. Tribology Letters. 2011;44:223-8
2. Comaish S, Bottoms E. The skin and friction: Deviations from Amonton's laws, and the effects of hydration and lubrication. Br J Dermatol. 1971;84:37-43.
3. Baussan E, Bueno MA, Rossi RM, Derler S. Analysis of current running sock structures with regard to blister prevention. Textile Research Journal. 2012;0(00):1-13.
4. Mailler EA, Adams BB. The wear and tear of 26.2: dermatological injuries reported on marathon day. British Journal of Sports Medicine. 2004;38:498-501.
5. Kogut KT, Rodewald LE. A field survey of the emergency preparedness of wilderness hikers. Journal of Wilderness Medicine. 1994 1994/06/01;5(2):171-8.
6. Polliack AA, Scheinberg S. A new technology for reducing shear and friction forces on the skin: Implications for blister care in the wilderness setting. Wilderness and Environmental Medicine. 2006;17:109-19.
7. Yavuz M, Davis BL. Plantar shear stress distribution in athletic individuals with frictional foot blisters. Journal of the American Podiatric Medical Association. 2010;100(2):116-20.
8. Yavuz M, Erdemir A, Botek G, Hirschman GB, Bardsley L, Davis BL. Peak Plantar Pressure and Shear Locations: Relevance to diabetic patients. Diabetes Care. 2007 October 1, 2007;30(10):2643-5.
9. Marieb EN, Hoehn K. Human Anatomy and Physiology. Seventh Edition ed: Pearson Education; 2007.
10. Martini FH, Nath JL. Fundamentals of Anatomy and Physiology. 8th Edition ed: Pearson Education Inc. ; 2009.
11. Escoffier C, De Rigal J, Rochefort A, Vasselet R, Leveque J-L, Agache PG. Age-related mechanical properties of human skin: an in vivo study. J Investig Dermatol. 1989;93(3):353-7.
12. Cua AB, Wilhelm K-P, Maibach HI. Elastic properties of human skin: relation to age, sex, and anatomical region. Archives of Dermatological Research. 1990;282:283-8.
13. Sandby-Moller J, Poulsen T, Wulf HC. Epidermal thickness at different body sites: relationship to age, gender, pigmentation, blood content, skin type and smoking habits. Acta Dermato Venereologica. 2003;83(6):410-3.
14. Grouios G. Corns and calluses in athletes' feet: a cause for concern. The Foot. 2004;14:175-84.
15. Sun JH, Cheng BK, Zheng YP, Huang YP, Leung JY, Cheing GL. Changes in the thickness and stiffness of plantar soft tissues in people with diabetic peripheral neuropathy. Archives of Physical Medicine and Rehabilitation. 2011;92:1484-9.
16. Hsu T-C, Wang C-L, Tsai W-C, Kuo J-K, Tang F-T. Comparison of the mechanical properties of the heel pad between young and elderly adults. Archives of Physical Medicine and Rehabilitation. 1998;79(9):1101-4.
17. Zheng Y-P, Choi Y, Wong K, Chan S, Mak AF. Biomechanical assessment of plantar foot tissue in diabetic patients using an ultrasound indentation system. Ultrasound in Medicine & Biology. 2000;26(3):451-6.

18. Kwan RL-C, Zheng Y-P, Cheing GL-Y. The effect of aging on the biomechanical properties of plantar soft tissues. Clinical Biomechanics. 2010;25(6):601-5.
19. Tomlinson SE, Lewis R, Carre MJ. Review of the frictional properties of finger-object contact when gripping. Proceedings of the Institution of Mechanical Engineers Part J-Journal of Engineering Tribology. 2007 Dec;221(J8):841-50.
20. OpenStax College. Layers of the Skin. Anatomy & Physiology2013.
21. Derler S, Gerhardt LC. Tribology of skin: Review and analysis of experimental results for the friction coefficient of human skin. Tribology Letters. 2012;45:1-27.
22. Pailler-Mattei C, Nicoli S, Pirot F, Vargiolu R, Zahouani H. A new approach to describe the skin surface physical properties in vivo. Colloids and Surfaces B: Biointerfaces. 2009;68(2):200-6.
23. Hendriks FM. Mechanical behaviour of human epidermal and dermal layers in vivo: Technische Universiteit Eindhoven; 2005.
24. Payne PA. Measurement of properties and function of skin. Clinical Physics and Physiological Measurement. 1991;12(2):105.
25. McGrath JA, Eady RAJ, Pope FM. Anatomy and Organization of Human Skin. Rook's Textbook of Dermatology: Blackwell Publishing, Inc.; 2008. p. 45-128.
26. Thomas SE, Dykes PJ, Marks R. Plantar Hyperkeratosis: A Study of Callosities and Normal Plantar Skin. J Investig Dermatol. 1985;85(5):394-7.
27. Gerhardt L-C, Schiller A, Müller B, Spencer ND, Derler S. Fabrication, characterisation and tribological investigation of artificial skin surface lipid films. 2009. 2009;34:81-93.
28. Liu X. Understanding the effect of skin mechanical properties on the friction of human finger-pads: The University of Sheffield; 2012.
29. Cua AB, Wilhelm KP, Maibach HI. Frictional properties of human skin: relation to age, sex and anatomical region, stratum corneum hydration and transepidermal water loss. Br J Dermatol. 1990;123(4):473-9.
30. Tomlinson SE, Lewis R, Carre MJ. The effect of normal force and roughness on friction in human finger contact. Wear. 2009 Jun;267(5-8):1311-8.
31. Liu X, Lu Z, Lewis R, Carre MJ, Matcher SJ. Feasibility of using optical coherence tomography to study the influence of skin structure on finger friction. Tribology International. 2013 Jul;63:34-44.
32. Tomlinson SE, Carre MJ, Lewis R, Franklin SE. Human finger contact with small, triangular ridged surfaces. Wear. 2011 Jul;271(9-10):2346-53.
33. Tomlinson SE, Lewis R, Carre MJ, Franklin SE. Human finger friction in contacts with ridged surfaces. Wear. 2013 Apr-May;301(1-2):330-7.
34. Tomlinson SE, Lewis R, Liu X, Texier C, Carre MJ. Understanding the Friction Mechanisms Between the Human Finger and Flat Contacting Surfaces in Moist Conditions. Tribology Letters. 2011 Jan;41(1):283-94.
35. Geerligs M, Oomens C, Ackermans P, Baaijens F, Peters G. Linear shear response of the upper skin layers. Biorheology. 2011;48(3):229-45.
36. Hendriks CP, Franklin SE. Influence of Surface Roughness, Material and Climate Conditions on the Friction of Human Skin. Tribology Letters. 2010 2010/02/01;37(2):361-73.
37. Edwards C, Marks R. Evaluation of biomechanical properties of human skin. Clinics in Dermatology. 1995;13(4):375-80.

38. Naylor PFD. The skin surface and friction. The British Journal of Dermatology. 1955;67:239-48.
39. Derler S, Gerhardt LC, Lenz A, Bertaux E, Hadad M. Friction of human skin against smooth and rough glass as a function of the contact pressure. Tribology International. 2009;42(11–12):1565-74.
40. Cottenden DJ, Cottenden AM. A study of friction mechanisms between a surrogate skin (Lorica soft) and nonwoven fabrics. Journal of the Mechanical Behavior of Biomedical Materials. 2013;28:410-26.
41. Sivamani RK, Goodman J, Gitis NV, Maibach HI. Coefficient of friction: tribological studies in man - an overview. Skin Research and Technology. 2003;9:227-34.
42. Gitis N, Sivamani R. Tribometrology of skin. Tribology Transactions. 2004;47:461-9.
43. Sivamani RK, Maibach HI. Tribology of skin. Journal of Engineering Tribology. 2006;220:729-37.
44. Bowden FP, Tabor D. The friction and lubrification of solids: Clarendon Press; 1954.
45. Hashmi F, Richards BS, Forghany S, Hatton AL, Nester CJ. The formation of friction blisters on the foot: the development of a laboratory-based blister creation model. Skin Research and Technology. 2012;19.
46. Naylor PFD. Experimental friction blisters. The British Journal of Dermatology. 1955;67:327-42.
47. Cua AB, WILHELM KP, Maibach H. Frictional properties of human skin: relation to age, sex and anatomical region, stratum corneum hydration and transepidermal water loss. Br J Dermatol. 1990;123(4):473-9.
48. Adams M, Briscoe B, Johnson S. Friction and lubrication of human skin. Tribology Letters. 2007;26(3):239-53.
49. Sivamani RK, Wu GC, Gitis NV, Maibach HI. Tribological testing of skin products: gender, age, and ethnicity on the volar forearm. Skin Research and Technology. 2003;9:299-305.
50. Koudine AA, Barquins M, Anthoine PH, Aubert L, Lêvêque J-L. Frictional properties of skin: proposal of a new approach. International Journal of Cosmetic Science. 2000;22:11-20.
51. Derler S, Schrade U, Gerhardt LC. Tribology of human skin and mechanical skin equivalents in contact with textiles. Wear. 2007;263:1112-6.
52. Cross R. Standing, walking, running, and jumping on a force plate. American Journal of Physics. 1999;67(4):304-9.
53. Stiles V, Dixon S. Sports surfaces, biomechanics and injuries. Dixon S, Fleming P, James I, Carré M, editors: Routledge; 2015.
54. Carré MJ, Clarke JD, Damm L, Dixon SJ. Friction at the Tennis Shoe-court Interface: How Biomechanically Informed Lab-based Testing can Enhance Understanding. Procedia Engineering. 2014;72:883-8.
55. Hennig EM, Milani TL. In-shoe pressure distribution for running in various types of footwear. Journal of Applied Biomechanics. 1995;11:299-.
56. Hayafune N, Hayafune Y, Jacob H. Pressure and force distribution characteristics under the normal foot during the push-off phase in gait. The Foot. 1999;9(2):88-92.
57. Kram R, Griffin TM, Donelan JM, Chang YH. Force treadmill for measuring vertical and horizontal ground reaction forces. Journal of Applied Physiology. 1998 August 1, 1998;85(2):764-9.

58. Swensson O, Langbein L, McMillan JR, Stevens HP, Leigh IM, McLean W. H. I., et al. Specialized keratin expression pattern in human ridged skin as an adaptation to high physical stress. Br J Dermatol. 1998;139:767-75.
59. Wang YN, Sanders JE. How does skin adapt to repetitive mechanical stress to become load tolerant? Medical hypotheses. 2003;61(1):29-35.
60. Comaish JS. Epidermal fatigue as a cause of friction blisters. The Lancet. 1973:81-3.
61. Sulzberger MB, Cortese TA, Fishman L, Wiley HS. Studies on blisters produced by friction I. Results of linear rubbing and twisting techniques. The Journal of Investigative Dermatology. 1966;47:456-65.
62. Nilsson J, Thorstensson A. Ground reaction forces at different speeds of human walking and running. Acta Physiologica Scandinavica. 1989;136(2):217-27.
63. Knapik JJ. Friction blisters: pathophysiology, risk factors, and prevention. US Army Center for Health Promotion and Preventive Medicine.1-4.
64. Cortese TA, Sams WM, Sulzberger MB. Studies on blisters produced by friction. II. The blister fluid. The Journal of Investigative Dermatology. 1968;50:47-53.
65. Brennan FH. Managing blisters in competitive athletes. Current Sports Medicine Reports. 2002;1:319-22.
66. Herring KM, Richie DH. Friction blisters and sock fiber composition: a double-blind study. J Am Podiatr Med Assoc. 1990;80(2):63-71.
67. Sun J-H, Cheng BK, Zheng Y-P, Huang Y-P, Leung JY, Cheing GL. Changes in the Thickness and Stiffness of Plantar Soft Tissues in People With Diabetic Peripheral Neuropathy. Archives of Physical Medicine and Rehabilitation. 2011;92(9):1484-9.
68. Yavuz M, Hetherington VJ, Botek G, Hirschman GB, Bardsley L, Davis BL. Forefoot plantar shear stress distribution in hallux valgus patients. Gait & Posture. 2009;30(2):257-9.
69. Knapik J, Harman E, Reynolds K. Load carriage using packs: A review of physiological, biomechanical and medical aspects. Applied Ergonomics. 1996;27:207-16.
70. Knapik J. Physiological, biomechanical and medical aspects of soldier load carriage. US Army Center for Health Promotion and Preventive Medicine. 2000:1-19.
71. Dai XQ, Li Y, Zhang M, Cheung JTM. Effect of sock on biomechanical responses of foot during walking. Clinical Biomechanics. 2006;21:314-21.
72. Herring KM, Richie DH. Comparison of cotton and acrylic socks using a generic cushion sole design for runners. Journal of the American Podiatric Medical Association. 1993 September 1993;83:515-22.
73. Reynolds K, Darrigrand A, Roberts D, Knapik J, Pollard J, Duplantis K, et al. Effects of an antiperspirant with emollients on foot-sweat accumulation and blister formation while walking in the heat. Journal of the American Academy of Dermatology. 1995 October 1995;33:626-30.
74. Costill DL. Sweating: It's composition and effects on body fluids*. Annals of the New York Academy of Sciences. 1977;301(1):160-74.
75. Kirkham S, Lam S, Nester C, Hashmi F. The effect of hydration on the risk of friction blister formation on the heel of the foot. Skin Research and Technology. 2014;20(2):246-53.
76. Kenins P. Influence of Fiber Type and Moisture on Measured Fabric-to-Skin Friction. Textile Research Journal. 1994 December 1, 1994;64(12):722-8.

77. Troynikov O, Ashayeri E, Fuss FK. Tribological evaluation of sportswear with negative fit worn next to skin. Proceedings of the Institution of Mechanical Engineers, Part J: Journal of Engineering Tribology. 2012 July 1, 2012;226(7):588-97.
78. Konopov I, Oggiano L, Chinga-Carrasco G, Troynikov O, Sætran L, Alam F. Aerodynamic and comfort characteristics of a double layer knitted fabric assembly for high speed winter sports. Procedia Engineering. 2010;2(2):2837-43.
79. Van Amber RR, Wilson CA, Laing RM, Lowe BJ, Niven BE. Thermal and moisture transfer properties of sock fabrics differing in fiber type, yarn, and fabric structure. Textile Research Journal. 2015;85(12):1269-80.
80. Bertaux E, Derler S, Rossi RM, Zeng X, Koehl L, Ventenat V. Textile, physiological, and sensorial parameters in sock comfort. Textile Research Journal. 2010;80(17):1803-10.
81. Pan N, Maibach HI, Williams K. Fabric and skin: contact, friction and interactions.: University of California2006.
82. Guerra CA. Development and investigation of synthetic skin simulant platform (3SP) in friction blister applications. Texas: Texas A&M University; 2010.
83. Shao F, Childs THC, Henson B. Developing an artificial fingertip with human friction properties. Tribology International. 2009;42(11–12):1575-81.
84. Kawabata S. The standardisation and analysis of hand evaluation. The Textile Machinery Society of Japan. 1980.
85. Kim JO, Slaten BL. Objective Evaluation of Fabric Hand. Textile Research Journal. 1999;69(1):59-67.
86. Quaynor L, Takahashi M, Nakajima M. Effects of Laundering on the Surface Properties and Dimensional Stability of Plain Knitted Fabrics. Textile Research Journal. 2000;70(1):28-35.
87. Bueno M-A, Lamy B, Renner M, Viallier-Raynard P. Tribological investigation of textile fabrics. Wear. 1996 1996/07/01;195(1):192-200.
88. Tasron D, Maiti R, Hemming M, Lewis R, Carré M. Investigating a methodology to measure moisture in skin–textile friction experiments. Footwear Science. 2015;7(sup1):S15-S6.
89. Carré M, Tasron D, Lewis R, Hashmi F. Investigating foot-sock friction: A comparison of two different methodologies. Procedia Engineering. 2016;147:759-64.
90. Tasron DN, Thurston TJ, Carré MJ. Frictional Behaviour of Running Sock Textiles Against Plantar Skin. Procedia Engineering. 2015;112:110-5.
91. Tasron D, Maiti R, Hemming M, Lewis R, Carré M. Frictional interaction between running sock fabrics and plantar aspect of first metatarsal head in different moisture conditions. Procedia Engineering. 2016;147:753-8.
92. Tasron D, Maiti R, Hemming M, Lewis R, Carré MJ. Frictional interaction between running sock fabrics and plantar aspect of first metatarsal head in different moisture conditions. Proceedings of the 11th Conference of the International Sports Engineering Association 2016 (in press). 2016.
93. Carré MJ, Tasron DN, Lewis R, Hashmi F. Investigating foot-sock friction: A comparison of two different methodologies. Proceedings of the 11th Conference of the International Sports Engineering Association 2016 (in press). 2016.
94. Tasron D, Nasir S, Troynikov O, Lewis R, Carré M, editors. Thermo-physiological comfort and frictional characteristics of running socks in different moisture conditions. Proceedings

of the 9th Conference of the Textile Bioengineering and Informatics Symposium (in press); 2016.

95. Tasron D, Nasir S, Troynikov O, Lewis R, Carré M, editors. Thermo-physiological comfort and frictional characteristics of running socks in different moisture conditions. Proceedings of the 9th Conference of the Textile Bioengineering and Informatics Symposium 2016; 2016.
96. Wright CR. The biophysical properties of plantar callus and the relationship between pressure and callus development and regression [Thesis]: University of Salford; 2015.
97. Fluhr JW, Gloor M, Lazzerini S, Kleesz P, Grieshaber R, Berardesca E. Comparative study of five instruments measuring stratum corneum hydration (Corneometer CM 820 and CM 825, Skicon 200, Nova DPM 9003, DermaLab). Part II. In vivo. Skin Research and Technology. 1999;5(3):171-8.
98. Fluhr JW, Gloor M, Lazzerini S, Kleesz P, Grieshaber R, Berardesca E. Comparative study of five instruments measuring stratum corneum hydration (Corneometer CM 820 and CM 825, Skicon 200, Nova DPM 9003, DermaLab). Part I. In vitro. Skin Research and Technology. 1999;5(3):161-70.
99. Hashmi F, Malone-Lee J. Measurement of skin elasticity on the foot. Skin Research and Technology. 2007;13:252-8.
100. Welzel J, Lankenau E, Birngruber R, Engelhardt R. Optical coherence tomography of the human skin. Journal of the American Academy of Dermatology. 1997;37(6):958-63.
101. Bogerd CP, Brühwiler PA, Rossi RM. Heat loss and moisture retention variations of boot membranes and sock fabrics: A foot manikin study. International Journal of Industrial Ergonomics. 2012;42:212-8.
102. Van Amber RR, Lowe BJ, Niven BE, Laing RM, Wilson CA, Collie S. The effect of fiber type, yarn structure and fabric structure on the frictional characteristics of sock fabrics. Textile Research Journal. 2014 July 16, 2014.
103. Laing RM, Wilson CA, Gore SE, Carr DJ, Niven BE. Determining the Drying Time of Apparel Fabrics. Textile Research Journal. 2007 August 1, 2007;77(8):583-90.
104. Gerhardt L-C, Strässle V, Lenz A, Spencer ND, Derler S. Influence of epidermal hydration on the friction of human skin against textiles2008.
105. Baussan E, Bueno MA, Rossi RM, Derler S. Experiments and modelling of skin-knitted fabric friction. Wear. 2010;268:1103-10.
106. Laing RM, Wilson CA, Dunn LA, Niven BE. Detection of fiber effects on skin health of the human foot. Textile Research Journal. 2015 February 24, 2015;0(00):1-15.
107. Chao CYL, Zheng Y-P, Cheing GLY. Epidermal Thickness and Biomechanical Properties of Plantar Tissues in Diabetic Foot. Ultrasound in Medicine & Biology. 2011;37(7):1029-38.
108. Wagner MB, Gerling GJ, Scanlon J, editors. Validation of a 3-D Finite Element Human Fingerpad Model Composed of Anatomically Accurate Tissue Layers. Haptic interfaces for virtual environment and teleoperator systems, 2008 haptics 2008 symposium on; 2008 13-14 March 2008.
109. Menz H. Foot problems in older people: assessment and management. 2008. Edinburgh: Churchill Livingstone Elsevier.
110. De Groote I, Humphrey LT. Body mass and stature estimation based on the first metatarsal in humans. American journal of physical anthropology. 2011;144(4):625-32.

111. Wang C-L, Hsu T-C, Shau Y-W, Shieh J-Y, Hsu K-H. Ultrasonographic measurement of the mechanical properties of the sole under the metatarsal heads. Journal of Orthopaedic Research. 1999;17(5):709-13.
112. Oliver WC, Pharr GM. An improved technique for determining hardness and elastic modulus using load and displacement sensing indentation experiments. Journal of Materials Research. 1992;7(06):1564-83.
113. Herbert E, Pharr G, Oliver W, Lucas B, Hay J. On the measurement of stress–strain curves by spherical indentation. Thin solid films. 2001;398:331-5.
114. Shao F, Childs TH, Barnes CJ, Henson B. Finite element simulations of static and sliding contact between a human fingertip and textured surfaces. Tribology International. 2010;43(12):2308-16.
115. Tasron D, Thurston T, Carré M. Frictional behaviour of running sock textiles against plantar skin. Procedia Engineering. 2015;112:110-5.
116. Cimilli S, Nergis BU, Candan C, Özdemir M. A comparative study of some comfort-related properties of socks of different fiber types. Textile Research Journal. 2010 1 June 2010;80(10):948-57.
117. Özdil N, Supuren G, Özcelik G, Pruchova J. A study on the moisture transport properties of the cotton knitted fabrics in single jersey structure. 2009.

Appendix 1: Publications

- Tasron D, Maiti R, Hemming M, Lewis R, and Carré M. Investigating a methodology to measure moisture in skin–textile friction experiments. Footwear Science. 2015; 7(sup1): S15-S6 [88]

- Tasron D, Thurston T, and Carré M. Frictional behaviour of running sock textiles against plantar skin. Procedia Engineering. 2015; 112: 110-5 [115]

- Carré M, Tasron D, Lewis R, and Hashmi F. Investigating foot-sock friction: A comparison of two different methodologies. Procedia Engineering. 2016;147:759-64 [89]

- Tasron D, Maiti R, Hemming M, Lewis R, and Carré M. Frictional interaction between running sock fabrics and plantar aspect of first metatarsal head in different moisture conditions. Procedia Engineering. 2016; 147: 753-8 [91]

- Tasron D, Nasir S, Troynikov O, Lewis R, and Carré M. Thermo-physiological comfort and frictional characteristics of running socks in different moisture conditions. Proceedings of the 9th Conference of the Textile Bioengineering and Informatics Symposium 2016 [95]

Appendix 2: Ethics Application 002074

The University Of Sheffield.

Downloaded: 16/10/2015
Approved: 03/02/2015

Raman Maiti
Medical School

Dear Raman

PROJECT TITLE: Investigation on the mechanical and material properties of the skin
APPLICATION: Reference Number 002074

On behalf of the University ethics reviewers who reviewed your project, I am pleased to inform you that on 03/02/2015 the above-named project was **approved** on ethics grounds, on the basis that you will adhere to the following documentation that you submitted for ethics review:

- University research ethics application form 002074 (dated 26/01/2015).
- Participant information sheet 004824 version 1 (26/01/2015).
- Participant consent form 004823 version 1 (26/01/2015).

If during the course of the project you need to deviate significantly from the above-approved documentation please inform me since written approval will be required.

Yours sincerely

Jean Lazenby
Ethics Administrator
Medical School

Appendix 3: Ethics Application 007424

The University Of Sheffield.

Downloaded: 23/02/2016
Approved: 15/02/2016

Raman Maiti
Infection and Immunity

Dear Raman

PROJECT TITLE: Investigation on the properties of the skin using mechanical and skin characteristic systems
APPLICATION: Reference Number 007424

On behalf of the University ethics reviewers who reviewed your project, I am pleased to inform you that on 15/02/2016 the above-named project was **approved** on ethics grounds, on the basis that you will adhere to the following documentation that you submitted for ethics review:

- University research ethics application form 007424 (dated 08/02/2016).
- Participant information sheet 1015207 version 1 (06/02/2016).
- Participant information sheet 1014814 version 3 (06/02/2016).
- Participant consent form 1015208 version 1 (06/02/2016).
- Participant consent form 1014810 version 2 (06/02/2016).

The following optional amendments were suggested:

The PIS needs the name of the study on it. The PIS and consent forms need dates and version numbers added as a footer / header.

If during the course of the project you need to deviate significantly from the above-approved documentation please inform me since written approval will be required.

Yours sincerely

Paula Blackwell
Ethics Administrator
Medical School

Appendix 4: Ethics Application HSCR 15-21

University of Salford MANCHESTER

Research, Innovation and Academic Engagement Ethical Approval Panel

College of Health & Social Care
AD101 Allerton Building
University of Salford
M6 6PU

T +44(0)161 295 2280
HSresearch@salford.ac.uk

www.salford.ac.uk/

14 May 2015

Dear Diyana,

RE: ETHICS APPLICATION HSCR 15-21 – Understanding the issues related to maintaining foot skin health within a shoe environment

Based on the information you provided, I am pleased to inform you that application HSCR15-21 has been approved.

If there are any changes to the project and/ or its methodology, please inform the Panel as soon as possible by contacting HSresearch@salford.ac.uk

Yours sincerely,

Sue McAndrew
Chair of the Research Ethics Panel

The University Of Sheffield.

Faculty of Engineering

Mechanical Engineering

General Risk Assessment : Unique ID 003321

Task or Activity : Using the Large Friction Rig (LFR) to measure the applied normal load and friction force between the human skin and various surfaces including the steel workplate of the LFR and fabrics/textiles. Participants are required to slide their skin site to be tested (e.g. the sole of the foot) along the material surface which has been securely adhered to the top of the workplate. STAFF AND STUDENTS SHOULD REFER TO THIS RISK ASSESSMENT PRIOR TO USING THE EQUIPMENT AND ADD ANY ADDITIONAL HAZARDS PRESENT AT THE SITE.

Valid until 27th November 2018

Persons At Risk : Staff , Postgraduates and Undergraduates

Name : Diyana Tasron

Supervisor : Dr Matt Carre

Location : Off Site (PORTABLE)

No Out of Hours Working Allowed

If ANY changes are made to the task or activity described on this form please create a new Risk Form.

Hazard Type	Risk of Injury & Details	Control Measures	Risk Rating
Repetitive Movements or Poor Posture	Risk of skin abrasion from the repetitive sliding. Participants could also experience discomfort and fatigue during the testing. Posture of hand, back and neck during the experiment.	Participants will be required to take a short break after each sliding to rest and allow the skin to return back to its initial condition. The hydration level and localised temperature of the tested skin site are also monitored at specific intervals by the Principal Investigator to ensure that no large changes have occurred. Longer break intervals with light refreshments are also provided for any testing lasting more than 30 minutes. In case of unforeseen accidents/injuries, dermatology experts (Prof. Mike Cork and Dr.Simon Danby) from the Royal Hallamshire Hospital will	1

Repetitive Movements or Poor Posture		**be consulted and adequate care and treatment will be provided. Investigators will ensure that participants maintain correct postures throughout testing. No testing will be conducted before 8.30am and after 4.30pm.**	**1**
General Hazards in the Laboratory	**Slipping due to spillages on the floor and tripping over while walking around the lab. In case where the test is conducted on the sole of foot, there is a risk of falling over during the sliding.**	**Preventing slipping and tripping: Good housekeeping is maintained and any spillages will be mopped up immediately. Work areas are kept clean and tidy at all times. Trailing leads and cables are kept away from walkways. Preventing falling: In order to prevent the participants from falling over, the LFR will be placed on a solid level floor surface and a fixed support will be provided for them to hold on to throughout the testing. Participants will also be shown some demonstrations on how the sliding should be done prior to the test by the Principal Investigator. The demonstrations will initially be shown in the form of recorded videos and then shown live by the Principal Investigator himself/herself. STAFF AND STUDENTS SHOULD HAVE GONE THROUGH GENERAL LABORATORY INDUCTION AND SIGNED THE RELEVANT DOCUMENTS. FOR EXAMPLE: GENERAL LABORATORY RULES NO.2370 FOR HIG LAB (MD16).**	**1**

Chemical	Allergies to the skin of the participants and investigators triggered by: 1) application of surgical spirit or any alcohol-based topical preparations and 2) use of latex gloves.	Participants will be given an Information Sheet prior to the test and therefore will be informed about the testing procedure and any skin preparations involved. They will also have to provide their written consent before taking part in the testing. Investigators will be using disposable vinyl and/or nitrile gloves when applying the alcohol-based topical preparations onto participant's skin. In case of unforeseen post-test allergies, dermatology experts (Prof. Mike Cork and Dr.Simon Danby) from the Royal Hallamshire Hospital will be consulted and adequate care and treatment will be provided. No testing will be carried out before 8.30am and after 5.30pm.	1
Manual Handling	Investigators risk injuries or back pain from handling heavy/bulky objects e.g. shifting the LFR and its accessories to the Royal Hallamshire Hospital for testing.	Investigators will be recommended to undertake the on-line Manual Handling Training. Trolley will be used to move items from the laboratory to the transporting vehicle and from the vehicle to the hospital. Heavy items are stored at the height closer to chest and staff in the Mechanical Workshop will be contacted for assistance in moving the LFR to the hospital if necessary.	1

Key		
High Risk	Medium Risk	Low Risk

The University Of Sheffield.

Faculty of Engineering

Mechanical Engineering

General Risk Assessment : Unique ID 003451

Task or Activity : Conducting an indentation test on skin to investigate its deformation behaviour in loading and unloading conditions. STAFF AND STUDENTS SHOULD REFER TO THIS RISK ASSESSMENT PRIOR TO USING THE EQUIPMENT AND ADD ANY ADDITIONAL HAZARDS PRESENT AT THE SITE.

Valid until 27th November 2018

Persons At Risk : Staff , Postgraduates and Undergraduates

Name : Diyana Tasron

Supervisor : Dr Matt Carre

Location : Off Site (PORTABLE)

No Out of Hours Working Allowed

If ANY changes are made to the task or activity described on this form please create a new Risk Form.

Hazard Type	Risk of Injury & Details	Control Measures	Risk Rating
Repetitive Movements or Poor Posture	Posture of hand, back and neck during the experiment.	Investigator(s) will ensure that the participants will maintain correct postures throughout testing.	1
Other	Risk of skin damage due to the indentation of the probe.	The load will be applied very gradually onto the tested area of the skin. Investigators will also ensure that the load applied to the skin is less than the damaging force to the skin. IMPORTANT: Before conducting an indentation test on any skin area, it is very crucial that the Investigators have good knowledge on the maximum (cut-off) force that the skin could withstand prior to carrying out the test on participants. They are also advised to consult their project supervisor(s) regarding this before proceeding with the test.	1

Chemical	Allergies to the skin of the participants and investigators triggered by the application of surgical spirit or any alcohol-based topical preparations.	Participants and investigators will be given an Information Sheet prior to the test and therefore will be informed about the testing procedure and any skin preparations involved. They will also have to provide their written consent before taking part in the testing.	1
General Hazards in the Laboratory	Slipping due to spillages on the floor and tripping over while walking around the lab.	Good housekeeping is maintained and any spillages will be mopped up immediately. Work areas are kept clean and tidy at all times. Trailing leads and cables are kept away from walkways. STAFF AND STUDENTS SHOULD HAVE GONE THROUGH GENERAL LABORATORY INDUCTION AND SIGNED THE RELEVANT DOCUMENTS.	1

Key		
High Risk	Medium Risk	Low Risk

Appendix 7: List of sock textiles used for testing

3.1 Pilot study 1: A comparison of two different methodologies in measuring foot-sock friction (please refer to page 49)

Sock type	Material compositions	Knit pattern	Mean thickness ± SD (mm)
Anti-blister "ABS"	99% nylon and 1% elastane	Simple jersey	1.18 ± 0.04
Cotton-rich "CRS"	70% cotton, 29% nylon, and 1%elastane	Terry jersey	2.62 ± 0.08

3.2 Pilot study 2: Investigating the friction between a sock and chosen shoe insole (please refer to page 58)

Sock type	Material compositions	Knit pattern
Cotton-rich "Sock A"	75% cotton, 17% polyester, 6% nylon, 2% elastane	Terry jersey
100% cotton "Sock B"	100% cotton	Simple jersey
Wool-rich "Sock C"	40% wool, 31% cotton, 19% nylon, 8% elastane	Terry jersey
Anti-blister "Sock D"	99% nylon, 1% elastane	Simple jersey
Double-layer (outer) "Sock E-o"	54% cotton, 44% nylon and 2% elastane	Simple jersey

3.3 Pilot study 3: Investigating the effects of strain on the frictional behaviour of sock fabrics (please refer to page 65)

Sock type	Fibre compositions	Knit pattern
Cotton-rich "Sock A"	75% cotton, 17% polyester, 6% nylon, 2% elastane	Terry jersey
100% cotton "Sock B"	100% cotton	Simple jersey
Wool-rich "Sock C"	40% wool, 31% cotton, 19% nylon, 8% elastane	Terry jersey
Anti-blister "Sock D"	99% nylon, 1% elastane	Simple jersey
Double-layer (outer) "Sock E-o"	54% cotton, 44% nylon and 2% elastane	Simple jersey

3.4 Pilot study 4: Investigating the effects of contact area on the frictional behaviour of sock fabrics against shoe insole in dry condition (please refer to page 69)

Sock type	Fibre compositions	Knit pattern
Cotton-rich "Sock A"	75% cotton, 17% polyester, 6% nylon, 2% elastane	Terry jersey
100% cotton "Sock B"	100% cotton	Simple jersey
Wool-rich "Sock C"	40% wool, 31% cotton, 19% nylon, 8% elastane	Terry jersey
Anti-blister "Sock D"	99% nylon, 1% elastane	Simple jersey
Double-layer (outer) "Sock E-o"	54% cotton, 44% nylon and 2% elastane	Simple jersey

3.5 Pilot study 5: Investigating the effects of varying moisture conditions on the sock-insole friction behaviour (please refer to page 73)

Sock type	Fibre compositions	Knit pattern
Cotton-rich "Sock A"	75% cotton, 17% polyester, 6% nylon, 2% elastane	Terry jersey
100% cotton "Sock B"	100% cotton	Simple jersey
Wool-rich "Sock C"	40% wool, 31% cotton, 19% nylon, 8% elastane	Terry jersey
Anti-blister "Sock D"	99% nylon, 1% elastane	Simple jersey
Double-layer (outer) "Sock E-o"	54% cotton, 44% nylon and 2% elastane	Simple jersey

3.6 Investigating the frictional behaviour of plantar skin against running sock fabrics in dry condition (please refer to page 77)

Sock types	Fibre compositions	Knit pattern
Cotton-rich "Sock A"	75% cotton, 17% polyester, 6% nylon, 2% elastane	Terry jersey
100% cotton "Sock B"	100% cotton	Simple jersey
Wool-rich "Sock C"	40% wool, 31% cotton, 19% nylon, 8% elastane	Terry jersey
Anti-blister "Sock D"	99% nylon, 1% elastane	Simple jersey
Double-layer (inner) "Sock E"	100% nylon	Simple jersey

3.7 Investigating the frictional behaviour of first metatarsal head (1MTH) against running sock fabrics in different moisture conditions (please refer to page 88)

Sock type	Material compositions	Knit pattern	Mean thickness ± SD (mm)
Anti-blister "ABS"	99% nylon and 1% elastane	Simple jersey	1.18 ± 0.04
Cotton-rich "CRS"	70% cotton, 29% nylon, and 1%elastane	Terry jersey	2.62 ± 0.08

4.5.2 Friction tests using a dynamic friction rig (please refer to page 127)

Sock type	Material compositions	Knit pattern	Mean thickness ± SD (mm)
Anti-blister "ABS"	99% nylon and 1% elastane	Simple jersey	1.18 ± 0.04
Cotton-rich "CRS"	70% cotton, 29% nylon, and 1%elastane	Terry jersey	2.62 ± 0.08

Appendix 8: Protocol for Study A (at TUOS)

NO.	TASK	DONE?	
1	Brief participant on testing protocol and obtain his/her written consent.		
2	Ask participant remove his/her footwear to allow the Principal Investigator to conduct Vascular and Neuropathy Assessments on both feet. Identify any presence of callus on the test foot.		
3	Allow the test foot to acclimatise to the room environments for 15 minutes.		
4	Obtain Corneometer (6 readings), Cutometer (1 reading), and Thermometer (5 readings) measurements on the 1MTH. **[Before Cleaning]**		
5	Obtain an OCT image of the 1MTH **[Before Cleaning]**		
6	Soak test foot in a water bath (at room temperature) for 30 seconds.		
7	Dry test foot using paper towels and let it acclimatise to the room environments for 10 minutes.		
8	During acclimatisation, ask participant to fill in the questionnaire.		
9	Obtain Corneometer (6 readings), Cutometer (1 reading), and Thermometer (5 readings) measurements on the 1MTH. **[After Cleaning]**		
10	Obtain an OCT image of the 1MTH **[After Cleaning]**		
11	Obtain Corneometer measurements on the 1MTH (6 readings) and the dry sock (3 readings). **[Before Friction Test 1]**		
12	**FRICTION TEST 1 -** on a dry sock (at 4 ranges of loads). Get 3 Corneometer readings on the sock after each run of friction test. **[After Friction Test 1_load 1, After Friction Test 1_load 2, After Friction Test 1_load 3, After Friction Test 1_load 4]**		
13	Obtain Corneometer (6 readings) and Thermometer (5 readings) measurements of the 1MTH **[After Friction Test 1]**		
14	Obtain an OCT image of the 1MTH **[After Friction Test 1]**		
15	Allow the test foot to acclimatise to the room environments for 8 minutes.		
16	Obtain Corneometer readings on the 1MTH (6 readings) and low moist sock (3 readings). **[Before Friction Test 2]**		
17	Obtain an OCT image of the 1MTH **[Before Friction Test 2]**		

NO.	TASK	DONE?	
18	**FRICTION TEST 2** - on a low moist sock (at 4 ranges of loads). Get 3 Corneometer readings on the sock after each run of friction test. **[After Friction Test 2_load 1, After Friction Test 2_load 2, After Friction Test 2_load 3, After Friction Test 2_load 4]**		
19	Obtain Corneometer (6 readings) and Thermometer (5 readings) measurements of the 1MTH **[After Friction Test 2]**		
20	Obtain an OCT image of the 1MTH **[After Friction Test 2]**		
21	Allow foot to acclimatise to the room environments for 8 minutes.		
22	Obtain Corneometer readings on the 1MTH (6 readings) and wet sock (3 readings). **[Before Friction Test 3]**		
23	Obtain an OCT image of the 1MTH **[Before Friction Test 3]**		
24	**FRICTION TEST 3** - on a wet sock (at 4 ranges of loads). Get 3 Corneometer readings on the sock after each run of friction test. **[After Friction Test 3_load 1, After Friction Test 3_load 2, After Friction Test 3_load 3, After Friction Test 3_load 4]**		
25	Obtain Corneometer (6 readings) and Thermometer (5 readings) measurements of the 1MTH **[After Friction Test 3]**		
26	Obtain an OCT image of the 1MTH **[After Friction Test 3]**		
27	Soak foot in a water bath (at room temperature) for 30 seconds, dry it using paper towels and let it acclimatise for 10 minutes before proceeding to the second part of the test using another sock type. Repeat step 9 to 26 for the second sock type.		

Appendix 9: Protocol for Study B (at UoS)

NO.	TASK	DONE?	
1	Brief participant on testing protocol and obtain his/her written consent.		
2	Ask participant remove his/her footwear to allow the Principal Investigator to conduct Vascular and Neuropathy Assessments on both feet. Identify any presence of callus on the test foot.		
3	Allow the test foot to acclimatise to the room environments for 15 minutes.		
4	Obtain Corneometer (6 readings), Cutometer (1 reading), and Thermometer (5 readings) measurements on the 1MTH. **[Before Cleaning]**		
5	Soak test foot in a water bath (at room temperature) for 30 seconds.		
6	Dry test foot using paper towels and let it acclimatise to the room environments for 10 minutes.		
7	During acclimatisation, ask participant to fill in the questionnaire.		
8	Obtain Corneometer (6 readings), Cutometer (1 reading), and Thermometer (5 readings) measurements on the 1MTH. **[After Cleaning]**		
9	Obtain Corneometer measurements on the 1MTH (6 readings) and the dry sock (3 readings). **[Before Friction Test 1]**		
10	**FRICTION TEST 1 -** on a dry sock (at 3 pressure levels). Check sock alignment on probe, set the pressure level, start logging, insert code, click save. Get 3 Corneometer readings on the sock after each run of friction test. **[After Friction Test 1_pressure 1, After Friction Test 1_pressure 2, After Friction Test 1_pressure 3]**		
11	Obtain Corneometer (6 readings) and Thermometer (5 readings) measurements of the 1MTH **[After Friction Test 1]**		
12	Allow the test foot to acclimatise to the room environments for 8 minutes.		
13	Obtain Corneometer readings on the 1MTH (6 readings) and low moist sock (3 readings). **[Before Friction Test 2]**		

NO.	TASK	DONE?	
14	**FRICTION TEST 2 -** on a low moist sock (at 3 pressure levels). Check sock alignment on probe, set the pressure level, start logging, insert code, click save. Get 3 Corneometer readings on the sock after each run of friction test. **[After Friction Test 2_pressure 1, After Friction Test 2_pressure 2, After Friction Test 2_pressure 3]**		
15	Obtain Corneometer (6 readings) and Thermometer (5 readings) measurements of the 1MTH **[After Friction Test 2]**		
16	Allow the test foot to acclimatise to the room environments for 8 minutes.		
17	Obtain Corneometer readings on the 1MTH (6 readings) and wet sock (3 readings). **[Before Friction Test 3]**		
18	**FRICTION TEST 3 -** on a wet sock (at 3 pressure levels). Check sock alignment on probe, set the pressure level, start logging, insert code, click save. Get 3 Corneometer readings on the sock after each run of friction test. **[After Friction Test 3_pressure 1, After Friction Test 3_pressure 2, After Friction Test 3_pressure 3]**		
19	Obtain Corneometer (6 readings) and Thermometer (5 readings) measurements of the 1MTH **[After Friction Test 3]**		
20	Soak foot in a water bath (at room temperature) for 30 seconds, dry it using paper towels and let it acclimatise for 10 minutes before proceeding to the second part of the test using another sock type. Repeat step 8 to 19 for the second sock type.		

Appendix 10: Physical and thermophysiological comfort characteristics of anti-blister and cotton-rich running socks (in collaboration with the RMIT University, Australia)

Introduction

This study was carried out as part of a collaboration project with Siti Hana Nasir and Professor Olga Troynikov based at the RMIT University, Melbourne, Australia. The purpose of the current study was to assess the properties of two commercially-available running socks influencing the thermophysiological comfort of the wearer and relate the findings to the frictional performance of the socks which will be described in the following chapter. The physical characteristics and thermophysiological tests were conducted by Siti Hana Nasir in the RMIT University whereas the friction experiments (described in section 3.6) were undertaken by the author of this thesis at the University of Sheffield, UK. The sock materials were supplied by the author for testing and the results obtained were processed and analysed together by the author and Siti Hana Nasir.

Sock materials and their physical characteristics

Two types of newly-purchased running socks of differing material compositions and fabric construction were selected for the purpose of this study which are a predominantly nylon sock and a cotton-rich sock. The characteristics of the socks are exactly the same as the ones described in Table 2.4.

In order to remove any contaminants trapped in the sock fibres as well as to maintain their dimensional stability, all socks were hand-washed using water and a mild liquid detergent and left to air-dry at room temperature for at least 72 hours prior to the test.

For the purpose of the physical characteristic tests, five specimens were obtained from each sock and the mean values of each measured parameter were included in Table 2.4. The number of wales and courses per unit length of fabric sample was measured according

to AS 2001.2.6-2001. For any knitted fabrics, the term ‘wales’ refer to the series of loops that are interwoven vertically whereas the term ‘courses’ refer to the series of loops that are connected horizontally.

The thickness of fabric samples was measured as the distance between the reference plate and parallel presser foot of the thickness tester. The mass per unit area was also calculated as the mean mass per unit area of five specimens.

It was found that despite having lower stitch density (determined by the number of wales and courses per cm), the cotton-rich fabric is 44% heavier than that of the predominantly nylon anti-blister fabric. It is also noted that due to the plush knitted structure on the next-to-skin side of the cotton-rich fabric, it is significantly thicker than the anti-blister fabric.

Experimental procedure for the thermophysiological comfort

The thermophysiological tests were carried out at the RMIT University by Siti Hana Nasir and was supervised by Professor Olga Troynikov, which include measuring the thermal resistance, water vapour resistance and moisture management properties of both sock fabrics. A sweating guarded hot-plate, which has been commonly used to simulate both heat and moisture transfer from a body surface to the environment through the fabric layers, was utilised to obtain the thermal and water vapour resistance in accordance to the ISO:11092 standard. However, due to the limited size of the sock fabric samples, some modifications in the testing procedure were made.

The liquid water transfer and distribution of each fabric sample in multiple directions was measured and recorded using the moisture management tester (MMT). This technique was carried out in accordance to the American Association of Textile Chemists and Colorists (AATCC) test method 195-2009. Five fabric samples with the size of 80 mm×80 mm were obtained from each sock fabric for testing. The fabric was in contact with the sensor rings which allows the liquid content and the liquid moisture transfer behaviour between the fabric surfaces to be assessed. The top surface on the MMT equipment is normally the next-to-skin

side (the surface in contact with the skin) and bottom surface of the fabric is the away-from-skin side (the surface closest to the neighbouring environment), as shown in Figure A10.1.

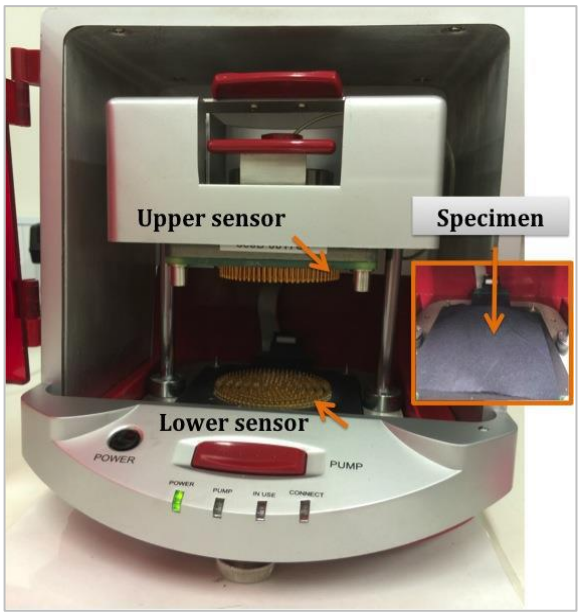

Figure A10.1: The moisture management tester (MMT).

Sock characteristics relevant to thermophysiological comfort

The experimental data showed that the anti-blister fabric has a lower thermal resistance and water vapour resistance than the cotton-rich fabric by 27% and 41% respectively. The paired t-test analysis of the data also shows that, in terms of their thermal resistance and water vapour resistance, both anti-blister and cotton-rich sock fabrics behaved significantly differently ($p < 0.005$). The thickness of the cotton-rich sock fabric contributes to higher value of thermal and water vapour resistance. Since the cotton-rich fabric is made from plush jersey, it increases the air volume contained within the thick knitted structure of the sock. This increases the passage of heat through the fabric from the skin to the environment leading to an increase in its thermal resistance. Fabric thickness has been reported by many researchers as one of the important fabric parameters influencing the thermal and water vapour resistance of a fabric [79, 116].

Figure A10.2 presents the results for the main indices of the moisture management properties of the sock fabrics. The moisture management capability of the fabric was mainly assessed on three indices which include the average moisture absorption rate at the top and bottom surfaces, accumulative one-way transport index (AOTI) and overall moisture management capacity (OMMC).

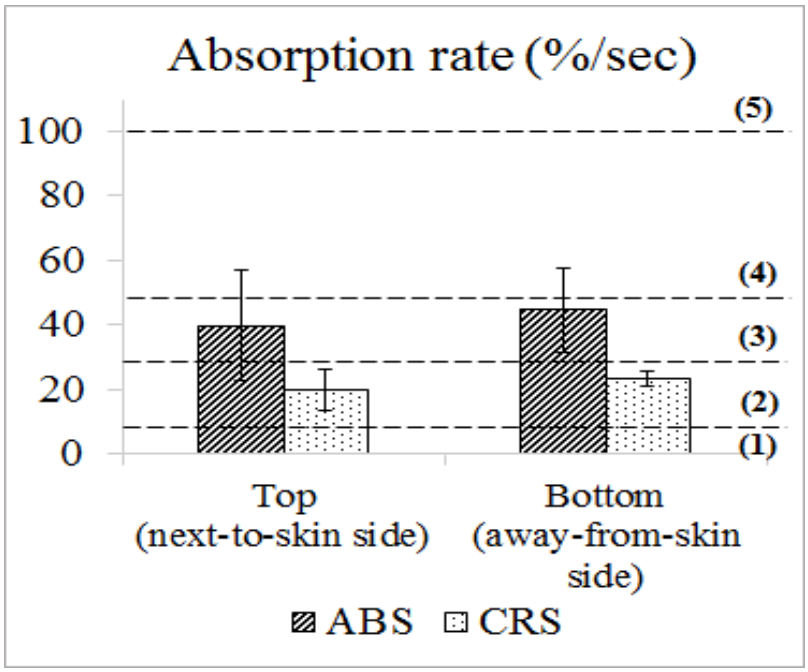

Figure A10.2: The average moisture absorption rate at the top (next-to-skin side) and bottom (away-from-skin side) surfaces for both anti-blister and cotton-rich socks. [Grading scale: (1): poor; (2): fair; (3): good; (4): very good; and (5): excellent]

It can be seen from Figure A10.2 that the absorption rate of the anti-blister fabric is almost twice as high as the cotton-rich fabric for both the top and bottom surfaces. According to Özdil et al. [117], a thinner and finer fabric will have a higher absorption rate compared to a thicker fabric due to its comprising finer yarn. The absorption rate on the bottom surface is slightly higher than the top surface for both fabrics which indicates that the liquid (sweat) diffuses efficiently from the next-to-skin side to the away-from-skin side and spreads on this side. In return, the top surface which would be in contact with the wearer's skin will remain drier than the bottom surface which is ideal for the wearer, ensuring comfort throughout.

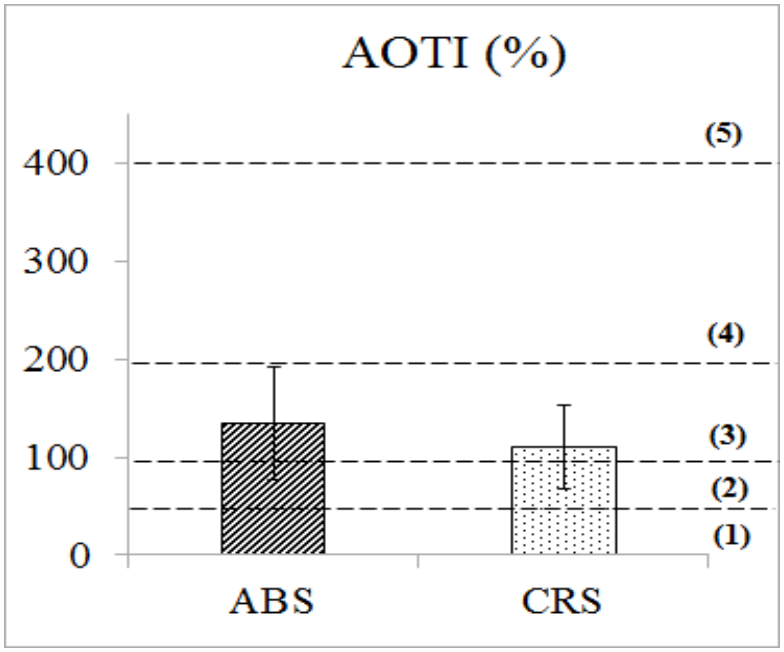

Figure A10.3: The accumulative one-way transport index (AOTI) for both anti-blister and cotton-rich socks.
[Grading scale: (1): poor; (2): fair; (3): good; (4): very good; and (5): excellent]

Figure A10.3 shows the comparison of the AOTI values measured from both sock fabrics, where fabric with lower AOTI value has low capability to quickly transport the liquid sweat quicker from next-to-skin side to the external environment. It can be seen that the AOTI of anti-blister fabric is slightly higher than that of the cotton-rich fabric, despite no significant difference found ($p > 0.05$). When the values of AOTI were converted into a grading scale, it showed that the anti-blister fabric has "good" one-way transport ability (3/5) whilst the cotton-rich fabric has "fairly-good" (2.5/5) one-way transport ability.

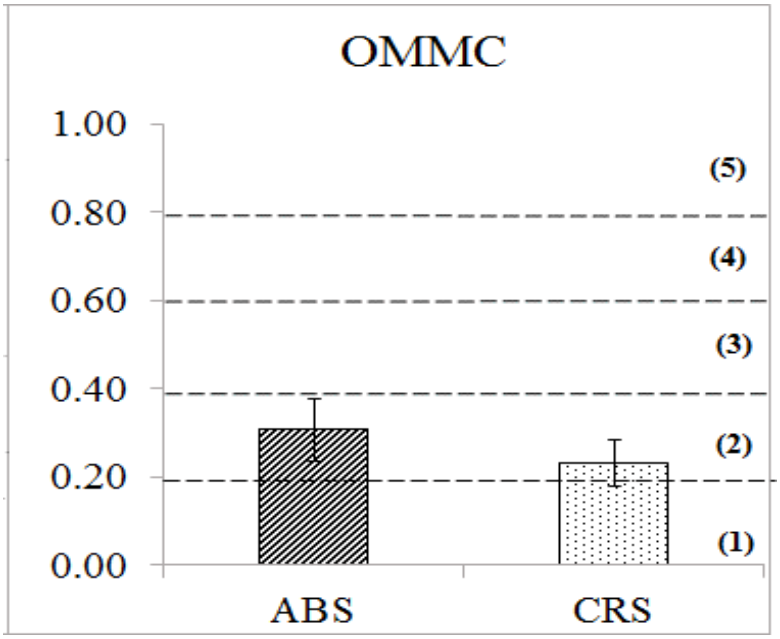

Figure A10.4: The overall moisture management capacity (OMMC) for both anti-blister and cotton-rich socks.
[Grading scale: (1): poor; (2): fair; (3): good; (4): very good; and (5): excellent]

Figure A10.4 illustrates the OMMC values of both sock fabrics. According to the grading scale, both fabrics are in the "fair" category in terms of their moisture management capacity. The moisture management properties of fabrics are critical in order for active sportswear to keep the skin dry and provide maximum comfort to the wearer. Factors such as fibre, yarn, fabric construction, and fabrics finishes are important to improve the moisture management performance of the fabrics, hence ensuring comfort to the wearer.

Relating the thermophysiological properties of running sock fabrics to their frictional performance

The dynamic coefficient of friction (DCOF) values were computed by dividing the predicted sliding friction force data by the 100N normal force for all participants. The mean DCOF values for all six fabric-moisture combinations were already presented in Table 3.8 (please refer to Section 3.7 in Chapter 3), along with the respective standard deviations and the level of significance obtained from an ANOVA test. All other comparisons were statistically significant ($p < 0.05$) apart from when comparing the "low moisture" cotton-rich fabric with

“wet” anti-blister fabric. The anti-blister fabric showed a slightly higher sliding friction than the cotton-rich fabric in dry condition. However, in the presence of moisture, the anti-blister fabric produced lower sliding friction than the cotton-rich fabric. This could be attributed to the fact that the anti-blister fabric has slightly better wicking properties compared with the cotton-rich fabric. Moreover, the anti-blister fabric demonstrated better water vapour transmission and due to its low resistance to water vapour and good one-way transport ability, allowing the water vapour from the added moisture to be transported through the air spaces and interstices between the sock fabric.

Moisture in the sock is dictated by the tribological properties [105] and hydrophobicity of the fabrics. During vigorous physical activity, the amount of perspiration produced could exceed the absorption capacity of any sock fabrics. In order for the dry in-shoe environment to be maintained, efficient wicking process is certainly required to transport the moisture away from the skin surface into the external environment. Based on the findings of this study, the anti-blister sock would more likely to remain dry within a shoe environment, hence producing lower sliding friction than the cotton-rich sock. This would not only reduce the probability of blistering but also help to ensure comfort to the wearer.